

AURORA GEOSCIENCES LTD.

**SRK CONSULTING ENGINEERS  
AND SCIENTISTS**

**GROUND PENETRATING RADAR  
AND SEISMIC REFRACTION  
SURVEYS AT THE FARO MINE,  
YUKON TERRITORY**

**M.A. Power, M.Sc., P.Geoph.**

Location: 62° 18' N, 133° 18' W  
NTS: 105 K/6  
Date: December 20, 2004

□

□

□

□

□

□

□

□

□

□

□

□

□

□

□

□

□

□

## SUMMARY

Ground penetrating radar (GPR) and seismic refraction surveys were conducted at the Faro Mine to map bedrock beneath overburden. The surveys were conducted at Vangorda Creek (1 GPR line), Grum Pit (2 GPR / 1 seismic line), Vangorda Pit (2 GPR / 1 seismic line), the north fork of Rose Creek ( 1 seismic line) and at Old Faro Creek (1 GPR line).

At the Old Faro Creek and North Fork of Rose Creek sites, surface topography was picked up by a survey contractor. At the other sites, the surface topography was picked up by the geophysical survey crew. Reference pickets consisting of marked full or half-length survey lathe were placed along the lines and the locations recorded with differential GPS receivers. The location of intermediate stations was calculated by linear interpolation.

The GPR survey was conducted with a RAMAC GPR using 25 and 50 MHz antennas. Conventional reflection data processing was applied incorporating geometric registration, statics, drift corrections, user gain, bandpass and F-k filtering, deconvolution, velocity analysis and depth conversion.

The seismic refraction survey was conducted with a 24 channel digital engineering seismograph using a 5 m phone spacing and explosives as the energy sources. For each spread, five shots were fired including 5 and 120 m offset shots and a centre spread shot. The data was interpreted using the delay time method incorporating velocity analysis and surface topographic corrections.

In general, the GPR survey detected few bedrock reflections and results were influenced by the azimuth of the survey line with respect to dominant bedrock foliation. Results on survey lines perpendicular to dominant foliation were better than on lines parallel to foliation. The seismic refraction survey detected very high second layer velocities and this layer may include, in part, weathered bedrock.

At the Vangorda Creek Site, no strong bedrock reflections were recorded in the GPR survey. At the Grum Pit site, bedrock was mapped by seismic refraction along one line at a depth of 9 to 18 m and by GPR on a parallel line at a depth of 8 to 12 m. At the Vangorda Pit site, a weak bedrock GPR reflection was recorded at depths of 6 to 20 m while on the orthogonal seismic refraction line, bedrock was mapped at depths of 6 to 25 m. Where the two lines intersected, apparent depths to bedrock recorded by the complementary surveys agreed within the limits of survey error. At the North Fork of Rose Creek (Rock Dump) site, the seismic refraction survey detected bedrock at a depth of 22 to 31 m. Finally, at Old Faro Creek near the mine entrance, the GPR survey mapped bedrock to a depth of 12 m, in agreement with available drill hole data.

## TABLE OF CONTENTS



1.0	INTRODUCTION .....	1
2.0	SITE DESCRIPTIONS AND TOPOGRAPHIC SURVEY CONTROL .....	1
3.0	GROUND PENETRATING RADAR - THEORY OF OPERATION .....	2
3.1	Radar wave propagation and attenuation .....	2
3.2	Radar wave reflection .....	4
3.3	System design and description .....	5
3.4	Survey methods .....	9
3.5	Electrical properties of earth materials at GPR frequencies .....	10
3.6	Response of discrete targets .....	12
4.0	SEISMIC REFRACTION METHOD - THEORY OF OPERATION .....	14
4.1	Basic theory .....	14
4.2	Seismic refraction surveys .....	16
4.3	Sources of error .....	18
4.4	Refraction interpretation methods .....	19
5.0	PERSONNEL AND EQUIPMENT .....	22
6.0	SURVEY SPECIFICATIONS .....	23
7.0	GPR DATA PROCESSING .....	25
8.0	RESULTS .....	27
8.1	Vangorda Creek .....	29
8.2	Grum Pit .....	30
8.3	Vangorda Pit .....	31
8.4	North Fork of Rose Creek (Rock Dump) .....	32
8.5	Old Faro Creek .....	34
8.6	General notes .....	34
9.0	CONCLUSIONS .....	36
10.0	RECOMMENDATIONS .....	38
	REFERENCES CITED .....	39
	APPENDIX A. PROJECT LOG .....	40
	APPENDIX B. INSTRUMENT SPECIFICATIONS .....	44
	APPENDIX C. SEISMIC REFRACTION INVERSION SUMMARY .....	45

1

2

3

4

5

6

7

8

9

10

11

12

13

14

15

16

17

18

19

## LIST OF FIGURES

Figure 1 Vangorda Creek site map . . . . .	Following page 27
Figure 2 Grum Pit site map . . . . .	Following page 27
Figure 3. Vangorda Pit site map . . . . .	Following page 27
Figure 4. North Fork of Rose Creek (Rock Dump) site map . . . . .	Following page 27
Figure 5. Old Faro Creek site map . . . . .	Following page 27



## 1.0 INTRODUCTION

Aurora Geosciences Ltd. was retained by SRK Consulting Engineers and Scientists to conduct ground penetrating radar (GPR) and seismic refraction surveys at five sites at the Faro Mine, Faro, Yukon Territory. The purpose of the surveys was to assist in the design of environmental mitigation measures by determining the depth to bedrock and the topography of bedrock at each site. This report describes the survey program and its results.

## 2.0 SITE DESCRIPTIONS AND TOPOGRAPHIC SURVEY CONTROL

The geophysical surveys were conducted at the following sites on the Faro Mine property:

Vangorda Creek  
Grum Pit  
Vangorda Pit  
North Fork of Rose Creek  
Old Faro Creek

The locations of the survey sites are shown in location maps in this report. In these diagrams, line locations are shown relative to NAD 27 (Yukon) UTM coordinates (Zone 8N). The survey lines are also shown relative to site topography in an AutoCADD drawing appended to this report on CD-ROM.

The locations of the geophysical lines at the Old Faro Creek and North Fork of Rose Creek (Rock Dump) sites were measured by Yukon Engineering Services and their data was used to locate the lines. At the other sites, the geophysical survey crew installed reference stations during the course of the surveys, recorded these locations with a differential GPS receiver, and determined corrected geographic coordinates for these points following the survey. On the GPR survey lines, pickets were placed at elevation inflection points or at least every 100 m along the survey lines. On the seismic survey lines, pickets were placed every 5 m and stations every 40 to 60 m along the lines were surveyed with the differential GPS receiver. The locations and elevations of intermediate stations were determined by linear interpolation, supplemented by elevations derived from laser range finder measurements.

### 3.0 GROUND PENETRATING RADAR - THEORY OF OPERATION

The GPR method involves directing a transient electromagnetic wave into the ground and recording waves reflected and refracted by subsurface interfaces. The transit time together with the velocity of the ground can be inverted to yield a cross section showing the depths to the reflecting surfaces in the ground. The theory behind the GPR method is summarized in Annan and Cosway (1991), Davis and Annan (1987) and Power (1994).

#### 3.1 Radar wave propagation and attenuation

Ground penetrating radar waves propagate according to Maxwell's Equations:

$$\nabla \times H = J + \frac{\partial D}{\partial t} \quad (1)$$

$$\nabla \times E = -\frac{\partial B}{\partial t} \quad (2)$$

$$\nabla \cdot D = \rho \quad (3)$$

$$\nabla \cdot B = 0 \quad (4)$$

where **E** is the electric field, **B** is the magnetic induction, **D** is the displacement current, **J** is the displacement current, *t* is time and  $\rho$  is the electrical charge. These are the vector forms of Ampere's, Faraday's and Gauss' Laws and the statement that there are no magnetic monopoles. Taking the curl of (2) and applying an elementary identity yields the Helmholtz equation for EM propagation in a source free medium:

$$\nabla^2 E - \mu\sigma \frac{\partial E}{\partial t} - \mu\epsilon \frac{\partial^2 E}{\partial t^2} = 0 \quad (5)$$

The solution to this equation in the most general form as a plane wave is in the form:

$$E(r, t) = E e^{-i(\omega t - k \cdot r)} \quad (6)$$

which, after substitution yields:

$$\kappa = \omega \frac{\sqrt{K^*}}{c} \quad (7)$$

where  $\omega$  is the angular frequency ( $2\pi f$ ) and  $K^*$  is the complex dielectric permittivity and  $c$  is the speed of light *in vacuo*. The complex dielectric permittivity governs both the attenuation and phase velocity of the radar wave.

Dielectric permittivity ( $\epsilon$ ) is the ease with which a material may be polarized in an electric field. Relative dielectric permittivity ( $K$ ) is the ratio of dielectric permittivity to free space dielectric permittivity. A material with abundant polar charges will have a higher dielectric permittivity than a material with comparatively fewer polar charges because per unit mass, the former will undergo more polarization than the latter. When the electric field changes, the polar material will resist the change in the field to a greater extent than the nonpolar substance. Consequently, materials with a high dielectric permittivity have a higher electrical impedance (greater attenuation) than materials with a lower dielectric permittivity. The phenomenon is log linear at low frequencies but increases rapidly when the applied frequency exceeds the natural oscillation frequency of the polar molecules. For water, the most important substance with respect to GPR system performance, this relaxation frequency is in the order of 1 Ghz.

Velocity is also affected by dielectric permittivity. The second term in the exponent of equation (6) must be dimensionless which indicates that  $\kappa$  must have dimensions of  $1/r$ . Consequently, the phase velocity must be:

$$v = \frac{c}{\sqrt{K^*}} \quad (8)$$

Radar waves thus slow down and shorten up in materials with high relative dielectric permittivity, and speed up and lengthen in materials with low relative dielectric permittivity.

Attenuation at radar frequencies is a function of dielectric permittivity and electrical conductivity. Davis and Annan (1987) derive an expression for attenuation in decibels per metre at radar frequencies using complex conductivity and relative dielectric permittivity:

$$\alpha_m = \frac{1.69 \times 10^3 \sigma^*}{\sqrt{K^*}} \quad (9)$$

In this relation, dielectric losses are incorporated into the complex conductivity  $\sigma^*$ .

### 3.2 Radar wave reflection

EM waves reflect at the boundaries between materials with different velocities. In the earth, these boundaries occur at the interface between materials with different relative dielectric permittivities. At normal incidence on a planar reflector, the strength of the reflection (Reflection coefficient - R) reduces to:

$$R = \frac{\sqrt{K_1} - \sqrt{K_2}}{\sqrt{K_1} + \sqrt{K_2}} \quad (10)$$

Thus the strength of the reflection is primarily a function of the contrast in relative dielectric permittivity.

The size and texture of the target affect the strength of the reflection. If the target is small, the strength of the reflection will be reduced and similarly, if the surface is rough, the incident energy will be absorbed or scattered. Smooth and small are terms defined relative to the wavelength of the radar wave. The power reflected back to the surface governed solely by the geometry of the target is the product of the backscatter gain and the target cross sectional area ( $g\phi$ ) (Annan and Davis 1977). For a planar reflector with reflection coefficient R at distance L, the backscatter gain is:

$$g\phi = \pi L^2 R \quad (11)$$

If the target is rough, with irregularities in the order of  $\lambda/4$  (quarter wavelength), the gain is reduced to:

$$g\phi = \frac{\pi \lambda L R}{2} \quad (12)$$

Finally if the target is very small with radius  $a \ll \lambda$ , the gain is further reduced to:

$$g\phi = 65\pi^5 a^6 \lambda^4 \quad (13)$$

In summary, the strength of a reflected wave depends strongly upon the size and roughness of the target.

### 3.3 System design and description

Ground radar systems consist of a transmitter and receiver, linked together by a controller. Both the transmitter and receiver consist of a electronic control unit and an antenna. The controller simultaneously triggers the transmitter and the receiver. Upon receipt of a signal from the controller, the transmitter sends a signal to the transmitting antenna which in turn radiates a radar wavelet into the earth where it reflects off various targets. The receiver is also triggered by a simultaneous pulse from the controller and it detects radiation at the same frequency as the transmitter. The receiver begins recording radar wave radiation as soon as it is triggered and ceases recording a short interval in the order of 1 or 2  $\mu$ s after initiation. Readings are stacked from 10 to 1000 times to improve the signal to noise ratio. A GPR system is sketched schematically in Figure GPR1.

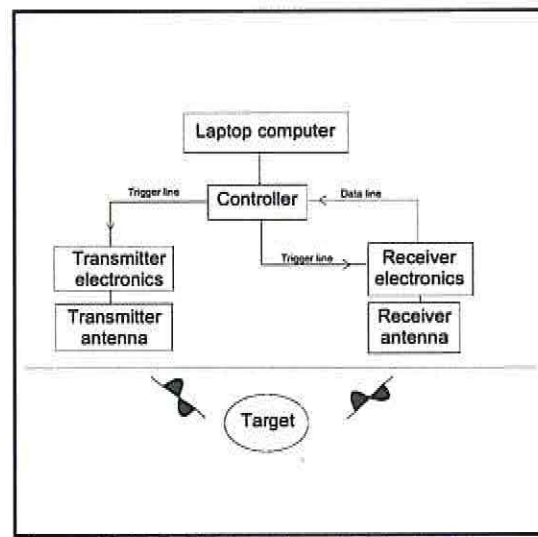


Figure GPR-1 GPR system block diagram.

GPR systems are made to operate at discrete frequencies spanning a spectrum from around 12.5 MHz to 1 GHz. The transmitted signal consists of a discrete pulse with a centre frequency (dominant frequency) approximately equal to its bandwidth. Thus a 100 MHz radar may generate a signal with a centre frequency of 100 MHz and bandwidth from 50 to 150 MHz. For this reason, the pulse period is inversely proportional to the centre frequency (Annan and Cosway 1991).

The table below shows the pulse wavelength in air and water for various GPR operating frequencies. Antenna design considerations require that the antennas be at least 1/3 of the system wavelength to ensure adequate propagation. Consequently, the lower the operating frequency, the larger the antennas required for the system. The practical lower limit is 12.5 MHz. The wavelength ( $\lambda$ ) also has implications for the target resolution as described in the previous section. For planar horizontal targets, the resolution is in the order of  $0.5\lambda$ .

Centre frequency (MHz)	$\lambda$ in air (m) (v=300 m/ms)	$\lambda$ in shale (m) (v=90 m/ $\mu$ s)	$\lambda$ in water (m) (v=30 m/ $\mu$ s)
500	0.6	0.18	0.06
200	1.5	0.45	0.15
100	3	0.9	0.3
50	6	1.8	0.6
25	12	3.6	1.2
12.5	24	7.2	2.4

The antenna radiation pattern imposes limitations on the system design. Figure GPR-2, adapted from Annan and Cosway (1991), illustrates the influence of the dielectric permittivity on the antenna radiation pattern. Earth materials display relative dielectric permittivities in the range of 5 to 40. At the lower end of this range, the radiation pattern

focuses the energy into two lobes oriented at an inclination of approximately 45° to the vertical. Annan and Cosway (*ibid*) cite a design relation for the optimum antenna separation S:

$$S = \frac{2 \cdot D}{\sqrt{K - 1}} \quad (14)$$

where D is the estimated depth to the target. In practice, antennas are commonly

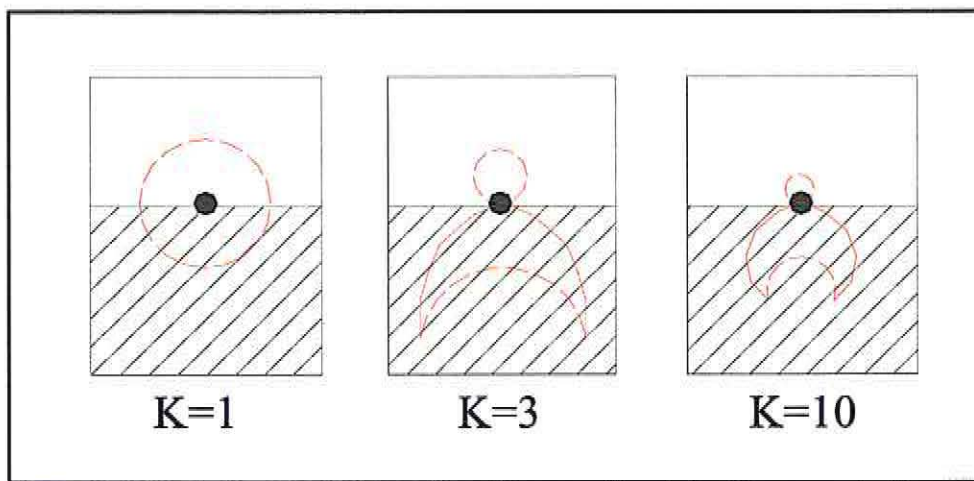


Figure GPR-2. Antenna radiation pattern (cross sectional view) for ground with different relative dielectric permittivity. Distance of curve from centre of antenna denotes strength of radiation in that direction. (after Annan and Cosway (1991))

separated at a distance equal to their length.

For optimal performance, the antennas should be oriented so that their electric field is parallel to the strike direction of the target. This normally implies that the antenna be oriented perpendicular to the direction of travel along a survey line. In practice, antennas are often oriented parallel to the direction of travel to facilitate the survey at the sacrifice of optimal coupling. If the target is equidimensional, there is no preferred direction for the antennas.

The GPR system is normally either worn and operated by a single operator for high frequency surveys, or is carried and guided by several operators with the controller being either worn or towed. Figure GPR-3 illustrates a 50 MHz RAMAC system in operation with a single operator and Figure GPR-4 illustrates a Pulse Ekko 25 MHz system in winter operations with two operators. The transmitter and receiver electronics are mounted on their respective antennas and linked via fibre optic cables to the controller unit which is either worn on a backpack or carried in a sled mounted hot box. Both radars are controlled by a laptop computer running interface software which

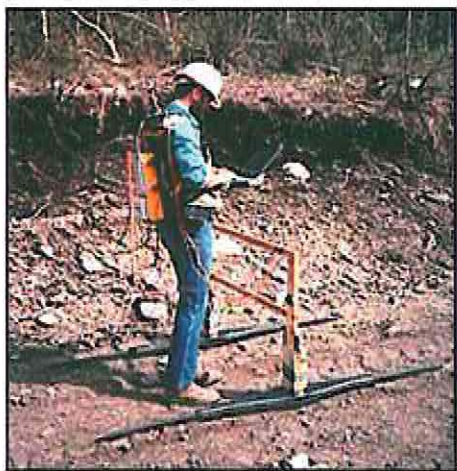


Figure GPR-3. RAMAC GPR operating at 50 MHz



Figure GPR-4. Pulse Ekko 100 GPR with 25 MHz antennas.

c  
o  
n  
f  
i  
g  
u  
r  
e  
s  
t  
e  
s  
y  
s  
t  
e  
m  
a  
n

d stores the collected data.

Annan and Davis (1977) describe overall radar system performance using the radar range equation:

$$Q = 10 \log \left[ \frac{\epsilon_{TX} \epsilon_{RX} G_{TX} G_{RX} v^2 g \sigma e^{-4\alpha r}}{64 \pi^3 f^2 r^2} \right] = 10 \log \left[ \frac{P_{min}}{P_{TX}} \right] \quad (15)$$

where:

- $Q$  - system performance factor or gain in dB
- $\epsilon_{TX}$  - transmitter antenna efficiency
- $\epsilon_{RX}$  - receiver antenna efficiency
- $G_{TX}$  - transmitter antenna gain
- $G_{RX}$  - receiver antenna gain
- $f$  - frequency (Hz)
- $r$  - range to target
- $\alpha$  - attenuation
- $v$  - earth radar velocity

$P_{MIN}$	- minimum detectable signal
$P_{TX}$	- output power from transmitter

This equation can be solved for  $r$  given known system parameters, target type, radar velocity and attenuation. Modern GPR systems have system gains in the range of 140 to 150 dB.

### 3.4 Survey methods

GPR surveys are commonly run in two modes. Profile surveys are the most common survey and are conducted to map subsurface layers and to locate discrete or compact targets within the earth. Velocity surveys are conducted to determine the radar velocity of the earth in the survey area by observing the change in arrival times with antenna separation. The two survey modes are displayed in Figure GPR-5 and are discussed in turn.

Profile surveys are run with the antennas spaced a fixed distance apart and conducted by moving the antenna pair along the survey lines. The data is plotted in radargrams which show the centre of the antennas ( $x$ ) on the horizontal axis and the signal on the  $y$ -axis as a function of time ( $t$ ), with arrival time increasing vertically downward. The reflections appear at various distances below the time zero line at the top of the radargram. These distances below the time zero line are proportional to the arrival times which in turn are roughly proportional to the depth to target. Thus the reflections display a pattern which generally correlates with their subsurface location. During data processing, the arrival times may be converted to depths and the reflections are then displayed at the apparent depths of the sources. Reflections may be displayed as wiggle traces (no fill), variable area traces (as shown) or as variable density colour or grey shade plots.

Velocity surveys are run by expanding the antenna separation and recording the change in the arrival times of the reflections from planar layers in the earth. The common mid-point (CMP) method requires that the antennas each be moved away from a common central point (as shown in Figure GPR-5) whereas the wide angle reflection and refraction (WARR) method requires that one antenna remain fixed while the other moves away from it. In situations where the principle reflectors are extensive and flat lying, either method will serve to derive the velocity structure. The data is plotted in radargrams which show the increase in antenna separation ( $x$ ) on the horizontal axis and the arrival time of the various reflections and refractions ( $t$ ) on the vertical axis with distance increasing from left to right and arrival time increasing from top to bottom in the radargram. A flat lying reflector will display a hyperbolic pattern in the radargram which can be fitted to the equation for normal move out (NMO) from seismic wave theory (Sheriff and Geldart 1995):

$$\frac{v^2 t^2}{4h^2} - \frac{x^2}{4h^2} = 1 \quad (15)$$

where  $h$  is the depth to the reflector,  $t$  is the arrival time,  $v$  is the layer velocity and  $x$  is the antenna separation. This equation can be rearranged yield the following:

$$t^2 = \frac{x^2}{v^2} + t_0^2 \quad (16)$$

where  $t_0$  is the arrival time at zero antenna separation. The slope of  $t^2$  as a function of  $x^2$  yields the inverse of the velocity squared. This method - the  $X^2 - T^2$  method - is used to derive radar velocities from the CMP or WARR radargrams.

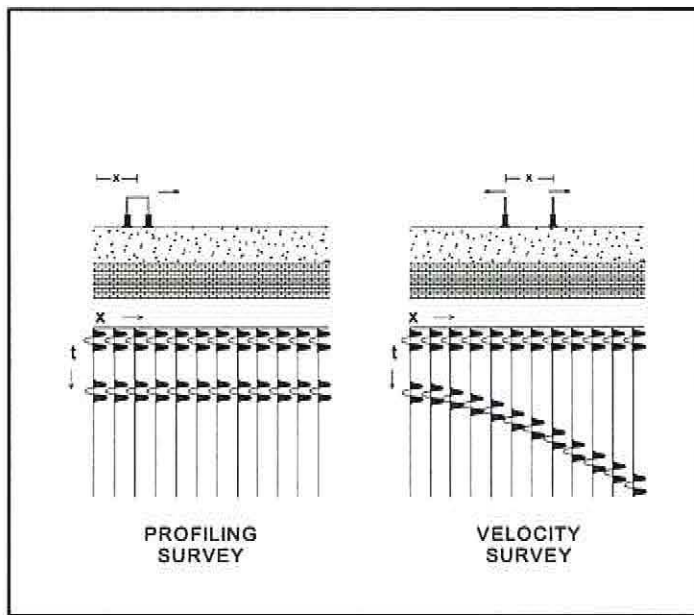


Figure GPR-5. GPR survey modes and corresponding radargrams.

### 3.5 Electrical properties of earth materials at GPR frequencies

The GPR method detects reflections from materials in the earth with contrasting electrical properties. While both electrical conductivity and relative dielectric permittivity affect radar velocity and attenuation, to a first approximation velocity is determined primarily by relative dielectric permittivity and attenuation is determined primarily by conductivity with a not inconsequential contribution from relative dielectric permittivity. The table below, modified after Annan and Davis (1987), summarizes the electrical

properties of materials commonly encountered during GPR surveys:

Material	K	$\sigma$ (mS/m)	v (m/ $\mu$ s)	$\alpha$ (dB/m)
Air	1	0	300	0
Fresh water	80	0.5	33	0.1
Saline water	80	30,000	10	1000
Dry sand	3-5	0.01	150	0.01
Saturated sand	20-30	0.1-1	60	0.03 - 0.3
Limestone	4-8	0.5-2	120	0.4 - 1
Shale	5-15	1-100	90	1-100
Silt	5-30	1-100	70	1-100
Clay	5-40	2 - 1000	60	1-300
Granite	4-6	0.01 - 1	130	0.01
Ice	3-4	0.01	160	0.01

The relative dielectric permittivity and GPR velocity of earth materials is largely controlled by the water content since water is both a strongly polar substance and is very common in the subsurface. Consequently, most GPR interpretation is concerned with the distribution of liquid water in the subsurface as this will exert the strongest influence on both velocity and the source of reflections.

Most earth materials are electrical insulators and electrical conduction occurs primarily within electrolyte solutions and, more rarely, within the few conducting minerals (eg. sulphides or graphite). The presence of water and the concentration of current carrying ions within it thus governs the conductivity of earth materials. McNeill (1980) summarizes the factors controlling electrical conductivity in earth materials:

- Porosity - if water filled
- Permeability - facilitates current flow in electrolytes
- Ion concentration - fresh water is a virtual insulator whereas saline water is a conductor.
- Saturation - water saturation determines the ability of a substance to carry electrical current.
- Temperature and phase of the electrolyte

Permafrost generally improves radar performance by suppressing attenuation due to liquid water. Bound water within clays however can persist well below 0° C and both attenuation due to conduction and surprising reflections can be found in overburden at temperatures down to -30° C. An example of this are clay rich saprolites in the Klondike district of the Yukon which are good reflectors within thoroughly frozen permafrost sections.

### 3.6 Response of discrete targets

Pipes, barrels and other compact 2D or 3D targets produce parabolas in GPR sections. This is caused by the target acting as almost a point source for reflections and by radar energy reflecting laterally off the target as the profiling antennas approach the target. The general signature consists of a symmetric hyperbolic response with an apex directly beneath the target.

Zeng and McMechan (1997) examined the GPR response of buried pipes and tanks in detail. A non-conductive barrel or tank may produce hyperbolas from both the top and bottom of the tank and, in some cases, at the fill line of any liquids. Tanks or barrels made of conductive material will only show a hyperbola originating from the top of the tank. Figure GPR-6 illustrates the general type of anomaly associated with a pipe, barrel or tank where the object is constructed of a non-conducting material which permits the GPR radiation to penetrate the target.

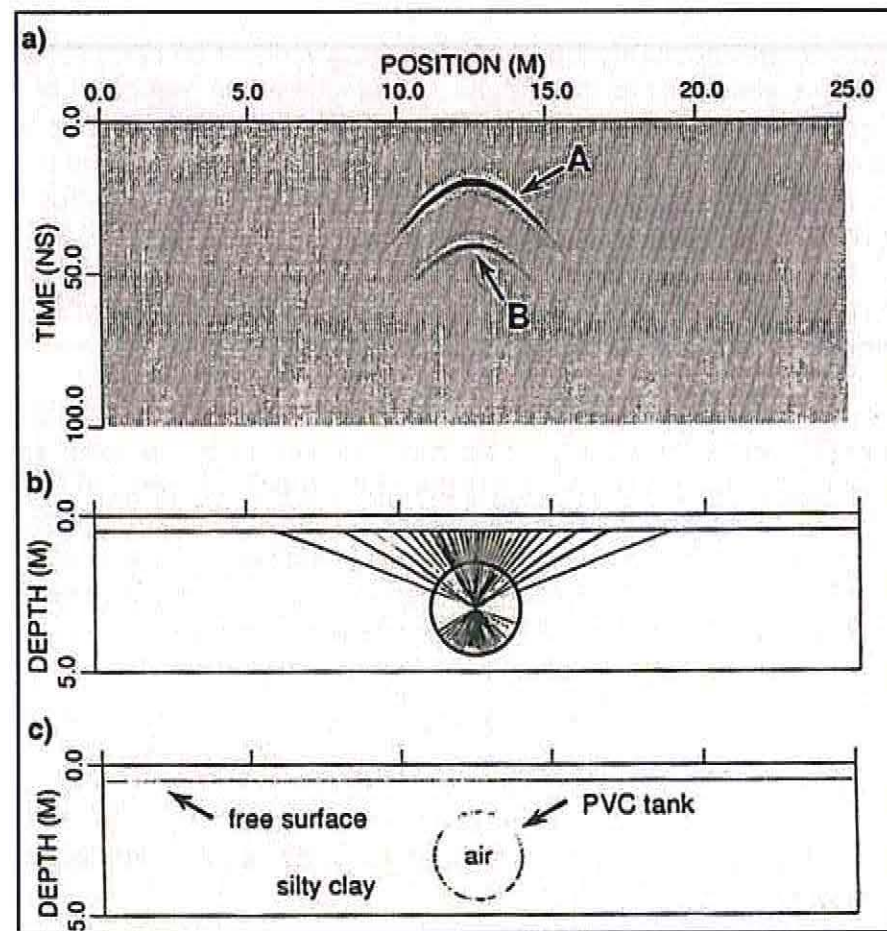


Figure GPR-6. GPR response of tanks, pipes and barrels. (a) Radargram showing reflection from top and bottom of target (b) Raypaths (c) Model. (Zeng and McMechan (1997)).

## 4.0 SEISMIC REFRACTION METHOD - THEORY OF OPERATION

The theory behind the seismic refraction method is summarized in Sheriff and Geldart (1995) and Telford *et. al.* (1990). This section summarizes the basic theory underlying the seismic refraction method and describes the methods used to interpret the data.

### 4.1 Basic theory

Seismic waves are mechanical perturbations, transmitted by compressing or shearing a medium as the wave passes through it. The elastic strain response of a solid body to stress is governed by Lame's Constants  $\lambda$  and  $\mu$ .  $\lambda$  is the strain response perpendicular to applied compressional force and is termed the *fluid incompressibility*. In effect it is the amount of elastic "lateral bulge" per unit volume when a mass is compressed.  $\mu$  is the *shear modulus* or resistance to shearing that the medium possess. Any solid or semi-solid has a measurable shear modulus; a liquid does not as it cannot store elastic energy when sheared. The shear modulus of a rigid rock would be high whereas that of compacted clay would be small.

Seismic wave propagate through a medium in one of two ways, shown in Figure RS-1 (a). Straightforward compression of the medium, similar to the generation of a sound wave, is termed a P-wave because it is the primary or first arrival in an earthquake or seismic record. A second wave is generated in response to stress transverse to the propagation direction of the seismic wave; this is similar to the wave on a string and is termed the S-wave as it is the secondary arrival in the seismic wave train recorded in an earthquake record. The velocity of the P-wave is governed by:

$$V_p = \sqrt{\frac{\lambda + 2\mu}{\rho}} \quad (1)$$

where  $\rho$  is the density of the rock and the other variables are defined as above. The S-wave velocity is:

$$V_s = \sqrt{\frac{\mu}{\rho}} \quad (2)$$

In water or air, the P-wave velocity reduces to:

$$V_p = \sqrt{\frac{\lambda}{\rho}} \quad (3)$$

Seismic refraction methods rely upon measuring and analyzing the first P-wave arrivals. It is apparent from the above relations that the velocity of a seismic wave decreases with increasing rock density but in practice, the increase in  $\lambda$  or  $\mu$  is much greater as density increases and consequently, seismic velocity tends to increase with density. The range of P-wave velocities commonly encountered in placer seismic refraction work is summarized in Table II. P-waves are the fastest and strongest waves measured by conventional seismic instruments and the remainder of this discussion will focus exclusively on their properties.

Seismic waves radiate away from a point source in all directions creating spherical wave fronts traveling through the medium. Huygen's Principle states that any point on a wave front is a point source for succeeding waves. The interference of these waves at any later time defines the new position of the moving wave front. It is useful to simplify a consideration of seismic wave motion by examining a ray path rather than the whole wave. Both the ray and wave obey the same physical laws but they are easier to visualize if the raypath is considered first. The wave front is nothing more than the sum of the possible ray paths.

Seismic waves are both reflected and refracted at the boundary between media with different seismic velocities. As shown in Figure RS-1(b), a portion of the seismic energy will reflect back towards the source and the residual will be transmitted through the boundary and be refracted upon entry into the second medium. For reflection, the angle of incidence - the angle between the incident ray and a normal to the reflecting surface - equals the angle of reflection. Refraction is governed by Snell's Law:

$$\frac{\sin \theta_i}{v_i} = \frac{\sin \theta_f}{v_f} \quad (4)$$

If the velocity in the lower medium is faster than that of the upper medium  $v_f > v_i$  and the ray will bend towards the velocity boundary. If the velocity in the lower medium is slower than that of the upper medium  $v_f < v_i$  and the ray will bend away from the velocity boundary.

**Table II. P-wave velocities of common rocks and sediments**  
 (after Sheriff and Geldart (1995))

Material	P-wave velocity (m/s)
Air	330
Water	1550
Gravel or sand (water saturated)	1500 - 1900
Gravel or sand (dry)	500 - 1500
Ice or permafrost	3500
Granite	4000 - 5500
Gabbro	5000 - 7000
Shale or schist	2000 - 5000

## 4.2 Seismic refraction surveys

Seismic survey methods involve placing vertical component microphones (geophones) with centre frequencies in the order of 10 Hz to 100 Hz in the ground and recording the arrivals of seismic waves after applying a shock to the ground using an energy source. For placer work, energy sources consist of small explosive charges at surface, 12 gauge shotgun slugs, rifle bullets, dropped weights or sledge hammer blows. The geophones are uniformly spaced at from 2 to 5 m depending upon the resolution required and are strung in line down the seismic survey line. In placer exploration surveys, the seismic lines are cut so as to cross the long axis of the stream bed and the geophone array is thus run across the stream channel to yield a profile of the stream channel once the data is interpreted. A trigger is connected from the energy source or its initiator back to the seismograph to start the seismograph when the energy is released. The trigger can be a switch which is momentarily opened and closed (hammer switch), a pulse from a blasting box or the simple breaking of a circuit if a wire is wrapped around explosives.

The seismic energy travels through the earth via a number of paths. In Figure RS-2(a) we consider the simple case of flat bedrock beneath overburden. A direct wave travels from the energy source directly through the low velocity near surface material. Near the energy source, this is the first wave to arrive. At greater distances, refracted waves are

the first arrivals.

At a distance from the source termed the critical distance, the angle of refraction becomes  $90^{\circ}$  and the refracted energy travels along the bedrock interface, generating upward traveling return waves as it skims along bedrock. The refracted wave will travel along bedrock at the faster velocity of bedrock and at a distance termed the cross-over distance, the first wave to reach the geophone will be the refracted rather than the direct wave. The refracted waves which travel into the lower medium in turn may be critically refracted along higher velocity boundaries in bedrock and also return to the surface although they will be refracted at the bedrock boundary on their return journey.

Seismic refraction data is collected by putting energy into the ground at a number of "shot points" while keeping the geophone array fixed. It is fairly common practice in seismic refraction work to take 5 shots: 2 at a considerable distance from either end of the geophone array, 2 at either end of the geophone array and 1 in the middle of the array. The shot pattern is sketched in Figure RS-2(b). Following or prior to the survey it is important to survey in the relative elevations of the geophones and the shot points in order to correct the data for surface elevation changes. If not corrected, these will appear as bedrock topography in the final interpreted section.

Seismic refraction data is processed and plotted in a very simple manner. The shot record or seismogram from each shot is examined to determine when the first energy was received at each geophone. This first deflection (first break) is timed and plotted in a graph of arrival time (vertically) versus distance (horizontally) (Figure RS-2(c)). The break in slope along the T-X curve indicates the cross over distance where the refracted energy overtook the direct wave energy to become the first arrival. Knowing the geometry of the geophone array and shot point, it is possible to analyze the graph and determine the velocity of the gravel and bedrock and from that, determine the depth to bedrock. In the simple case of a flat bedrock surface and overburden with a single velocity ( $V_1$ ) slower than bedrock ( $V_2$ ), the velocities of the bedrock and overburden are the reciprocals of the slopes of the lines along the refracted and direct wave arrivals respectively. The equation of the line connecting the refracted arrivals is:

$$t = \frac{x}{v_2} + t_i \quad (5)$$

where  $t_i$  is the intercept time and  $x$  is the distance from the energy source. The velocities of the overburden and bedrock can be used to determine the critical angle:

$$\theta_c = \arcsin \frac{v_1}{v_2} \quad (6)$$

and this angle can be used to calculate the depth to bedrock from the known velocities and the intercept time:

$$z = \frac{v_1 t_i}{2 \cos \theta_c} \quad (7)$$

This method works only on the very simplest case of flat bedrock beneath homogeneous overburden. Seismic refraction interpretation methods must account for several velocity layers (eg. dry overburden, wet overburden, bedrock) and be able to map irregular boundaries. A following section describes delay time methods commonly used to deal with these circumstances.

#### 4.3 Sources of error

Seismic refraction surveys are prone to several sources of error. The first class of problems are directly related to acquisition and the second are violations of the underlying assumptions behind the interpretation methods.

Sources of error in acquisition include poor elevation surveys, timing errors (either shot or geophone), static errors and phase shifts. The requirement for elevation surveys was discussed above. Small near surface elevation errors can translate into large bedrock topography errors because the near surface velocity is very slow - commonly 1/4 to 1/3 that of the underlying overburden. Thus a one metre error in near surface elevation can translate into a 3 or 4 metre error in bedrock elevation.

Timing errors occur if there is a delay in initiating an energy source (eg. slow cap) or if a phone is not properly planted or the first arrival properly identified. A shot timing error affects all the arrivals from the shot and is sometimes difficult to identify or discriminate from a geological feature. A timing error for an individual geophone is generally more easily spotted and corrected.

Sometimes a geophone is planted in particularly slow ground (eg. squirrel's nest or duff) and all the arrival times recorded at that geophone from every shot appear to be slow. These errors are termed static errors and are often visible in the T-X curve when the arrival at a phone is "pulled up" on every T-X curve.

The final source of error is phase shift or change in shape of the first arriving energy. The strength and shape of the first arrival will change with offset distance from the source as different waves at different angles of incidence are recorded as first arrivals at each geophone. A common error, particularly with a weak energy source, is to lose a first arrival train and start picking second or third arrivals which are much clearer and coherent, lower down in the seismic record. These errors, if not detected, can result in calculated bedrock depths which are too great and topography which is in error.

The second class of errors directly affects the interpretation method. The seismic refraction method, properly employed and interpreted, will yield depth determinations accurate to within  $\pm 10\%$  provided the following underlying assumptions are valid:

- a. The earth consists of several layers with relatively uniform velocity.
- b. The velocity of each layer is lower than the velocity of the layer beneath it.
- c. The layer boundaries are relatively smooth and continuous.
- d. The layers are thick enough to be resolved by the geophone array being used.

The validity of these assumptions determines the accuracy of the bedrock profile derived from the refraction data. If the velocity of the overburden varies dramatically along a seismic line over a distance equal to or less than a spread length, the interpretation will yield a bedrock surface with relief introduced solely by the varying overburden velocity (Figure SR-3(a)).

If the overburden contains a low velocity layer, then the refracted wave will bend downwards and there will be no indication of this refraction in the travel time curve (Figure SR-3(b)). Instead, the seismic velocity of the overburden will be over-estimated and the depths to bedrock will be too deep. This situation - termed a velocity inversion - is common in areas with discontinuous permafrost where thawed ground may occur below faster frozen ground and bedrock. This is the principle reason seismic refraction surveys are not recommended in areas affected by discontinuous permafrost.

A third problem occurs if there is a thin, high velocity layer which is too thin to produce a discernable response in the travel time curve. The seismic velocity of the overburden will be underestimated and the calculated depth to bedrock will be too shallow. This situation could be caused by a thin bed of frozen ground in otherwise thawed overburden. It is normally the least significant of the three problems.

#### **4.4 Refraction interpretation methods**

The simple depth determination method outlined in Section 4.2 is suitable only for a very preliminary field approximation of depth. Increasingly complex calculations are required to deal with multiple planar refractors and with refractors of varying dip. It is worthwhile to consider qualitatively several aspects of refractor responses visible in the T-X curves.

Figure SR-4(a) shows the response from a single dipping refractor measured with a single spread and two shots at either end. The portions of the travel time curves from

the uppermost layers have the same slope ( $1/V_1$ ) while the slopes of the T-X curves from the refractors differ. The shot placed on the down-dip side of the refractor (ie. shooting up dip) has a faster apparent velocity ( $1/V_u$ ) than the down-dip apparent velocity ( $1/V_d$ ). The average of the two velocities is a close approximation to the true refractor velocity.

So far, this summary has been confined to the refraction response of planar refractors. Figure SR-4(b) illustrates the effect of an irregular refractor on the T-X curves. If the refractor contains either a depression or rise, indications of these will appear in mirror images on the T-X curve. A depression will increase the travel time in the vicinity of the low and a high will decrease the travel time in the area of a high. It is useful to qualitatively identify possible refractor relief in order to assess the results of more formal automated interpretation.

The data described in this report was interpreted using a computerized delay time method. The theory behind this method is summarized in Telford et. al. (1990), Sheriff and Geldart (1995) and Scott (1973). The delay time is defined with reference to Figure SR-4(c), considering the simplest possible case. For a shot at point A and a geophone at D, the total travel time includes the time to cover sections AB, BC and CD. Now suppose that the shot point and geophone were moved vertically down to the first refractor and shot from there. The travel time along EF would be much faster, traveling with velocity  $V_2$  along the refractor. The delay time is the difference between the travel time along ABCD less the travel time along EF. Since the transit time along BC is common, the delay time can be calculated from:

$$\delta = \left( \frac{AB}{V_1} - \frac{EB}{V_2} \right) + \left( \frac{CD}{V_1} - \frac{CF}{V_2} \right) = \delta_s + \delta_g \quad (8)$$

where  $\delta_s$  and  $\delta_g$  are the shot and geophone delay times respectively. For a horizontal to shallow dipping refractor, the horizontal distance between the shot and geophone (AD) is the same as EF. The velocities  $V_1$  and  $V_2$  can be determined from the reciprocals of the slopes of the T-X curves. Thus it is easy to calculate the delay time as this will be the observed travel time less the calculated travel time along the refractor:

$$\delta = t_{AD} - \frac{EF}{V_2} \quad (9)$$

The shot delay time can be calculated for any shot if two or more geophones recorded the shot. Similarly, the geophone delay time at any phone can be calculated if two or shots are recorded at the geophone. Thus it is easy to solve for the shot and phone delay times for any reversed spread (ie. a spread where shots are fired from either side

of the geophone.

Scott (1973) describes a computerized application of delay time analysis to seismic refraction data. This method has been repackaged for commercial use as the Rimrock Geophysics SIP (seismic interpretation program) software package and was used to invert the data collected during this project. The basic steps in the algorithm are:

1. Operator assigns layers to various segments of the refractor T-X curve (ie. identify the number of velocity layers and which portions of the travel time curve are from each segment.)
2. Analyze each segment using least-squares analysis to determine a best-fit velocity.
3. Correct geophone arrival times and shot times for local static errors and for elevation above a datum within the top layer. This correction is applied using the calculated upper layer velocity (V1).
4. For the first refractor, calculate total delay times for each shot and calculate individual shot point and geophone delay times. From these, calculate the position of the points where the rays intercept the first refractor (ie. shot entry points and geophone exit points). Average points to determine the mean position of the refractor.
5. Verify the refractor location by ray tracing each shot from the shot point to the geophones. Adjust the position of the refractor by moving the shot entry and geophone exit points iteratively where necessary to optimize the fit.
6. Strip away the delay times and reposition the shots and geophones on the next refractor.
7. Repeat steps 4 through 6 for the second and subsequent refractors until all the layers identified by the operator in step 1 have been processed and a solution for their location determined.

It is critical to the inversion that the interpreter accurately determine the number of layers apparent in the T-X curves. It is possible to derive an apparently good solution to the interpretation problem which is completely incorrect if a layer is missed. The common sources of error in this process are irregular refractors which are misinterpreted as indicating extra layers. Alternatively, two layers may be grouped together and identified as being a single refractor with a depression in it. A knowledge of the local geology is essential in discriminating between the various possible scenarios.

The results of the inversion show the locations of the calculated ray entry and exit points. In a good solution, these tend to be clustered about the mean refractor location; in a poor solution these are scattered. An additional check on accuracy is to compare the overburden velocities for adjacent spreads; in most areas these should not vary significantly.

## 5.0 PERSONNEL AND EQUIPMENT

The geophysical surveys were performed by the following personnel:

Mike Power, M.Sc. P.Geoph.	Crew chief
Dave Hildes, Ph.D.	Geophysicist
Raanan Bodzin, M.Sc.	Technician
Gary Lee, P.Eng.	Technician

The crew was equipped with the following instruments and equipment:

Seismograph: Geometrics Strataview R-48 digital engineering seismograph (s/n 75162)

Seismic equipment:

- 1 - 24 channel cable w/ 10 m takeouts
- 1 - Bison HVB-1 high voltage seismic blaster / trigger
- 29 - Mark Products 40Hz vertical component geophones
- 2 - Type 6 explosives magazines
- 1 - Impulse laser range finder / digital clinometer & level
- 1 - Blasting wire, spool & winder
- 4 - VHF radios & chargers

- GPR system:
- 1 - RAMAC GPR (s/n 4679) w/  
controller, Tx and Rx consoles
  - 1 - 50 MHz dipole antenna assembly
  - 1 - 25 MHz dipole antenna assembly
  - 1 - 50 MHz rough terrain antenna (s/n  
12095)
  - 1 - Hip chain trigger
  - 1 - External monitor / computer  
controller
  - 1 - Li ion battery packs, chargers
  - 1 - Reflex processing and  
interpretation software package
- Other:
- 2 - 1.8 Ghz laptop computers
  - 1 - Trimble Geoexplorer I differential  
GPS receiver
  - 1 - 1Ton 4x4 GMC truck
  - 1 - Electronic and general repair tools

Instrument specifications are contained in Appendix B.

## 6.0 SURVEY SPECIFICATIONS

The seismic refraction survey was conducted according to the following general specifications:

- Channels: 24
- Receiver spacing: 5 m
- Receivers: single phone at each receiver station
- Sampling: 0.250 ms
- Record length: 256 ms
- Pre-acquisition filters: 500 Hz high cut

<u>Channels:</u>	24
<u>Storage format:</u>	SEG-Y digital file & paper shot record copy.
<u>Shot spacing:</u>	<p>2 - 120 m off either end of the receiver array</p> <p>2 - 5 m off either end of the receiver array</p> <p>1 - mid-spread, offset 5 m left or right of line to clear the cable</p>
<u>Energy source:</u>	High explosives (Dyno-Nobel Powerfrac™) initiated with StaticMaster seismic detonators. Single blast at each shot point with charges on surface / no mud-capping. Charges varied from 5 sticks (centre spread) to 25 sticks (offset shots)
<u>Topography:</u>	As provided by YES or surveyed with laser range finder, supplemented by DGPS receiver

The GPR survey was conducted according to the following specifications:

<u>Centre Frequency:</u>	50 MHz and 25 MHz
<u>Station spacing:</u>	20 cm
<u>Time window:</u>	700 ns after groundwave first arrival
<u>Sampling interval:</u>	1.25 ns per sample
<u>Antenna separation:</u>	2.0 m (4.0 m - 25 MHz) maintained using a rope between antenna pullers
<u>Triggering:</u>	Automated chainbox (Hipchain)

**Station registration:**

The apparent horizontal distance at which each surveyed control line picket was encountered was recorded manually and used in the data processing to register the lines.

Where no data was provided by Yukon Engineering Services, the survey lines were registered to geographic coordinates by taking differential GPS position measurements at control pickets and by calculating the location of intermediate stations using linear interpolation. The differential GPS measurements consisted of 120 repeated measurements taking at 1 second intervals and corrected using base station data from the Geodetic Survey of Canada GPS observation station in Whitehorse, Yukon. This station cycles using a 30 s reading epoch. The final station position is the average of all corrected positions recorded for that site. Estimated position accuracy using this procedure at this range is approximately  $\pm 1$  m.

Along the seismic lines, differential GPS measurements were taken at stations 40 to 60 m apart and the intervening stations were surveyed in using the laser rangefinder. This instrument provides both horizontal and vertical distance information.

## 7.0 GPR DATA PROCESSING

The GPR data was processed with the Gradix software package developed by Interpex Ltd. using the following procedures in the order they are described:

1. *Geometric corrections:* Radargrams were registered to grid coordinates by interpolating the true horizontal and vertical distances for each trace using the surveyed location of the control pickets and the apparent distances of each trace from these reference pickets. The coordinates shown on the top of each radargram are the horizontal distance in metres from the start of the profile line.
2. *Trace kills.* Bad traces caused by toppling antennas or by riding over brush or snow were deleted.
3. *Drift correction:* The radar records data from a time zero set about 20 ns before the first energy arrival in the ground wave. The arrival time of the ground wave may vary across the length of the radargram due to instrument drift and to changes in the velocity of the ground wave. The drift correction aligns all traces to a common datum based on the arrival of the first radar wave energy. The method employed selects the sample with the greatest positive amplitude on each trace within a small window. Each trace is time shifted so that the samples with maximum amplitude occur at the same time. For the 50 MHz data, the search time window was 0-22 ns; for the 25 MHz data, the search time window

was 0-33 ns. On some radargrams where the first trough was more regular than the first peak, the search was conducted for the sample with the greatest negative amplitude.

4. *Set time zero:* After drift correction, the time zero line on the radargrams was reset to the first arrival of the ground wave. This generally involved a time shift of 15 to 20 ns.

5. *Dewow:* Low frequency antenna-to-antenna reverberations were removed by examining the frequency spectra from a representative set of 10 traces and applying a low cut filter to remove frequencies below the first trough in the average frequency spectrum calculated from the representative traces. The first trough commonly represents the upper cutoff frequency of low frequency wow.

6. *F-k filtering.* Some 25 MHz radargrams were F-k filtered to remove dipping arrivals which appeared to be lateral diffractions from above ground objects (eg. road embankment, pipes, trees). This was only necessary at the Old Faro Creek site.

7. *Gain.* Applied time varying and trace balancing gain to boost signal in the reflection window and to balance trace amplitudes across the sections.

8. *Deconvolution.* Spiking deconvolution was applied on some traces at 25 MHz using a 0 - 400 ns autocorrelation window and a 60 ns operator length.

9. *Bandpass filtering.* A trapezoidal bandpass filter with low truncation, low cutoff, high cutoff and high truncation of 0, 2, 20 and 60 MHz was applied to some 25 MHz data. This attenuated high frequency diffractions and reflections from lateral above ground objects.

10. *Velocity analysis.* GPR velocity was estimated by interactively fitting velocity hyperbolas to complete or partial diffraction hyperbolas. The average of the velocities derived from fitting the diffraction hyperbolas was used as the single constant velocity in the depth conversion.

11. *Interpretation:* At this stage, anomalies which may be caused by subsurface debris or contaminants were identified and annotated on the radargrams.

12. *Printing and annotation:* Radargrams were converted to jpeg files and annotated.

## 8.0 RESULTS

The following products are appended to this report in the back pockets:

SITE	SURVEY	FIGURES
Vangorda Creek	GPR	R-1. Line GPR-1 50 MHz radargram
		R-2. Line GPR-1 25 MHz radargram
Grum Pit	GPR	R-3. Line GPR-2 25 MHz radargram
		R-4. Line GPR-2 50 MHz radargram
	Seismic	R-5. Line GPR-3 25 MHz radargram
		R-6. Line GPR-3 50 MHz radargram
Vangorda Pit	GPR	E-1. Line SL-1 - Elevation section
		R-7. Line GPR-4 25 MHz radargram
	Seismic	R-8. Line GPR-4 50 MHz radargram
		R-9. Line GPR-5 25 MHz radargram
	Seismic	R-10. Line GPR-5 50 MHz radargram
		E-2. Line SL-2 - Elevation section
North Fork - Rose Creek (Rock Dump)	Seismic	E-3. Line SL-3 - Elevation section
Old Faro Creek	GPR	R-11. Line GPR-6 25 MHz radargram
		R-12. Line GPR-6 50 MHz radargram

In addition, a CD-ROM is included in the back pocket of this report. The CD contains the following data, organized by site unless otherwise specified:

DATA	SPECIFICATIONS
------	----------------

Topographic survey - line & station locations	\Topo data\\Final corrected coordinates of geophysical grid station pickets in UTM coordinates (NAD 27 (Yukon) / Zone 8N projection - Elevations in metres above mean sea level)
Radargrams	\<site>\Radargrams\\Annotated final radargrams in JPEG format.
Seismic elevation sections	\<site>\Elevation sections\\Annotated elevation sections showing layers, velocities and interpretation, corrected for surface elevation in JPEG format
Topography plan	Site topography in AutoCADD LT2000 format with survey lines superimposed.
Digital copy of report	PDF copy of the report text. Some stock theory diagrams not included as PDFs.

The location of survey lines at each site is shown in Figures 1 to 5. Each location plot shows the location of the survey lines with respect to UTM coordinates (NAD 1927 (Yukon) / Zone 8N). Location maps for sites located in areas covered by digital topography are shown with the digital topography as an underlay for additional reference.

The radargrams show the horizontal position along the x-axis and both travel time and apparent depth along the y-axis. The radargrams have been compensated for topography and some are plotted with considerable vertical exaggeration. The reflections are plotted as alternating black (positive) and white (negative) bands. The first arrival - a triplet which is continuous across the section- is the ground wave between the antennas and not a feature of interest. Reference picket locations are shown beneath the reflection section. Each radargram contains a raw reflection section and an interpreted reflection section on which the apparent bedrock reflection is indicated in green. There are linear, sharp, moderately dipping linear arrivals which are likely diffractions from above ground targets adjacent to the antennas. Many of these were timed and found to have a velocity equal to that of air (0.30 m/ns). On most sections there is considerable ringing, particularly in the 25 MHz data. This is manifested by parallel bands of recurring reflections which tend to run across the section and obliterate any weaker reflections arriving in the same time window. The presence of these effects suggest strong attenuation of deep reflections by ohmic losses along the profile line.

The seismic refraction elevation sections show the horizontal position along the x-axis

and elevation in metres above mean sea level along the y-axis. The boundaries between layers with contrasting seismic velocity are shown as black lines and the layers are indicated by varying colours. In general, the shape of the travel time curves dictated that the inversions be performed with three layer models. These models invoked an uppermost layer with a velocity from about 330 to 800 m/s, a deeper layer with a velocity of 1400 to 2000 m/s and a basal layer with a velocity of about 5000 m/s. These three layers correspond to dry material above the water table, to water saturated and compacted overburden, and to fresh bedrock. In each model and elevation section, the lowermost layer is interpreted to be bedrock and the boundary between the lowermost layer and the layer above is the interpreted top of bedrock. The horizontal distance coordinates along the seismic line are also shown in plan view in the corresponding location map for the survey site.

The inversion results from which the elevation sections were constructed are compiled in Appendix C. They summarize the results of the seismic refraction interpretation, containing a listing of arrival times, velocity analysis, travel time curves, depth point compilations, scattergrams and final depth models. The layer boundaries are best-fit curves through a scatter of depth points depicted in the scattergrams and the quality of each inversion and hence the reliability of each depth section can be estimated looking at the dispersion of the depth points about the best fit curves in the scattergrams.

## 8.1 Vangorda Creek

A single GPR profile was surveyed at the Vangorda Creek site. The location of the survey line is shown in Figure 1. The line was surveyed at both 25 MHz and 50 MHz. Very poor reflections were recorded on both profiles and it is difficult to discriminate between bedrock and overburden reflections. There is no continuous bedrock reflection evident in either radargram. The depth conversion was performed with a velocity of 0.12 m/ns, computed from an average of velocities determined by analysis of diffraction hyperbolas.

Figures R-1 and R-2 are radargrams recorded at 50 and 25 MHz respectively. The interpreted bedrock reflection is identified in green in the right hand panel of each section. At 50 MHz (Figure R-1), there are two plausible bedrock reflections in the western end of the section. There is no definitive strong bedrock reflection visible in either section and the reflection identified as the bedrock reflection was selected on the basis of its relationship to events above and below; its limited amplitude standout; and the shape of the reflection.

## 8.2 Grum Pit

Two GPR profile lines and a single seismic reflection survey line were surveyed at the site near the Grum Pit. The location of the survey lines are shown in Figure 2. Seismic

refraction line SL-1 is coincident with Line GPR-2 and both sections are plotted in the same direction (ie. looking north).

Line GPR-2 was surveyed at both 25 MHz and 50 MHz and the results are shown in Figures R-3 and R-4 . Very poor reflections were recorded and it is difficult to determine which are bedrock and which are from overburden. There is no continuous bedrock reflection evident in either radargram. The depth conversion was performed with a velocity of 0.12 m/ns, computed from an average of velocities determined from analyses of diffraction hyperbolas. Several reflections in the 50 MHz radargrams which might be caused by bedrock are identified in green.

Line SL-1 was surveyed in three spreads from west to east and is coincident with Line GPR-2. The velocities of layers 1 and 3 (uppermost and lowermost layers) were unconstrained but the velocity of the middle layer was constrained to 2000 m/s. The inversion scattergrams suggest error in depth determinations of the lowermost layer in the order of 2 to 3 m. The elevation section along Line SL-1 is shown in Figure E-1. The lower layer with a velocity of 5200 m/s is interpreted to be fresh bedrock. This velocity is consistent with those recorded on other lines on the property. The second layer, interpreted to be compacted, water saturated till, has a high seismic velocity and may, in part, include weathered bedrock.

Line GPR-3 was surveyed at both 25 MHz and 50 MHz and the results are shown in Figures R-5 and R-6. The depth conversion was performed using an average section velocity of 0.85 m/ns, determined by averaging the results of hyperbolic diffraction curve analyses. No deconvolution or bandpass filtering was performed on these sections. The 25 MHz profile shows ringing also seen at the Vangorda Creek site and the 50 MHz profile appears to contain the best reflection section. A series of reflections at 8 to 12 m depths have characteristics associated with bedrock reflections. In particular, diffraction hyperbolas are rooted in these reflections; the reflections truncate both overlying and underlying reflections; and these reflections are characterized by a slight amplitude standout. The reflection between registration points 3-2 and 3-4 most clearly exemplifies these properties.

The lack of any drill hole data and the absence of any correlation between the GPR and seismic refraction results along Lines SL-1 / GPR-2 complicate the interpretation. On Lines SL-1 and GPR-2, there is no correlation between the radar reflections and the seismic refraction results. The best radar response is at 50 MHz (Figure R-4) and reflections in the interval from P20 to P30 are at a depth of about 6 m. The seismic refraction results suggest that the depth to bedrock in this interval is in the range of 15 m. Consequently, it would appear that the discontinuous reflections in the radar profiles along Line GPR-2 are from overburden layers. On Line GPR-3, stronger reflections with characteristics suggesting bedrock origin are present at depths of 8 to 12 m. The depth to bedrock indicated by the seismic survey along Line SL-1 ranges from 9 to 18 m

and thus the radar reflections are within a depth range similar to that indicated by the seismic survey.

### 8.3 Vangorda Pit

Two GPR profile lines and a single seismic reflection survey line were surveyed at the site near the Vangorda Pit. The location of the survey lines are shown in Figure 3. Lines GPR-5 and SL-2 are coincident and the profiles for both data sets are projected from north to south (ie. looking east).

Line GPR-4 was surveyed at both 25 and 50 MHz and the results are shown in Figures R-7 and R-8. The polarity of the 50 MHz data was reversed to accommodate an apparent reversal in antenna orientation relative to the 25 MHz survey. Velocity analyses of hyperbolic diffractions indicated overburden velocities ranging from 0.85 to 0.13 m/ns and an average of 0.11 m/ns was used in the depth conversion. The 25 MHz data shows ringing similar to that seen in the profiles at Vangorda Creek and the Grum Pit while the 50 MHz data shows few deep reflections. In both sections, there are west-plunging reflections at depths of 8 to 14 m near reference station P 4-9. In the 25 MHz data there is a very weak, discontinuous, low frequency reflection which extends across the section from the east end to reference station P 4-4 in the west. This reflection is interpreted to be the bedrock reflection based on the presence of rooted diffraction hyperbolas, amplitude standout, and the relationship between this reflection and those above and below it. At reference station 5-55, which is the intersection with Line GPR-5 and SL-2, the indicated depth to the bedrock reflection is approximately 20 m.

Line GPR-5 was surveyed at both 25 and 50 MHz and the results are shown in Figures R-9 and R-10. The polarity of the 50 MHz data was reversed to accommodate an apparent reversal in antenna orientation relative to the 25 MHz survey. The data was bandpass filtered using a 12-25-75-100 MHz trapezoid for the 25 MHz data and 2-12-78-35 MHz trapezoid for the 50 MHz data. An average velocity of 0.12 m/ns was used in the depth conversion. In general, the radar signal was screened at depths greater than 10 - 15 m but there are a few weak reflections at greater depths. Deeper reflections which could be caused by bedrock are identified in green. The 50 MHz data appears to have imaged the shallower bedrock reflections on the north end of the line.

The seismic reflection survey was conducted on Line SL-2, coincident with Line GPR-5. The velocities of the upper and lowermost layers were unconstrained in the inversion while the overburden velocity was constrained to 2000 m/s. The inversion scattergrams suggest errors in the depth determination in the order of  $\pm$  3 m with the worst scatter being in the intervals from 115 - 230 and 350 - 470. As in profile SL-1, the three layers present appear to be unconsolidated, dry overburden (Layer 1), compacted overburden

below the water table (Layer 2) and bedrock (Layer 3). The Layer 3 velocity is within the range expected for bedrock in this area. Apparent depths to bedrock range from 6 to 25 m and the overall profile suggests that bedrock topography is not reflected in the surface topography over the rise in the centre of the line.

The GPR response on Line GPR-4 was significantly better than that along the cross-line, Line GPR-5. The reflection identified as the bedrock reflection on Line GPR-4 is at a depth of approximately 20 m and the depth to bedrock at this point on the orthogonal seismic line SL-2 is 21.4 m. This concurrence between the GPR indicated depth to bedrock on Line GPR-4 and the seismic indicated depth to bedrock on the cross-cutting seismic line is reassuring in this case where there is no subsurface information with which to constrain geophysical interpretation.

#### 8.4 North Fork of Rose Creek (Rock Dump)

A single deviated refraction seismic line was surveyed at the North Fork of Rose Creek or Rock Dump site. The line location is shown in Figure 4. The line consisted of three separate 115 m spreads, numbered sequentially from east to west. Line inflections occur at each spread boundary. Offset shots were placed in-line with each spread (ie. off in the bush and not along the adjacent spreads) and shot locations were surveyed in relative to the last phones on the spread. All spreads overlapped the adjacent spread (s) by one phone.

The final elevation section is plotted in Figure E-3. All inversion velocities were unconstrained and were calculated using the identified first arrivals. The three spreads were inverted separately on account of the crooked line geometry. The data in each case best fit a three layer model and the velocities used in the inversions are summarized below:

Spread	$V_1$ (m/s)	$V_2$ (m/s)	$V_3$ (m/s)
1	597	1562	3075
2	354	1500	3637
3	564	1562	4281

The uppermost layer ( $V_1$ ) has a velocity expected of dry, relatively unconsolidated material. The middle layer velocity is in the range expected for water saturated overburden. The velocity of the lowermost layer is in the range expected for bedrock in this area on Spread 3; it is anomalously slow on the other two spreads, particularly on Spread 1. The boundary between layers 2 and 3 (the lowermost boundary in each model) is tentatively interpreted to be bedrock. The scatter in depth points about the

best-fit layer boundary can be taken as a qualitative indication of the quality of goodness-of-fit in the final solution. It is an inevitable feature of the inversion process that the scatter of points below lower boundaries is substantially greater than the scatter of points about the upper layer boundaries.

The mis-tie between the spreads is important in assessing the validity of the final solutions because the spreads were inverted separately. The mis-tie in elevation between Spreads 1 and 2 at Station 24 is 3.0 m and the mis-tie between Spreads 2 and 3 at Station 47 is 4.6 m. Seismic refraction surveys are typically accurate to  $\pm 10\%$ ; consequently the difference between the two end-points could be as much as 20% of the total depth. Given the average depth of 20 to 30 m, a maximum discrepancy of 4 to 6 m could be anticipated. Consequently, the mis-ties, while larger than hoped, are within the bounds of expected error. The apparent bedrock scarp at 235 m and the change in elevation of the low velocity layer at 115 m are likely inversion artifacts.

## 8.5 Old Faro Creek

A single GPR profile line was surveyed at Old Faro Creek (Line GPR-6). The location of this line is shown in Figure 5.

Line GPR-6 was surveyed at both 25 and 50 MHz and the results are shown in Figures R-11 and R-12 respectively. F-k filtering, spiking deconvolution and bandpass filtering were applied to the 25 MHz data. A velocity of 0.100 m/ns, derived from the analysis of diffraction hyperbolas was used in the depth conversion. The Old Faro Creek site has a section consisting of fine grained, conductive tailings overlying glacial till on fresh bedrock. Drill indicated depths to bedrock in two holes at 90 m and 100 m along the survey line are approximately 12 m. Only the 25 MHz radiation effectively penetrated the section and it appears that there is a discontinuous bedrock reflection in this data set. The two drill holes are shown in orange and the apparent bedrock reflection is shown in green in Figure R-11.

## 8.6 General notes

The results of the geophysical surveys cannot be properly evaluated without drill testing. The seismic data, while generally of good quality, was difficult to interpret at two sites because of the very high apparent second layer velocities. In part, the second layer may contain decomposed bedrock or even fresh phyllite (Grum Pit lines).

The GPR survey failed to elicit strong bedrock reflections at any site. In part, the GPR signal appears to be attenuated by scattering as there are abundant diffraction events in the 50 MHz data. This cannot be the entire cause of signal loss however as the 25 MHz data contains far less diffraction events and yet still does not contain strong bedrock reflections. At some sites, the persistent ringing in the 25 MHz data and absence of

reflections indicates attenuation through ohmic losses. Interference from culverts, pipes and other large metallic objects was a problem only at the Vangorda Pit site.

The rocks at the Faro Mine site may be electrically anisotropic and this has implications for GPR survey design. At Vangorda Creek site, the GPR survey results along an essentially east-west line were poor. At the Vangorda Pit site, the GPR survey along the north-south line produced better results than the survey along the east-west line. Although some good reflections were recorded in a portion of one line at the Grum Pit site, in general the results were poor along the east-west lines. The results at the Old Faro Creek site along a north-south line were good despite the presence of conductive overlying tailings. Surveys for BGC Engineering also elicited similar results; surveys along Rose Creek generated poorer results than those across the creek axis. Foliated rocks can display electrical anisotropy in which electrical conductivity varies with azimuth. The reason for this is the fact that electric currents can more readily be conducted along foliation planes than across them. If the foliation is steeply dipping, electrical anisotropy will be strongly azimuth-dependent. The following table summarizes a comparison of GPR survey results with dominant foliation, based on discussions with Lee Pigage, P.Geo., a Yukon Geological Survey geologist responsible for conducting detailed mapping in the Faro District:

<b>Site</b>	<b>Dominant Foliation</b>	<b>Results</b>
Rose Creek (BGC)	Parallel to Rose Creek	Poor results in line along Rose Creek; good reflections on orthogonal cross lines
Old Faro Creek	250°	Good results on single GPR line perpendicular to foliation
Grum Pit	Foliation subparallel to GPR survey lines	Poor results
Vangorda Pit	0°	Good results on east-west Line GPR-4; poor results on orthogonal Line GPR-5.
Vangorda Creek	Dominant foliation at both 0 and 145°	Poor results; inconclusive relation to foliation because of strike variation and absence of orientation data.

These observations suggest that line orientation should be orthogonal to dominant bedrock foliation where possible. In situations where the dominant foliation cannot be estimated, surveys could be conducted in two directions to ensure that strong bedrock reflections are recorded.

## 9.0 CONCLUSIONS

The results of the geophysical surveys at the Faro Mine site support the following conclusions:

### Vangorda Creek site

- a. No strong reflections apparently originating from bedrock were recorded at this site.

### Grum Pit site

- a. No definitive bedrock reflections were detected in the GPR survey along Line GPR-2. The seismic refraction survey along the coincident line SL-1 detected a high velocity layer which is likely fresh bedrock at depths ranging from 9 to 18 m.
- b. On Line GPR-3, the GPR survey detected reflections possibly originating from bedrock at depths from 8 to 12 m.

### Vangorda Pit site

- c. On Line GPR-4, there is a very weak, discontinuous, low frequency reflection in the 25 MHz data which extends across the section. This reflection occurs at a depth of 6 to 20 m and has a character which suggests that it originates from bedrock.
- d. No definitive bedrock reflections were recorded in the GPR survey along Line GPR-5. The seismic refraction survey along the coincident line SL-2 located a high velocity layer which is likely fresh bedrock at depths ranging from 6 to 25 m.
- e. At the junction between Lines GPR-4 and SL-2, the depth to the seismic high velocity layer interpreted to be bedrock and the depth to the GPR reflection interpreted to originate from bedrock agree within the bounds of measurement error.

### North Fork of Rose Creek site (Rock Dump site)

- f. The seismic refraction survey along Line SL-3 located a high velocity layer likely representing fresh bedrock at a depth of from 22 to 31 m.

### Old Faro Creek

- g. On Line GPR-6, the GPR survey at 25 MHz mapped bedrock at depths ranging from 6 to 12 m. This interpretation is supported by logs from nearby drill holes.

General conclusions

- h. The GPR survey failed to conclusively map bedrock at most sites because of signal attenuation and scattering and the absence of a strong bedrock reflection.
- i. The rocks at the Faro Mine may be electrically anisotropic and GPR surveys may have to be conducted in a preferential direction to elicit strong reflections. It appears that surveys conducted across the strike of foliation generate stronger reflections than those conducted in along the strike of foliation.
- j. Seismic refraction interpretation is complicated by the high velocity of the second layer. This layer may consist of both compacted till and weathered bedrock.

## 10.0 RECOMMENDATIONS

The conclusions of this report support the following recommendations:

- a. The apparent bedrock depths derived from the GPR and seismic refraction interpretation should be drill tested at selected locations to verify and refine the interpretations
- b. Where possible, GPR surveys should be run across the strike of dominant foliation or, in areas with no subsurface control, surveys should be run in two orthogonal directions.

Respectfully submitted,  
**AURORA GEOSCIENCES LTD.**

Mike Power, M.Sc., P.Geoph.  
Geophysicist

## REFERENCES CITED

- Annan, A.P. and J. L. Davis (1977) Radar range analysis for geological materials. Geological Survey of Canada Paper 77-1B, pp. 117-122.
- Annan, A.P. and S.W. Cosway (1991). Ground penetrating radar survey design. Paper presented at the 53<sup>rd</sup> Annual Meeting of the European Association of Exploration Geophysicists.
- Davis, J. L. and A. P. Annan (1987) Ground penetrating radar for high resolution mapping of soil and rock stratigraphy. Paper presented at Exploration '87.
- McNeill, J. D. (1980) Electrical Conductivity of Soils and Rocks. Geonics Ltd: Technical Note TN-5.
- Power, M.A. (1994) An evaluation of ground penetrating radar as a tool in placer exploration. Indian and Northern Affairs Canada: Yukon Region. Open File 1994-

Sheriff, R.E. and L.P. Geldart (1995) Exploration Seismology - Second Edition. New York: Cambridge University Press.

Zeng, X. and G.A. McMechan (1997) GPR characterization of buried tanks and pipes. *Geophysics* Vol. 62, No. 3, pp. 797-806.



## APPENDIX A. PROJECT LOG





**AURORA GEOSCIENCES LTD.**  
**FARO SEISMIC AND GPR SURVEYS**  
**JOB BGC-04-002-YT / SRK-04-002-YT**  
**BGC ENGINEERING INC.**  
**SRK CONSULTING ENGINEERS AND SCIENTISTS LTD.**

**Period:** October 7<sup>th</sup> - October 18<sup>th</sup>, 2004

**Personel:**  
 Mike Power (MP) - Crew chief  
 Dave Hildes (DH) - Geophysicist  
 Raanan Bodzin (RB) - Technician  
 Gary Lee (GL) - Technician

**Thu 07 Oct 04** Mobe  
 Crew loaded gear at 0730 and explosives at 1000 hrs. Arrived in Faro at 1430 and drove to mine site. Met Dana Hagar and were briefed on mine site procedures. After inspecting buttress lines, stashed explosives off site in a secure location. Returned to Faro and checked in. Made up seismic cables to survey length, sorted and checked gear, set up seismograph.

**Fri 08 Oct 04** Survey Faro Pit Buttress  
 Left Faro at 0800 hrs. Picked up powder and packed gear into Line 3. Survey operations hampered by rough terrain on top of waste pile and steep, now frozen, slopes of waste pile. Set up Line 3 and began firing around 1045 hrs. Two repeated shots due to recording problem. Completed Line 3 (1.5 spreads) at about 1630 hrs, tore down equipment and moved to Line 2. Set up line 2. Returned to Faro at 1830 hrs. Wx: cloudy with snow, fog and wind by early afternoon; accumulation about 2 cm.

**Production:** 2 spreads (overlapped)

**Sat 09 Oct 04** Survey Faro Pit Buttress  
 Left Faro at 0800 hrs. After picking up powder, set up shots and began firing Line 2 at 0915 hrs. Line completed at 1400 hrs. Very slippery with fresh snow on the waste rock pile. Survey stations had been painted on rocks and were difficult to find. Tore down line and moved gear back to the truck as we have to be offsite for Sunday / Monday. Moved gear down to SRK Line and packed equipment into the site. Conducted topo survey on the line and dug in phones. Returned to Faro at 1700 hrs. Wx: cloudy, some snow flurries, clearing a bit as the day progressed.

- Sun 10 Oct 04**
- Production: 2 spreads (overlapped)  
 Survey SRK Line  
 Left Faro at 0800 hrs. Set up and began firing first spread at 0915 hrs. Fired 3 spreads to finish line. Unable to put in full (120 m) offset shots because shot points were on the rock pile. Finished at 1700 hrs and returned to Faro. Wx: cloudy, snow in the afternoon.
- Production: 3 spreads.
- Mon 11 Oct 04**
- Survey Rose Creek Diversion  
 Left Faro at 0830 hrs after sorting gear. Encountered problems with Ramac computer unit. The crew was able to get the instrument running with a spare computer but were forced to return to the truck during the mid-afternoon to recharge the computer for 1 hr in order to finish. Finished survey at 1815 and returned to Faro by 1900 hrs.
- Production GPR - 2.3 line-km (50 MHz).
- Tues 12 Oct 04**
- Survey Faro Pit Buttress  
 Left Faro at 0930 hrs. Picked up powder and packed gear into Line 1. Waste pile very slippery, movement slow. Fired 2 spreads, packed up gear.
- Production: 2 spreads (overlapped)
- Wed 13 Oct 04**
- Survey SRK Mudflats  
 DH and RB left Faro at 0845, MP stayed in town to process data and await replacement+line cutting crew. Intermittent problems again Ramac computer unit and further problems with communications with spare computer. Ready to go by 1100, but heavy sleet prevented survey. Waited for over an hour, no sign of a break so packed seismic gear into Rose Creek Diversion. Weather improved by 1530 and GPR survey proceeded with 3 sets of antennae. Returned to Faro by 1700. Garry Lee (GL) arrives to replace MP, and line cutting crew (Calvin Delwisch and Mitch Smasslaat) arrives.
- Production: GPR - 0.250 line-km (50 (X2) & 25 MHz).
- Thur 14 Oct 04**
- Survey Rose Creek Diversion  
 Seismic & SRK line cutting. Left Faro at 0815. Pack the rest of seismic gear down line. Fire three spreads, pack all gear out. Back in Faro by 1930. Line cutters locate, cut and chain Seismic line 1 (GPR line 2) and GPR line 3 (no cutting required). A locked gate blocked access to the rest of the lines. Line cutters back in Faro by 1730.
- Production: Seismic - 3 spreads. Line cutting - 1.0 km

- Fri 15 Oct 04 Survey SRK Grum Pit  
seismic and line cutting. Left Faro at 0800. Set up on Seismic Line 1, fired 3 spreads (last 2 overlapping) and surveyed line. Line cutters explore for best access to GPR line 1, then locate, cut and chain GPR line 1 but then have some difficulty locating GPR lines 4 and 5 (note indicated line 4 was along road, when in fact it was along cat trail). Snow flurries begin in early afternoon and become heavy by end of day. Back in Faro by 1830.  
Production: Seismic - 3 spreads. Line cutting - 0.2 km.
- Sat 16 Oct 04 Survey SRK Grum Pit  
Seismic and line cutting. Leave Faro at 0800. Locate GPR lines 4 and 5 (identical to seismic line 2). Set up seismic gear on seismic line 2, fire 4 spreads. Line cutters brush-out, chain and survey GPR lines 4 and 5. Back in Faro by 1815. Wx: Partly cloudy.  
Production: Seismic - 4 spreads. Line cutting - 1.1 km.
- Sun 17 Oct 04 Survey SRK Grum Pit  
GPR, line cutters demob. Leave Faro at 0800, load up explosive magazines and GPR lines 1, 2, 3 and 4 (50 MHz only). Survey lines 1 and 3. Back in Faro at 1800. Wx: Partly cloudy.  
Production: GPR - 1.2 km (50 and 25 MHz), 0.7 (50 MHz)
- Mon 18 Oct 04 Survey SRK Grum Pit  
GPR and demob. Leave Faro at 0800. Complete GPR on line 4 and line 5. Pack up all gear, back in Faro at 1315. Leave for Whitehorse at 1400.  
Production: GPR - 0.450 km (50 and 25 MHz), 0.7 (25 MHz)



## APPENDIX B. INSTRUMENT SPECIFICATIONS



## APPENDIX C. SEISMIC INVERSION RESULTS



AURORA GEOSCIENCES LTD.

**LINE SL-1 - GRUM PIT**



SIPT2 V-4.1 --- SEISMIC REFRACTION INTERPRETATION PROGRAM --- RIMROCK  
GEOPHYSICS, INC.

DATA FILE: GRUM1.SIP

PRINT FILE: C:\DATA\GRUM\GRUM1.OUT  
11-09-2004 at 10:56

RUN DATE AND TIME:

TITLE: SRK Grum Line 1 - West to East

## PROGRAM CONTROL DATA

Printer Plot Scales Datum Plane Control Points Plot Control Special  
Control Parameters

Sprds	Exit	Layers	V-Over	Elev	Horiz	Time	Point 1	Point 2	Elevations	Trace	Off	L					
				m/col	m/row	ms/col	Elev	X-Loc	Elev	X-Loc	Top	Bottom	BLim	TLim	Print		
									SP	Dip							
3	6	3	1	0.0	0.0	0.0	0.0	0.0	0.0	0.0	0	0	0.5	10.0	0	0	0

## VELOCITY OVERRIDES for GRUM1.SIP

Layer	Spread 1		Spread 2		Spread 3	
	Vv	Vh	Vv	Vh	Vv	Vh
2	2000	2000	2000	2000	2000	2000

## SHOTPOINT AND GEOPHONE INPUT DATA for GRUM1.SIP

Spread A, 5 Shotpoints, 24 Geophones, X-Shift = 0.0, X-True = 1, Units: Meters.

SP	Elev	X-Loc	Y-Loc	Depth	UpHole	T	Fudge	T	End	SP
A	1302.1	-54.9	12.7	0.0	0.0	0.0	0.0	0.0	0	
B	1299.7	-5.0	0.0	0.0	0.0	0.0	3.0	0.0	1	
C	1301.0	53.2	-2.0	0.0	0.0	0.0	3.0	0.0	0	
D	1304.8	118.2	-3.0	0.0	0.0	0.0	0.0	0.0	2	
E	1306.3	218.4	-2.0	0.0	0.0	0.0	0.0	0.0	0	

## Arrival Times + Fudge T and Layers represented

Geo	Elev	X-Loc	Y-Loc	SP A		SP B		SP C		SP D		SP E	
				T-L	T-L	T-L	T-L	T-L	T-L	T-L	T-L		
1	1299.7	0.0	0.0	29.0	2	11.4	1	32.8	3	42.9	3	58.6	3
2	1299.5	4.7	0.0	31.1	2	16.5	1	32.6	3	42.5	3	57.9	3
3	1299.4	9.5	0.0	32.9	2	22.8	2	32.0	3	42.3	3	57.1	3
4	1299.4	14.4	0.0	33.4	3	25.5	2	31.1	3	41.5	3	56.9	3
5	1299.5	19.2	0.0	34.0	3	26.5	3	30.6	3	41.0	3	56.9	3
6	1299.4	24.1	0.0	35.5	3	26.8	3	27.9	2	39.3	3	56.1	3
7	1300.0	29.2	0.0	36.1	3	27.8	3	26.4	2	38.3	3	54.9	3
8	1300.3	34.2	0.0	37.1	3	29.5	3	24.0	2	36.8	3	53.3	3
9	1300.5	39.3	0.0	38.5	3	31.0	3	21.4	2	36.0	3	52.0	3
10	1300.6	44.1	0.0	40.1	3	32.3	3	16.9	1	35.5	3	51.4	3
11	1301.0	49.2	0.0	40.8	3	33.6	3	12.4	1	33.9	3	50.4	3
12	1301.3	54.3	0.0	42.3	3	34.6	0	7.9	1	33.1	3	49.4	3
13	1301.5	59.2	0.0	43.3	3	35.5	3	13.4	1	32.1	3	47.8	3
14	1301.5	64.4	0.0	43.9	3	36.9	3	22.8	2	31.4	3	46.8	3
15	1301.9	69.3	0.0	44.6	3	38.3	3	24.4	2	30.1	3	45.3	3
16	1302.2	74.2	0.0	44.9	3	38.6	3	25.3	2	28.5	3	44.5	3
17	1302.6	79.3	0.0	45.6	3	40.4	3	28.1	3	27.3	3	43.9	3
18	1302.8	83.8	0.0	46.1	3	41.5	3	29.8	3	26.3	3	42.9	3
19	1303.2	89.2	0.0	47.4	3	42.4	3	30.5	3	24.9	2	42.0	3
20	1303.2	94.3	0.0	47.9	3	42.6	3	30.8	3	22.8	2	40.1	3
21	1303.8	99.2	0.0	48.4	3	42.6	3	31.4	3	20.0	2	38.8	3
22	1304.2	104.0	0.0	49.1	3	43.6	3	32.0	3	17.5	2	38.1	3

23	1304.7	109.1	0.0	49.8	3	44.5	3	34.0	3	15.3	2	37.5	3
24	1304.8	114.2	0.0	50.1	3	45.9	3	35.0	3	11.9	1	36.8	3

## SHOTPOINT AND GEOPHONE INPUT DATA for GRUM1.SIP

Spread B, 5 Shotpoints, 24 Geophones, X-Shift = 0.0, X-True = 1, Units: Meters.

SP	Elev	X-Loc	Y-Loc	Depth	UpHole	T	Fudge	T	End	SP
A	1299.7	-5.0	0.0	0.0	0.0	0.0	0.0	0.0	0	
B	1304.7	109.6	2.0	0.0	0.0	0.0	0.0	0.0	1	
C	1307.4	171.5	2.0	0.0	0.0	0.0	0.0	0.0	0	
D	1305.1	233.5	1.0	0.0	0.0	0.0	0.0	0.0	2	
E	1305.8	288.0	-4.0	0.0	0.0	0.0	0.0	0.0	0	

Arrival Times + Fudge T and Layers represented

Geo	Elev	X-Loc	Y-Loc	SP A	SP B	SP C	SP D	SP E					
				--T--L	--T--L	--T--L	--T--L	--T--L					
1	1304.8	114.2	0.0	42.9	3	13.0	1	33.3	3	41.8	3	59.4	0
2	1305.0	119.0	0.0	44.6	3	18.8	3	32.9	3	41.1	3	58.1	0
3	1305.3	123.8	0.0	46.1	3	20.1	3	32.4	3	40.5	3	55.1	3
4	1305.5	129.1	0.0	46.8	3	21.9	3	30.6	2	39.6	3	54.9	3
5	1305.6	134.1	0.0	48.4	3	23.6	3	29.4	2	39.1	3	54.5	3
6	1305.9	139.2	0.0	49.1	3	24.8	3	28.4	2	38.4	3	53.3	3
7	1305.9	144.2	0.0	50.0	3	26.3	3	26.5	2	37.5	3	50.9	3
8	1306.2	148.9	0.0	51.3	3	27.5	3	24.9	2	36.8	3	51.1	3
9	1306.3	154.1	0.0	52.9	3	29.3	3	22.9	2	35.8	3	50.4	3
10	1306.6	159.1	0.0	54.5	3	30.4	3	19.8	1	34.5	3	50.1	3
11	1307.1	164.1	0.0	56.1	3	31.6	3	14.8	1	33.8	3	49.4	3
12	1307.2	168.9	0.0	56.9	3	32.6	3	6.8	1	33.0	3	48.1	3
13	1307.5	174.0	0.0	58.1	3	33.9	3	7.4	1	32.5	3	46.9	3
14	1307.9	178.8	0.0	59.1	3	35.1	3	19.4	1	31.4	3	46.0	3
15	1307.9	183.8	0.0	60.1	3	35.9	3	22.8	2	30.4	3	44.8	3
16	1307.8	189.1	0.0	60.8	3	36.9	3	24.9	2	28.4	3	43.5	3
17	1307.6	194.0	0.0	61.9	3	37.5	3	26.1	2	27.4	2	42.9	3
18	1307.5	198.9	0.0	62.6	3	38.5	3	28.3	3	26.1	2	42.9	3
19	1307.4	204.0	0.0	63.3	3	39.4	3	29.5	3	24.6	2	41.8	3
20	1307.0	208.9	0.0	63.6	3	40.0	3	29.1	3	22.6	2	40.5	3
21	1306.7	213.8	0.0	63.9	3	40.4	3	30.1	3	20.8	2	39.3	3
22	1306.3	218.4	0.0	64.1	3	40.4	3	31.0	3	19.1	2	38.4	3
23	1305.8	223.7	0.0	64.6	3	40.6	3	30.8	3	14.6	2	37.8	3
24	1305.9	228.7	0.0	65.0	3	41.0	3	31.3	3	11.6	1	36.8	3

## SHOTPOINT AND GEOPHONE INPUT DATA for GRUM1.SIP

Spread C, 5 Shotpoints, 24 Geophones, X-Shift = 0.0, X-True = 1, Units: Meters.

SP	Elev	X-Loc	Y-Loc	Depth	UpHole	T	Fudge	T	End	SP
A	1301.0	53.2	2.0	0.0	0.0	0.0	0.0	0.0	0	
B	1307.4	171.5	2.0	0.0	0.0	0.0	-3.0	1		
C	1305.5	231.1	4.0	0.0	0.0	0.0	7.0	0		
D	1305.8	288.0	-4.0	0.0	0.0	0.0	0.0	0.0	2	
E	1316.2	360.6	0.4	0.0	0.0	0.0	0.0	0.0	0	

Arrival Times + Fudge T and Layers represented

Geo	Elev	X-Loc	Y-Loc	SP A	SP B	SP C	SP D	SP E					
				--T--L	--T--L	--T--L	--T--L	--T--L					
1	1307.5	174.0	0.0	47.5	3	2.3	1	34.6	3	46.0	3	55.0	3

2	1307.9	178.8	0.0	47.8	3	14.9	1	34.0	3	45.8	3	54.4	3
3	1307.9	183.8	0.0	48.4	3	19.4	2	33.0	2	45.1	3	53.8	3
4	1307.8	189.1	0.0	48.5	3	21.8	2	31.9	2	44.5	3	53.0	3
5	1307.6	194.0	0.0	49.1	3	24.3	2	30.8	2	43.9	3	52.8	3
6	1307.5	198.9	0.0	49.8	3	25.9	2	29.8	2	42.6	3	52.0	3
7	1307.4	204.0	0.0	50.6	3	26.6	2	28.6	2	41.6	3	50.8	3
8	1307.0	208.9	0.0	51.3	3	27.5	3	27.0	2	40.8	3	49.3	3
9	1306.7	213.7	0.0	51.8	3	28.4	3	25.1	2	39.9	3	48.0	3
10	1306.3	218.3	0.0	52.3	3	28.8	3	22.1	2	38.6	3	46.9	3
11	1305.8	223.7	0.0	52.6	3	29.1	3	16.9	2	37.8	3	45.9	3
12	1305.9	228.7	0.0	54.0	3	29.9	3	13.8	1	36.1	3	45.1	3
13	1305.1	233.4	0.0	55.1	3	30.1	3	15.0	1	35.3	3	44.4	3
14	1304.7	238.7	0.0	55.3	3	31.1	3	16.8	2	34.4	3	43.6	3
15	1304.3	243.7	0.0	56.1	3	32.3	3	20.5	2	33.5	3	42.6	3
16	1304.3	248.7	0.0	57.4	3	33.5	3	24.8	2	32.5	3	42.1	3
17	1304.1	253.5	0.0	58.6	3	34.1	3	26.5	2	31.3	2	41.9	3
18	1304.4	258.5	0.0	59.9	3	35.4	3	27.9	2	29.5	2	40.5	3
19	1304.6	263.4	0.0	61.5	3	37.1	3	30.4	2	28.9	2	39.3	3
20	1304.8	268.3	0.0	63.8	3	39.0	3	32.4	2	27.6	2	38.5	3
21	1305.2	273.2	0.0	64.9	3	40.9	3	34.0	2	25.8	2	37.3	3
22	1305.4	278.2	0.0	66.8	3	42.1	3	35.3	3	22.1	2	36.5	3
23	1305.4	283.1	0.0	68.6	3	43.3	3	37.3	3	13.0	1	36.3	3
24	1305.8	288.0	0.0	70.4	3	44.5	3	38.9	3	5.6	1	36.3	3

## Layer 1 Velocity from direct arrivals

Spread A SP Geo DD V Avg V

B	1	5.0	439
B	2	9.7	588
			513
C	10	9.3	552
C	11	4.5	361
C	12	2.3	291
C	13	6.3	473
			419
D	24	5.0	420
			420

Spread B SP Geo DD V Avg V

B	1	5.0	386
			386
C	10	12.6	636
C	11	7.7	518
C	12	3.3	483
C	13	3.2	433
C	14	7.6	391
			492
D	24	5.0	428
			428

Spread C SP Geo DD V Avg V

B	1	3.2	1393
B	2	7.6	509
			951
C	12	4.7	339
C	13	4.6	309
			324
D	23	6.3	488
D	24	4.0	714

601

---

 Wtd Avg Velocity computed for Layer 1 = 508

Layer 2 Velocity computed by regression of raw uncorrected arrivals

Spread A

V	Ti	Geos	<-SP->	Geos	Ti	V	Avg V	Avg Ti	Pts
				A	1 3	5.4 2384	2384	5.4	3
				B	3 4	14.8 1815	1815	14.8	2
2305	15.5	6 9	C	14 16	20.0 3897	2794	17.8	7	
1995	10.4	19 23	D			1995	10.4	5	
Avg = 2306 for 17 Pts									

Spread B

V	Ti	Geos	<-SP->	Geos	Ti	V	Avg V	Avg Ti	Pts
3230	17.8	4 9	C	15 17	18.8 3057	3170	18.3	9	
2453	12.1	17 23	D			2453	12.1	7	
Avg = 2811 for 16 Pts									

Spread C

V	Ti	Geos	<-SP->	Geos	Ti	V	Avg V	Avg Ti	Pts
				B	3 7	15.2 2699	2699	15.2	5
2712	17.0	3 11	C	14 21	14.3 2045	2351	15.6	17	
2900	19.7	17 22	D			2900	19.7	6	
Avg = 2511 for 28 Pts									

Avg of all regression velocities: 2519 for 61 points in Layer 2.

Layer 2 Velocity computed by Hobson-Overton method

Spread C

SPs	Geos	Avg	Std Err	4 Highest	Std Err at geophones								
	V	TdSP	Overall	Err Geo	Err Geo	Err Geo	Err Geo						
B C	3 7	3394	-2.8	0.508	0.697	5	-0.662	7	-0.430	3	0.425	6	
C D	17 21	3001	-0.9	0.095	-0.137	19	0.119	21	0.088	17	-0.065	20	
Avg = 3198 for 10 Pts													

Avg of all Hobson-Overton velocities: 3198 for 10 points in Layer 2.

---

 Wtd Avg Velocity computed for Layer 2 = 2687

Override Velocity assigned to Layer 2

Spread	A	B	C
	2000	2000	2000

---

Layer 3 Velocity computed by regression of raw uncorrected arrivals

Spread A

V	Ti	Geos	<-SP->	Geos	Ti	V	Avg V	Avg Ti	Pts
				A	4 24	22.2 5803	5803	22.2	21

		B	5	24	21.7	4777	4777	21.7	19		
8126	26.4	1	5	C	17	24	23.7	5658	6406	25.1	13
				D				4878	4878	19.8	18
				E				4886	4886	15.2	24

Avg = 5212 for 95 Pts

Spread B

V	Ti	Geos	<SP->	Geos	Ti	V	Avg V	Avg Ti	Pts		
				A	1	24	20.6	4978	4978	20.6	24
				B	2	24	19.0	4780	4780	19.0	23
10673	27.9	1	3	C	18	24	25.9	10266	10385	26.9	10
				D				5845	5845	21.9	16
				E				5549	5549	26.2	22

Avg = 5492 for 95 Pts

Spread C

V	Ti	Geos	<SP->	Geos	Ti	V	Avg V	Avg Ti	Pts		
				A	1	24	21.6	5181	5181	21.6	24
				B	8	24	17.5	4530	4530	17.5	17
7945	27.4	1	2	C	22	24	18.0	2714	3685	22.7	5
				D				5184	5184	25.1	16
				E				5573	5573	21.9	24

Avg = 5019 for 86 Pts

Avg of all regression velocities: 5241 for 276 points in Layer 3.

#### Layer 3 Velocity computed by Hobson-Overton method

Spread A

SPs	Geos	Avg	Std Err	4 Highest	Std Err at geophones								
	V	TdSP	Overall	Err Geo	Err Geo	Err Geo	Err Geo						
A C	4	5	8647	-1.4	0.000	0.000	4	-0.000	5				
A D	4	18	4854	-1.0	0.497	-1.034	5	0.778	12	0.767	13	-0.740	18
A E	4	24	5162	2.5	0.901	-1.897	24	1.582	13	1.479	15	-1.393	5
B D	5	18	4393	2.5	0.358	0.577	11	-0.542	14	-0.512	7	0.409	8
B E	5	24	4690	7.4	0.899	1.599	15	-1.476	24	-1.407	6	-1.401	23
C D	17	18	3327	4.7	0.000	0.000	18	-0.000	17				
C E	17	24	5128	6.7	0.301	0.475	18	-0.470	17	-0.413	22	0.193	23

Avg = 4905 for 80 Pts

Spread B

SPs	Geos	Avg	Std Err	4 Highest	Std Err at geophones								
	V	TdSP	Overall	Err Geo	Err Geo	Err Geo	Err Geo						
A C	1	3	4687	-3.6	0.024	0.034	2	-0.017	1	-0.017	3		
A D	1	16	4833	1.0	0.482	-0.914	7	-0.860	8	0.649	11	-0.645	6
A E	3	24	5352	-2.2	1.077	-2.213	24	-1.746	23	1.664	16	1.643	15
B C	2	3	5301	-6.0	0.000	0.000	2	-0.000	3				
B D	2	16	4590	0.7	0.298	0.627	10	-0.526	15	0.405	9	-0.362	13
B E	3	24	5212	-4.7	1.209	-2.575	24	-2.059	23	1.801	16	-1.592	4
C E	18	24	6606	-4.8	0.470	0.828	22	-0.473	18	0.420	21	-0.388	24

Avg = 5166 for 87 Pts

Spread C

		Avg	Std Err	4 Highest	Std Err at geophones
--	--	-----	---------	-----------	----------------------

SPs	Geos	V	Td	SP Overall	Err Geo				
A C 1 2	10646	6.9	0.000	-0.000	2	0.000	1		
A D 1 16	6153	-1.4	0.780	1.772	1	-1.057	11	-1.022	5
A E 1 24	5369	1.7	1.536	3.047	1	2.337	23	2.309	24
B D 8 16	5725	-6.1	0.322	-0.510	11	0.471	16	-0.396	13
B E 8 24	5128	-0.5	1.150	-2.251	17	1.531	22	-1.498	18
C E 22 24	5142	5.9	0.144	0.204	23	-0.102	22	-0.102	24

Avg = 5672 for 71 Pts

Avg of all Hobson-Overton velocities: 5229 for 238 points in Layer 3.

Wtd Avg Velocity computed for Layer 3 = 5234

Arrival times Td corrected to datum. (Datum Elev = 1300.884 + 0.025x) for GRUM1.SIP

Spread A

	SP A	SP B	SP C	SP D	SP E
--	------	------	------	------	------

Datum Elev ..... 1299.5 1300.8 1302.2 1303.8 1306.3

Geo .	X-Loc	Cor T	0.0	2.1	2.4	-1.9	0.0	
	--	--	--Td--	--Td--	--Td--	--Td--	--Td--	
1	1300.9	0.0	2.3	31.3	15.8	37.5	43.3	60.9
2	1301.0	4.7	3.0	34.1	21.5	37.9	43.5	60.9
3	1301.1	9.5	3.4	36.3	28.3	37.8	43.7	60.5
4	1301.2	14.4	3.6	37.0	31.2	37.1	43.2	60.5
5	1301.4	19.2	3.7	37.7	32.3	36.6	42.7	60.6
6	1301.5	24.1	4.1	39.6	33.0	34.4	41.5	60.2
7	1301.6	29.2	3.2	39.3	33.1	31.9	39.5	58.1
8	1301.7	34.2	2.8	39.9	34.4	29.2	37.7	56.1
9	1301.9	39.3	2.7	41.2	35.8	26.4	36.7	54.7
10	1302.0	44.1	2.7	42.8	37.1	22.0	36.3	54.1
11	1302.1	49.2	2.2	43.0	37.9	16.9	34.1	52.6
12	1302.2	54.3	1.8	44.1	38.5	12.1	33.0	51.2
13	1302.4	59.2	1.7	45.0	39.3	17.5	31.8	49.5
14	1302.5	64.4	1.9	45.8	40.9	27.1	31.4	48.7
15	1302.6	69.3	1.4	46.0	41.8	28.2	29.5	46.7
16	1302.7	74.2	1.0	45.9	41.7	28.7	27.6	45.5
17	1302.9	79.3	0.5	46.1	43.0	31.0	25.9	44.4
18	1303.0	83.8	0.3	46.4	43.9	32.5	24.7	43.2
19	1303.1	89.2	-0.2	47.2	44.3	32.7	22.8	41.8
20	1303.2	94.3	0.0	47.9	44.7	33.2	20.9	40.1
21	1303.3	99.2	-0.9	47.5	43.8	32.9	17.2	37.9
22	1303.5	104.0	-1.5	47.6	44.2	32.9	14.1	36.6
23	1303.6	109.1	-2.2	47.6	44.4	34.2	11.2	35.3
24	1303.7	114.2	-2.1	48.0	45.9	35.2	7.8	34.7

Spread B

	SP A	SP B	SP C	SP D	SP E
--	------	------	------	------	------

Datum Elev ..... 1300.8 1303.6 1305.1 1306.7 1308.0

Geo .	X-Loc	Cor T	0.0	-2.2	-4.5	3.1	0.0	
	--	--	--Td--	--Td--	--Td--	--Td--	--Td--	
1	1303.7	114.2	-2.1	40.8	8.7	26.7	42.8	57.3
2	1303.8	119.0	-2.3	42.3	14.3	26.1	41.9	55.8
3	1304.0	123.8	-2.7	43.4	15.3	25.3	41.0	52.4
4	1304.1	129.1	-2.8	44.0	17.0	23.4	39.9	52.1
5	1304.2	134.1	-2.7	45.7	18.7	22.2	39.5	51.8
6	1304.3	139.2	-3.1	46.0	19.6	20.9	38.4	50.2
7	1304.5	144.2	-2.8	47.2	21.3	19.2	37.8	48.1

8	1304.6	148.9	-3.2	48.1	22.1	17.2	36.7	47.9
9	1304.7	154.1	-3.1	49.8	24.0	15.3	35.8	47.3
10	1304.8	159.1	-3.5	51.0	24.8	11.9	34.1	46.6
11	1305.0	164.1	-4.2	51.9	25.2	6.1	32.7	45.2
12	1305.1	168.9	-4.2	52.7	26.2	-1.8	31.9	43.9
13	1305.2	174.0	-4.5	53.6	27.2	-1.6	31.1	42.4
14	1305.3	178.8	-5.1	54.0	27.9	9.9	29.4	40.9
15	1305.4	183.8	-4.8	55.3	28.9	13.5	28.7	40.0
16	1305.6	189.1	-4.4	56.4	30.4	16.1	27.1	39.1
17	1305.7	194.0	-3.8	58.1	31.6	17.9	26.8	39.1
18	1305.8	198.9	-3.3	59.3	33.0	20.5	25.9	39.6
19	1305.9	204.0	-2.9	60.4	34.4	22.2	24.8	38.9
20	1306.1	208.9	-1.8	61.8	36.0	22.8	23.9	38.7
21	1306.2	213.8	-1.0	62.9	37.2	24.6	22.9	38.3
22	1306.3	218.4	0.0	64.1	38.2	26.5	22.2	38.4
23	1306.4	223.7	1.2	65.8	39.7	27.6	19.0	39.0
24	1306.6	228.7	1.3	66.3	40.1	28.1	16.0	38.1

Spread C	SP A	SP B	SP C	SP D	SP E
----------	------	------	------	------	------

Datum Elev . . . . .	1302.2	1305.1	1306.6	1308.0	1309.8
----------------------	--------	--------	--------	--------	--------

Geo .	X-Loc	Cor T	0.0	-4.5	2.2	4.4	0.0	
---	---	---	--Td--	--Td--	--Td--	--Td--	--Td--	
1	1305.2	174.0	-4.5	43.0	-6.7	32.3	45.9	50.5
2	1305.3	178.8	-5.1	42.7	5.4	31.1	45.1	49.3
3	1305.4	183.8	-4.8	43.6	10.1	30.4	44.6	49.0
4	1305.6	189.1	-4.4	44.1	13.0	29.7	44.5	48.6
5	1305.7	194.0	-3.8	45.3	16.1	29.2	44.5	49.0
6	1305.8	198.9	-3.3	46.5	18.1	28.7	43.7	48.7
7	1305.9	204.0	-2.9	47.7	19.3	27.9	43.1	47.9
8	1306.1	208.9	-1.8	49.5	21.2	27.4	43.3	47.5
9	1306.2	213.7	-1.0	50.8	22.9	26.3	43.3	47.0
10	1306.3	218.3	-0.0	52.3	24.3	24.3	43.0	46.9
11	1306.4	223.7	1.2	53.8	25.9	20.3	43.4	47.1
12	1306.6	228.7	1.3	55.3	26.7	17.3	41.8	46.4
13	1306.7	233.4	3.1	58.2	28.7	20.3	42.8	47.5
14	1306.8	238.7	4.1	59.4	30.8	23.1	42.9	47.7
15	1306.9	243.7	5.2	61.3	33.0	27.9	43.1	47.8
16	1307.1	248.7	5.4	62.8	34.5	32.4	42.3	47.5
17	1307.2	253.5	6.1	64.7	35.7	34.8	41.7	48.0
18	1307.3	258.5	5.7	65.6	36.6	35.8	39.6	46.2
19	1307.4	263.4	5.6	67.1	38.2	38.1	38.8	44.9
20	1307.5	268.3	5.4	69.2	39.9	40.0	37.4	43.9
21	1307.7	273.2	4.8	69.7	41.3	41.0	35.0	42.1
22	1307.8	278.2	4.7	71.5	42.3	42.2	31.2	41.2
23	1307.9	283.1	4.9	73.5	43.8	44.4	22.3	41.2
24	1308.0	288.0	4.4	74.8	44.4	45.5	14.4	40.7

Arrival times Tc corrected to top of Layer 2 and Elev of top of Layer 2 for GRUM1.SIP

Spread A	SP A	SP B	SP C	SP D	SP E
----------	------	------	------	------	------

Elev . . . . .	0.0	1294.8	1296.7	1302.9	0.0
----------------	-----	--------	--------	--------	-----

Geo .	X-Loc	Cor T	9.6	9.6	8.5	3.8	3.8	
---	---	---	--Tc--	--Tc--	--Tc--	--Tc--	--Tc--	
1	1295.0	0.0	9.2	0.1	0.0	15.0	29.9	29.6
2	1295.0	4.7	8.9	2.5	0.0	15.1	29.8	29.2
3	1294.9	9.5	8.9	4.3	4.3	14.6	29.6	28.5
4	1295.0	14.4	8.8	8.6	7.1	13.8	29.0	28.4
5	1295.3	19.2	8.1	9.8	8.8	13.9	29.1	29.0

6	1295.6	24.1	7.5	11.9	9.7	11.9	28.0	28.9
7	1295.9	29.2	8.1	11.9	10.1	9.7	26.4	27.0
8	1296.1	34.2	8.2	12.8	11.6	7.2	24.8	25.3
9	1296.3	39.3	8.3	14.2	13.1	4.6	24.0	24.0
10	1296.4	44.1	8.5	15.5	14.2	0.0	23.2	23.1
11	1296.6	49.2	8.8	15.9	15.2	0.0	21.3	21.9
12	1296.7	54.3	9.1	17.2	0.0	0.0	20.2	20.6
13	1297.3	59.2	8.1	19.1	17.8	0.0	20.2	19.9
14	1297.9	64.4	7.1	20.7	20.2	7.1	20.5	19.9
15	1298.7	69.3	6.3	22.2	22.4	9.6	20.0	19.3
16	1299.6	74.2	5.2	23.6	23.8	11.5	19.5	19.5
17	1299.8	79.3	5.4	24.1	25.4	14.2	18.1	18.8
18	1300.0	83.8	5.5	24.5	26.4	15.7	17.0	17.6
19	1300.3	89.2	5.7	25.6	27.1	16.3	15.4	16.6
20	1300.5	94.3	5.4	26.4	27.6	16.9	13.6	15.0
21	1300.9	99.2	5.7	26.7	27.3	17.2	10.6	13.4
22	1301.5	104.0	5.4	27.6	28.6	18.1	8.3	13.0
23	1301.9	109.1	5.5	28.2	29.4	20.0	6.0	12.3
24	1302.5	114.2	4.7	29.3	31.6	21.7	0.0	12.3

## Spread B                    SPA    SP B    SP C    SP D    SP E

Elev ..... 0.0 1302.0 1304.0 1301.6 0.0

Geo .	X-Loc	Cor T	5.4	5.4	6.7	6.9	6.9	
---	---	---	--Tc--	--Tc--	--Tc--	--Tc--	--Tc--	
1	1302.5	114.2	4.7	8.6	0.0	21.9	30.2	0.0
2	1303.0	119.0	4.0	11.0	9.4	22.2	30.2	0.0
3	1304.2	123.8	2.1	14.4	12.6	23.6	31.4	31.2
4	1305.5	129.1	0.1	17.1	16.4	23.8	32.6	33.1
5	1305.3	134.1	0.6	18.2	17.6	22.1	31.5	32.1
6	1304.8	139.2	2.1	17.4	17.3	19.6	29.4	29.5
7	1304.6	144.2	2.7	17.7	18.3	17.1	27.9	26.5
8	1304.4	148.9	3.5	18.2	18.6	14.7	26.4	25.9
9	1304.2	154.1	4.1	19.2	19.8	12.1	24.8	24.6
10	1304.1	159.1	5.0	19.9	20.1	0.0	22.6	23.4
11	1304.0	164.1	5.8	20.7	20.4	0.0	21.1	21.9
12	1303.8	168.9	6.6	20.7	20.6	0.0	19.4	19.7
13	1304.2	174.0	6.6	21.9	21.9	0.0	19.0	18.6
14	1304.9	178.8	5.6	23.9	24.2	0.0	18.9	18.7
15	1305.6	183.8	4.5	26.0	26.0	11.6	19.0	18.6
16	1305.5	189.1	4.5	26.7	27.0	13.7	17.0	17.3
17	1305.5	194.0	4.1	28.2	28.0	15.3	16.4	17.1
18	1305.3	198.9	4.3	28.7	28.8	17.3	14.9	16.9
19	1305.0	204.0	4.7	29.0	29.3	18.1	13.0	15.3
20	1304.0	208.9	5.9	28.1	28.7	16.5	9.7	12.8
21	1303.3	213.8	6.7	27.6	28.4	16.7	7.2	10.9
22	1303.0	218.4	6.5	28.0	28.6	17.8	5.7	10.2
23	1303.0	223.7	5.5	29.5	29.7	18.6	2.2	10.6
24	1302.0	228.7	7.8	27.6	27.9	16.8	0.0	7.3

## Spread C                    SPA    SP B    SP C    SP D    SP E

Elev ..... 0.0 1304.0 1301.8 1300.9 0.0

Geo .	X-Loc	Cor T	6.7	6.7	7.3	9.6	9.6	
---	---	---	--Tc--	--Tc--	--Tc--	--Tc--	--Tc--	
1	1304.2	174.0	6.6	9.9	0.0	20.7	29.8	30.0
2	1304.9	178.8	5.6	11.2	0.0	21.1	30.6	30.4
3	1305.6	183.8	4.5	12.9	8.2	21.2	31.0	30.9
4	1305.5	189.1	4.5	13.0	10.6	20.1	30.4	30.1
5	1305.5	194.0	4.1	14.0	13.5	19.4	30.2	30.3
6	1305.3	198.9	4.3	14.5	14.9	18.2	28.7	29.3

7	1305.0	204.0	4.7	14.9	15.2	16.5	27.3	27.6
8	1304.0	208.9	5.9	14.4	14.9	13.7	25.3	24.9
9	1303.3	213.7	6.6	14.2	15.1	11.1	23.7	22.9
10	1303.0	218.3	6.5	14.8	15.6	8.3	22.5	22.0
11	1303.0	223.7	5.5	16.1	16.9	4.1	22.7	22.0
12	1302.0	228.7	7.8	15.2	15.4	0.0	18.7	18.9
13	1301.6	233.4	6.9	17.2	16.5	0.0	18.8	19.0
14	1301.3	238.7	6.7	17.6	17.7	2.8	18.1	18.5
15	1300.7	243.7	7.1	18.0	18.5	6.1	16.8	17.1
16	1300.4	248.7	7.6	18.8	19.2	9.8	15.3	16.0
17	1300.6	253.5	6.8	20.7	20.6	12.3	14.9	16.6
18	1301.0	258.5	6.7	22.2	22.0	13.9	13.2	15.4
19	1301.0	263.4	7.2	23.3	23.2	15.9	12.1	13.7
20	1300.8	268.3	7.9	24.8	24.4	17.1	10.0	12.1
21	1301.1	273.2	8.2	25.7	26.0	18.5	8.0	10.7
22	1301.0	278.2	8.6	27.2	26.8	19.4	3.9	9.5
23	1301.0	283.1	9.1	28.5	27.5	20.9	0.0	8.8
24	1300.9	288.0	9.6	29.8	28.2	22.0	0.0	8.3

GRUM1.SIP  
SRK Grum Line 1 - West to East

SRK Grum Line 1 - West to East

Spread A Points of emergence of refracted rays below target geophones for GRUM1.SIP

Geo	SP A		SP B		SP C		SP D		SP E	
	L	L	L	L	L	L	L	L	L	L
1	X-Loc	-1.0 2	---	1	2.1 3	2.5 3	2.3 3			
	Elev	1295.0	---		1291.3	1290.5	1290.9			
2	X-Loc	3.4 2	---	1	6.3 3	6.5 3	6.3 3			
	Elev	1295.0	---		1290.1	1289.6	1290.2			
3	X-Loc	8.2 2	8.2 2		11.2 3	11.5 3	11.2 3			
	Elev	1294.9	1294.9		1289.3	1288.4	1289.7			
4	X-Loc	10.5 3	13.2 2		16.7 3	16.9 3	16.8 3			
	Elev	1289.3	1294.9		1288.8	1287.7	1288.4			
5	X-Loc	15.4 3	16.0 3		22.3 3	22.7 3	22.6 3			
	Elev	1289.0	1290.0		1287.8	1286.7	1286.8			
6	X-Loc	19.8 3	21.0 3		25.3 2	28.4 3	28.7 3			
	Elev	1287.3	1289.7		1295.7	1286.7	1285.9			
7	X-Loc	26.0 3	26.7 3		30.5 2	33.7 3	34.0 3			
	Elev	1288.4	1290.4		1296.0	1287.7	1287.0			
8	X-Loc	31.4 3	31.8 3		35.5 2	38.2 3	38.5 3			
	Elev	1288.7	1289.9		1296.2	1288.7	1288.1			
9	X-Loc	36.1 3	36.5 3		40.5 2	43.2 3	43.2 3			
	Elev	1288.5	1289.5		1296.3	1288.7	1288.6			
10	X-Loc	40.5 3	41.0 3		— 1	48.2 3	48.1 3			
	Elev	1287.8	1289.2		—	1288.3	1288.4			
11	X-Loc	45.8 3	46.1 3		— 1	52.6 3	52.8 3			
	Elev	1288.8	1289.6		—	1289.6	1289.0			
12	X-Loc	51.0 3	— 0		— 1	57.4 3	57.5 3			
	Elev	1288.7	—		—	1289.6	1289.3			
13	X-Loc	54.5 3	55.2 3		— 1	62.2 3	62.1 3			
	Elev	1288.1	1289.5		—	1288.9	1289.2			
14	X-Loc	58.7 3	59.0 3		63.9 2	68.3 3	68.1 3			
	Elev	1287.4	1287.9		1297.8	1287.3	1287.9			
15	X-Loc	62.7 3	62.6 3		69.0 2	75.4 3	75.0 3			
	Elev	1286.9	1286.7		1298.7	1287.0	1287.9			
16	X-Loc	67.2 3	67.1 3		74.0 2	81.2 3	81.2 3			
	Elev	1286.7	1286.5		1299.5	1287.3	1287.3			

17	X-Loc	73.1 3	72.4 3	73.3 3	86.5 3	86.9 3
	Elev	1287.2	1285.8	1287.6	1288.4	1287.7
18	X-Loc	79.1 3	78.4 3	78.3 3	91.8 3	92.2 3
	Elev	1287.7	1285.6	1286.8	1289.1	1288.4
19	X-Loc	86.0 3	85.6 3	86.0 3	90.0 2	97.1 3
	Elev	1288.2	1286.6	1288.1	1300.3	1289.2
20	X-Loc	92.2 3	92.0 3	92.2 3	95.3 2	100.9 3
	Elev	1289.1	1287.9	1289.2	1300.5	1290.1
21	X-Loc	97.2 3	97.0 3	97.2 3	100.3 2	104.3 3
	Elev	1290.6	1289.9	1290.5	1301.1	1291.2
22	X-Loc	101.3 3	101.0 3	101.3 3	104.9 2	109.0 3
	Elev	1291.1	1290.1	1291.2	1301.6	1291.1
23	X-Loc	105.4 3	104.9 3	104.9 3	110.0 2	113.6 3
	Elev	1291.9	1290.6	1290.6	1302.0	1290.9
24	X-Loc	109.8 3	108.7 3	108.9 3	—1	118.6 3
	Elev	1292.1	1289.6	1289.9	—	1289.6

## Spread A Points of entry of refracted rays below source shotpoints:

L=2	Right	X-Loc	-3.5	-3.5	54.9	—	—
	Elev	1295.0*	1295.0	1296.7	—	—	—
L=2	Left	X-Loc	---	---	52.1	117.7	—
	Elev	---	—	1296.5	1302.7	—	—
L=3	Right	X-Loc	-2.5	-2.5	56.3	—	—
	Elev	1290.1*	1290.1	1288.5	—	—	—
L=3	Left	X-Loc	---	---	49.6	113.3	113.3
	Elev	---	—	1288.9	1291.1	1291.1*	—

## SRK Grum Line 1 - West to East

## Spread B Points of emergence of refracted rays below target geophones for GRUM1.SIP

Geo	—	SP A	SP B	SP C	SP D	SP E
		—L	—L	—L	—L	—L
1	X-Loc	110.3 3	—1	118.3 3	117.8 3	—0
	Elev	1293.4	—	1290.4	1291.9	—
2	X-Loc	113.9 3	114.8 3	121.7 3	121.4 3	—0
	Elev	1291.9	1293.9	1289.2	1291.0	—
3	X-Loc	116.6 3	117.7 3	128.8 3	128.2 3	128.1 3
	Elev	1290.2	1292.3	1286.8	1288.8	1289.2
4	X-Loc	118.0 3	118.6 3	129.1 2	136.7 3	136.8 3
	Elev	1288.9	1289.9	1305.5	1286.7	1286.4
5	X-Loc	122.0 3	122.6 3	134.2 2	142.7 3	142.8 3
	Elev	1288.4	1289.2	1305.3	1286.7	1286.3
6	X-Loc	131.3 3	131.4 3	139.5 2	149.9 3	149.8 3
	Elev	1289.2	1289.5	1304.8	1288.2	1288.4
7	X-Loc	137.3 3	137.2 3	144.5 2	154.9 3	153.7 3
	Elev	1289.6	1289.3	1304.5	1289.1	1290.8
8	X-Loc	143.4 3	143.3 3	149.3 2	158.8 3	158.3 3
	Elev	1290.1	1289.8	1304.4	1290.1	1290.9
9	X-Loc	150.9 3	150.8 3	154.6 2	163.0 3	162.7 3
	Elev	1290.5	1290.0	1304.2	1291.1	1291.5
10	X-Loc	156.5 3	156.5 3	—1	166.8 3	167.1 3
	Elev	1291.2	1291.3	—	1292.7	1292.1
11	X-Loc	161.5 3	161.6 3	—1	169.3 3	169.6 3
	Elev	1292.3	1292.8	—	1293.8	1293.2
12	X-Loc	166.7 3	166.8 3	—1	173.5 3	173.5 3
	Elev	1293.3	1293.6	—	1294.1	1294.0
13	X-Loc	170.4 3	170.5 3	—1	178.5 3	178.3 3
	Elev	1293.4	1293.6	—	1293.5	1294.2
14	X-Loc	174.2 3	174.2 3	—1	182.4 3	182.3 3

		Elev	1293.1	1293.1	—	1293.2	1293.7
15	X-Loc	176.9 3	177.0 3	183.6 2	188.1 3	187.9 3	
	Elev	1291.8	1292.0	1305.6	1291.9	1292.5	
16	X-Loc	180.8 3	180.7 3	188.5 2	195.0 3	195.0 3	
	Elev	1291.8	1291.7	1305.5	1292.6	1292.5	
17	X-Loc	185.9 3	186.1 3	193.4 2	194.5 2	201.7 3	
	Elev	1290.9	1291.3	1305.5	1305.5	1292.0	
18	X-Loc	191.4 3	191.4 3	191.3 3	199.3 2	207.5 3	
	Elev	1290.9	1291.0	1290.7	1305.3	1291.5	
19	X-Loc	198.3 3	198.3 3	198.0 3	204.1 2	212.7 3	
	Elev	1291.5	1291.4	1290.7	1305.0	1292.5	
20	X-Loc	205.5 3	205.4 3	205.5 3	209.3 2	214.7 3	
	Elev	1293.3	1292.8	1293.3	1303.9	1293.8	
21	X-Loc	211.8 3	211.7 3	211.7 3	214.5 2	218.5 3	
	Elev	1295.1	1294.5	1294.4	1303.2	1294.7	
22	X-Loc	216.1 3	216.0 3	215.7 3	219.3 2	222.8 3	
	Elev	1295.8	1295.5	1294.4	1303.0	1294.5	
23	X-Loc	220.9 3	220.9 3	220.7 3	223.7 2	228.1 3	
	Elev	1295.6	1295.6	1294.9	1303.0	1293.2	
24	X-Loc	226.1 3	226.1 3	225.8 3	— 1	231.4 3	
	Elev	1298.0	1298.0	1297.1	—	1294.9	

Spread B Points of entry of refracted rays below source shotpoints:

L=2	Right	X-Loc	—	—	172.8	—	—
		Elev	—	—	1304.0	—	—
L=2	Left	X-Loc	—	—	170.9	232.5	—
		Elev	—	—	1303.8	1301.6	—
L=3	Right	X-Loc	114.0	114.0	175.6	—	—
		Elev	1292.0*	1292.0	1293.6	—	—
L=3	Left	X-Loc	—	—	168.2	229.6	229.6
		Elev	—	—	1291.6	1294.1	1294.1*

#### SRK Grum Line 1 - West to East

Spread C Points of emergence of refracted rays below target geophones for GRUM1.SIP

Geo		SP A	SP B	SP C	SP D	SP E
		—	—	—	—	—
1	X-Loc	169.5 3	— 1	178.9 3	177.9 3	177.8 3
	Elev	1291.0	—	1291.3	1294.4	1294.6
2	X-Loc	173.5 3	— 1	183.4 3	182.6 3	182.5 3
	Elev	1291.7	—	1290.4	1293.1	1293.7
3	X-Loc	176.3 3	183.6 2	184.2 2	188.2 3	188.1 3
	Elev	1291.2	1305.6	1305.6	1291.4	1292.0
4	X-Loc	181.0 3	188.4 2	189.7 2	195.8 3	195.5 3
	Elev	1291.8	1305.5	1305.5	1290.6	1291.4
5	X-Loc	186.2 3	193.5 2	194.4 2	202.7 3	202.6 3
	Elev	1291.4	1305.5	1305.5	1290.1	1290.4
6	X-Loc	191.7 3	198.2 2	199.3 2	207.8 3	207.9 3
	Elev	1291.5	1305.4	1305.3	1291.0	1290.8
7	X-Loc	198.5 3	203.3 2	204.1 2	213.0 3	213.0 3
	Elev	1292.0	1305.1	1305.0	1292.1	1292.1
8	X-Loc	205.5 3	205.4 3	209.3 2	215.3 3	214.9 3
	Elev	1293.3	1292.7	1303.9	1292.7	1293.4
9	X-Loc	211.7 3	211.6 3	214.4 2	219.3 3	218.7 3
	Elev	1294.9	1293.9	1303.2	1293.3	1294.5
10	X-Loc	215.8 3	215.6 3	219.2 2	223.4 3	222.9 3
	Elev	1295.3	1294.4	1303.0	1293.6	1294.6
11	X-Loc	220.9 3	220.6 3	223.7 2	228.2 3	227.7 3
	Elev	1295.3	1294.4	1303.0	1292.4	1293.6

12	X-Loc	225.5 3	225.3 3	— 1	231.3 3	231.3 3
	Elev	1296.7	1296.4	—	1295.0	1295.2
13	X-Loc	229.9 3	230.2 3	— 1	236.4 3	236.4 3
	Elev	1295.5	1296.2	—	1293.7	1293.8
14	X-Loc	235.6 3	235.6 3	237.7 2	242.2 3	242.2 3
	Elev	1295.9	1295.7	1301.4	1293.1	1293.1
15	X-Loc	241.1 3	240.8 3	242.1 2	247.1 3	247.1 3
	Elev	1296.0	1295.4	1300.8	1293.2	1293.3
16	X-Loc	246.5 3	246.3 3	247.4 2	251.6 3	251.8 3
	Elev	1296.2	1295.7	1300.4	1293.6	1293.2
17	X-Loc	250.7 3	250.8 3	252.8 2	254.7 2	257.0 3
	Elev	1295.1	1295.3	1300.6	1300.7	1291.5
18	X-Loc	255.1 3	255.2 3	257.9 2	259.3 2	261.1 3
	Elev	1294.7	1294.9	1301.0	1301.0	1291.9
19	X-Loc	259.1 3	259.1 3	262.4 2	264.1 2	265.9 3
	Elev	1294.3	1294.4	1301.0	1300.9	1292.3
20	X-Loc	263.2 3	263.5 3	267.0 2	269.8 2	270.8 3
	Elev	1293.2	1293.7	1300.7	1300.8	1292.5
21	X-Loc	268.4 3	268.2 3	272.5 2	274.2 2	275.8 3
	Elev	1293.2	1292.8	1301.0	1301.1	1292.8
22	X-Loc	272.1 3	272.3 3	270.0 3	279.3 2	282.1 3
	Elev	1292.3	1292.7	1289.1	1301.0	1293.2
23	X-Loc	279.1 3	279.5 3	277.8 3	— 1	287.5 3
	Elev	1291.1	1292.1	1287.5	—	1292.1
24	X-Loc	283.8 3	284.4 3	282.5 3	— 1	290.4 3
	Elev	1291.2	1292.8	1287.8	—	1294.8

## Spread C Points of entry of refracted rays below source shotpoints:

L=2	Right	X-Loc	---	172.8	231.9	---	---
	Elev	---	---	1304.0	1301.6	---	---
L=2	Left	X-Loc	---	---	230.0	286.6	---
	Elev	---	---	---	1301.7	1300.9	---
L=3	Right	X-Loc	176.6	176.6	235.1	---	---
	Elev	1294.5*	1294.5	1291.1	---	---	---
L=3	Left	X-Loc	---	---	226.9	283.4	283.4
	Elev	---	---	1293.0	1290.5	1290.5*	---

## SRK Grum Line 1 - West to East

## Spread A Depth and Elev of layers directly beneath SPs and Geos for GRUM1.SIP

SP	Surface		Layer 2		Layer 3	
	X-Loc	Elev	Depth	Elev	Depth	Elev
B	-5.0	1299.7	4.6	1295.1	9.7	1290.0
C	53.2	1301.0	4.3	1296.7	12.3	1288.7
D	118.2	1304.8	1.9	1302.9	14.5	1290.3
				Geo		
1	0.0	1299.7	4.7	1295.0	9.6	1290.1
2	4.7	1299.5	4.5	1295.0	9.3	1290.2
3	9.5	1299.4	4.5	1294.9	9.8	1289.6
4	14.4	1299.4	4.4	1295.0	10.5	1288.9
5	19.2	1299.5	4.2	1295.3	11.2	1288.3
6	24.1	1299.4	3.8	1295.6	11.4	1288.0
7	29.2	1300.0	4.1	1295.9	11.9	1288.1
8	34.2	1300.3	4.2	1296.1	11.9	1288.4
9	39.3	1300.5	4.2	1296.3	11.9	1288.6
10	44.1	1300.6	4.2	1296.4	11.9	1288.7
11	49.2	1301.0	4.4	1296.6	12.2	1288.8

12	54.3	1301.3	4.6	1296.7	12.6	1288.7
13	59.2	1301.5	4.2	1297.3	13.2	1288.3
14	64.4	1301.5	3.6	1297.9	13.8	1287.7
15	69.3	1301.9	3.2	1298.7	14.7	1287.2
16	74.2	1302.2	2.6	1299.6	15.2	1287.0
17	79.3	1302.6	2.8	1299.8	15.4	1287.2
18	83.8	1302.8	2.8	1300.0	15.2	1287.6
19	89.2	1303.2	2.9	1300.3	14.8	1288.4
20	94.3	1303.2	2.7	1300.5	13.9	1289.3
21	99.2	1303.8	2.9	1300.9	13.7	1290.1
22	104.0	1304.2	2.7	1301.5	13.5	1290.7
23	109.1	1304.7	2.8	1301.9	13.7	1291.0
24	114.2	1304.8	2.3	1302.5	14.2	1290.6

## SRK Grum Line 1 - West to East

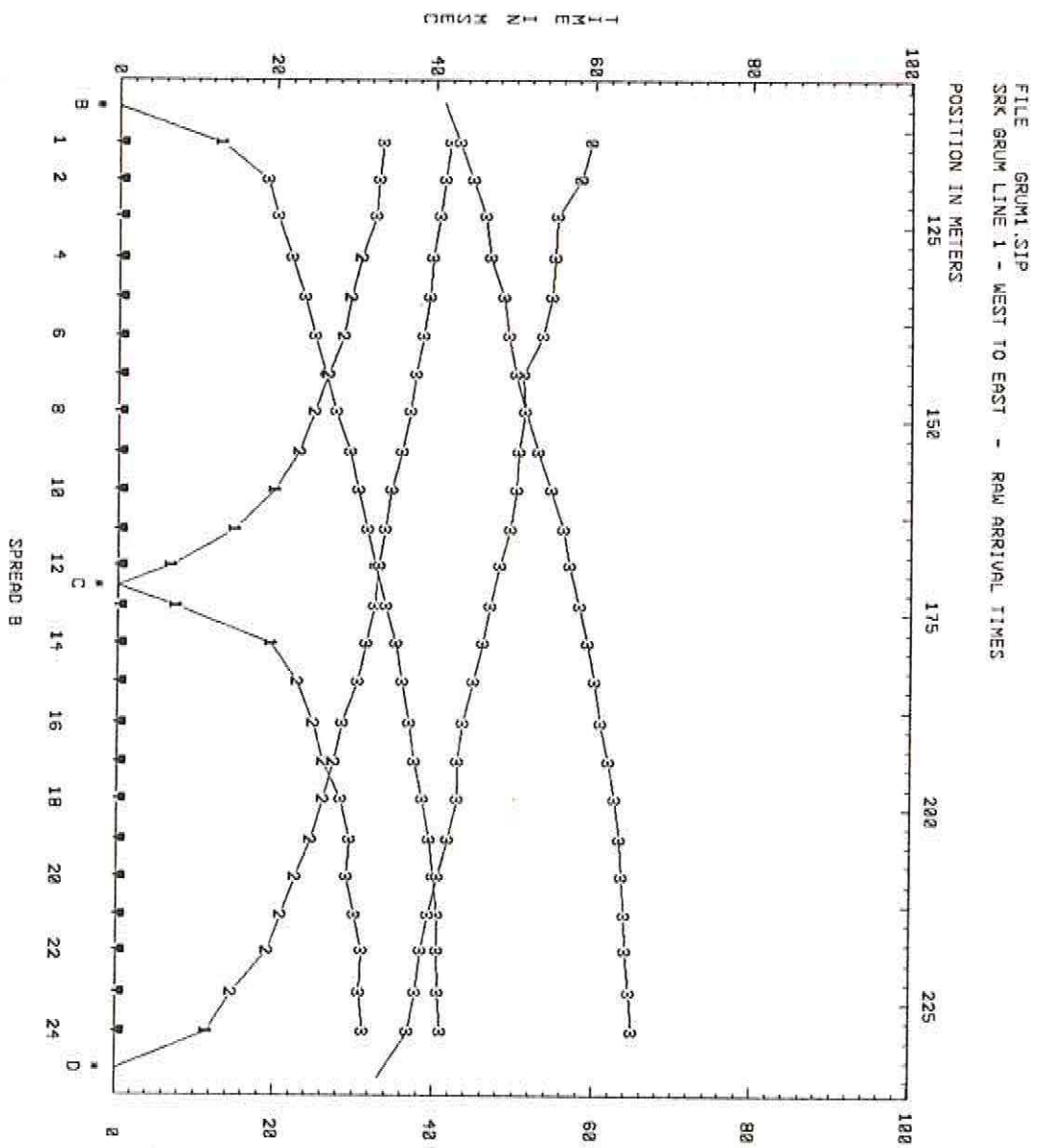
Spread B Depth and Elev of layers directly beneath SPs and Geos for GRUM1.SIP

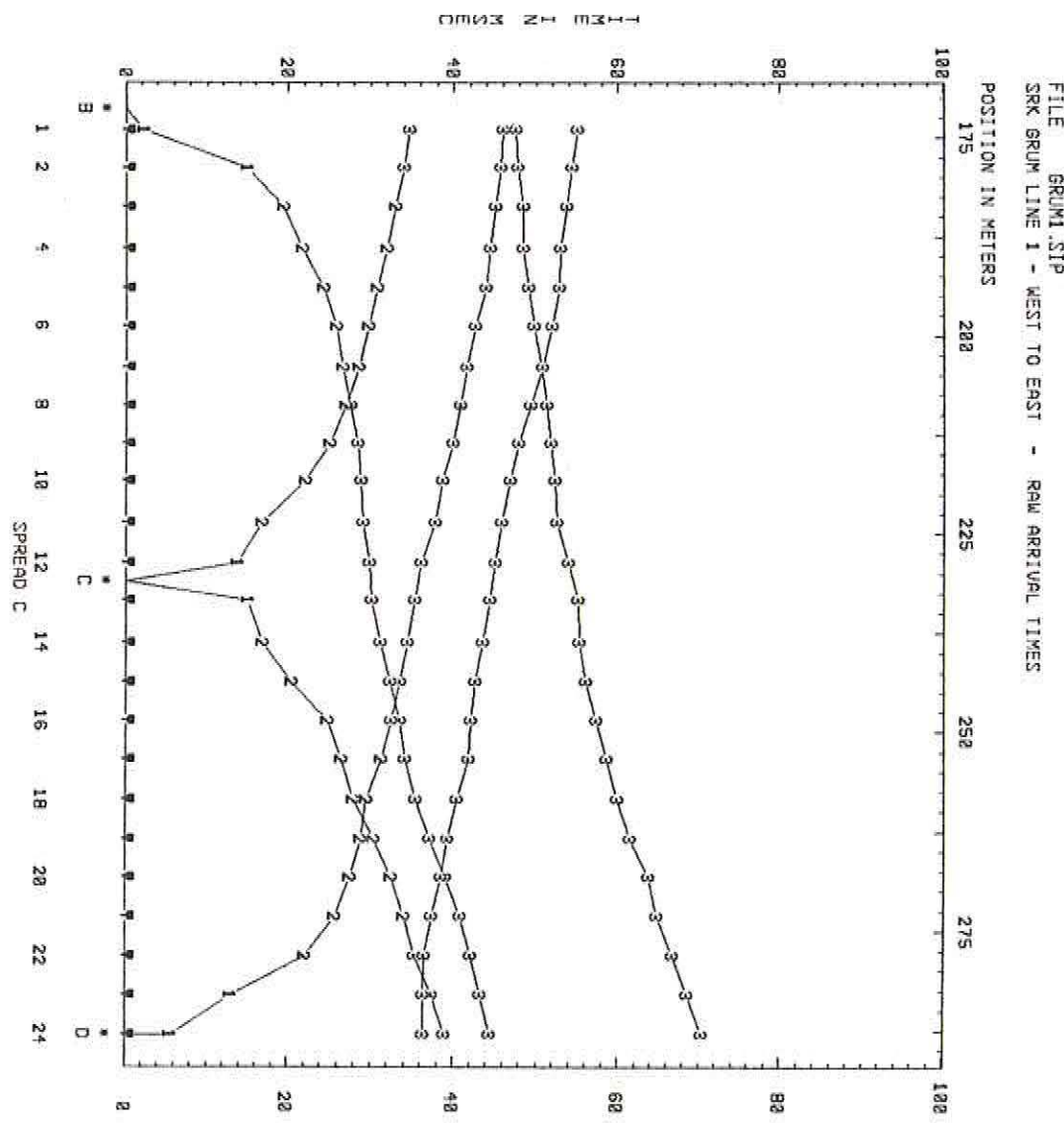
SP	Surface		Layer 2		Layer 3	
	X-Loc	Elev	Depth	Elev	Depth	Elev
B	109.6	1304.7	2.7	1302.0	13.7	1291.0
C	171.5	1307.4	3.4	1304.0	14.5	1292.9
D	233.5	1305.1	3.5	1301.6	10.4	1294.7
				Geo		
1	114.2	1304.8	2.3	1302.5	14.2	1290.6
2	119.0	1305.0	2.0	1303.0	14.8	1290.2
3	123.8	1305.3	1.1	1304.2	15.8	1289.5
4	129.1	1305.5	0.0	1305.5	16.7	1288.8
5	134.1	1305.6	0.3	1305.3	17.2	1288.4
6	139.2	1305.9	1.1	1304.8	17.7	1288.2
7	144.2	1305.9	1.3	1304.6	17.3	1288.6
8	148.9	1306.2	1.8	1304.4	17.0	1289.2
9	154.1	1306.3	2.1	1304.2	16.2	1290.1
10	159.1	1306.6	2.5	1304.1	15.5	1291.1
11	164.1	1307.1	3.1	1304.0	15.1	1292.0
12	168.9	1307.2	3.4	1303.8	14.4	1292.8
13	174.0	1307.5	3.3	1304.2	14.5	1293.0
14	178.8	1307.9	3.0	1304.9	15.2	1292.7
15	183.8	1307.9	2.3	1305.6	15.8	1292.1
16	189.1	1307.8	2.3	1305.5	16.2	1291.6
17	194.0	1307.6	2.1	1305.5	16.2	1291.4
18	198.9	1307.5	2.2	1305.3	16.0	1291.5
19	204.0	1307.4	2.4	1305.0	15.3	1292.1
20	208.9	1307.0	3.0	1304.0	14.1	1292.9
21	213.8	1306.7	3.4	1303.3	12.8	1293.9
22	218.4	1306.3	3.3	1303.0	11.8	1294.5
23	223.7	1305.8	2.8	1303.0	11.0	1294.8
24	228.7	1305.9	3.9	1302.0	10.9	1295.0

## SRK Grum Line 1 - West to East

Spread C Depth and Elev of layers directly beneath SPs and Geos for GRUM1.SIP

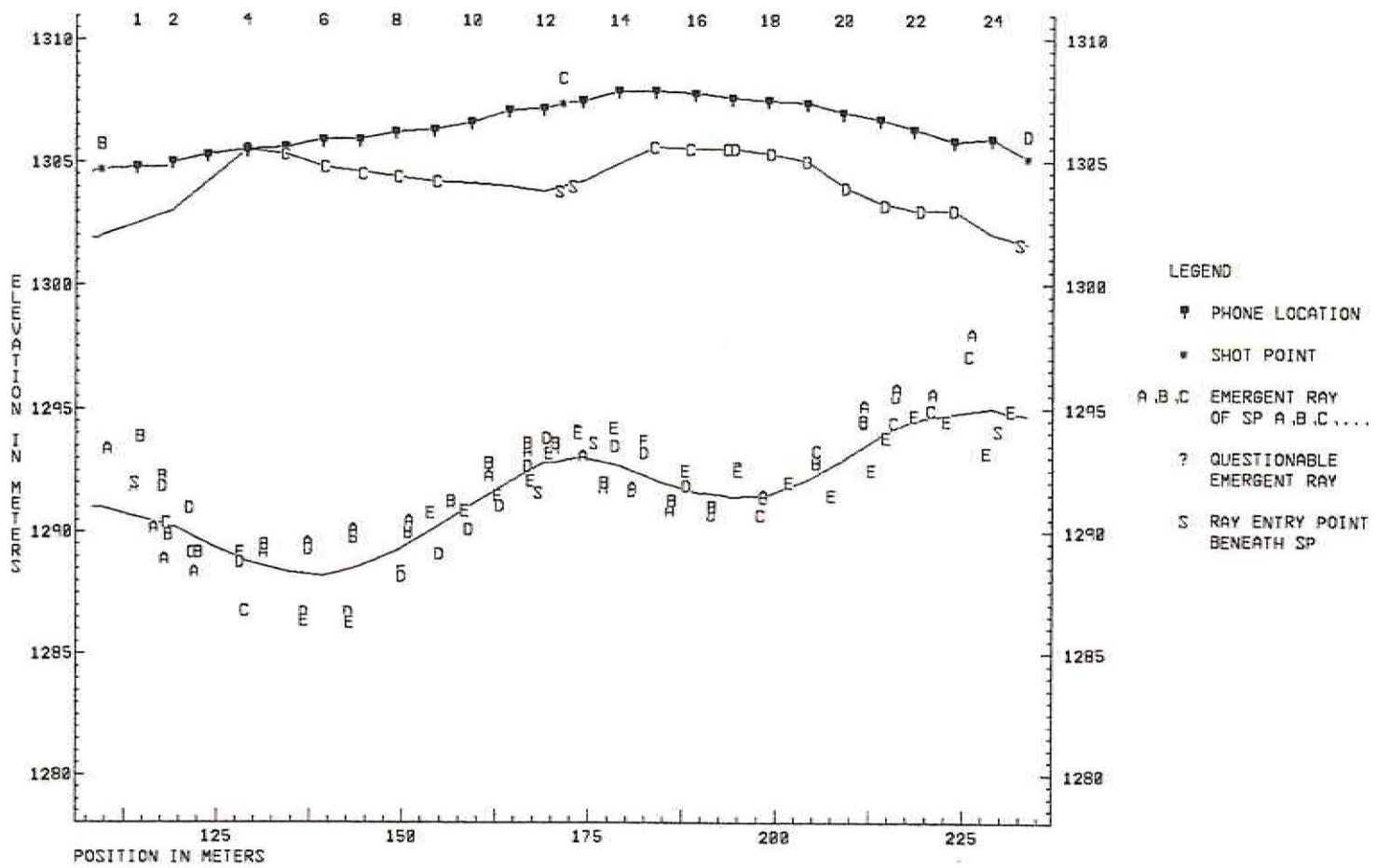
SP	Surface		Layer 2		Layer 3	
	X-Loc	Elev	Depth	Elev	Depth	Elev
B	171.5	1307.4	3.4	1304.0	14.5	1292.9

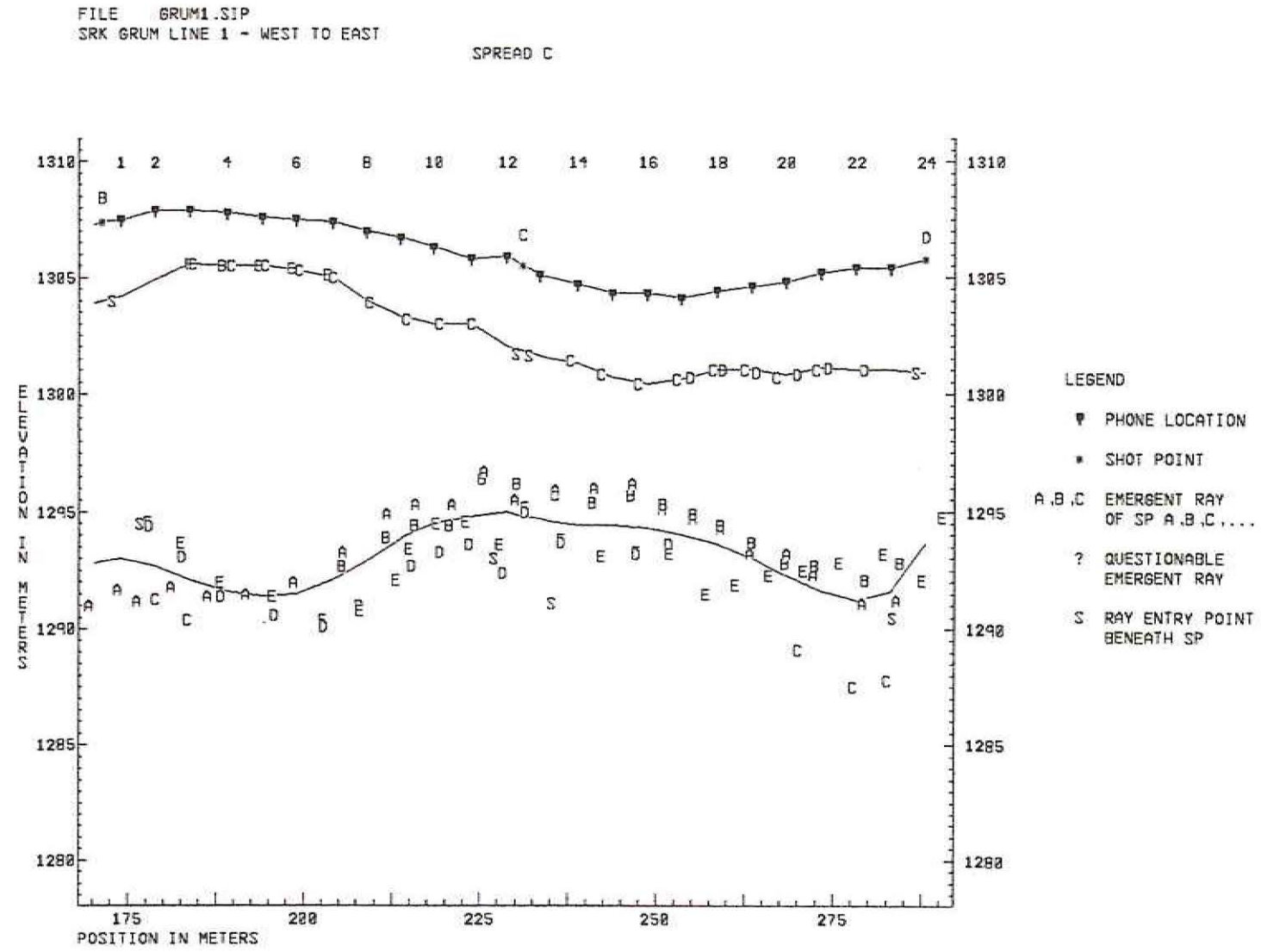




FILE GRUM1.SIP  
SRK GRUM LINE 1 - WEST TO EAST

SPREAD B





AURORA GEOSCIENCES LTD.

**LINE SL-2 - VANGORDA PIT**



## SIPT2 V-4.1 — SEISMIC REFRACTION INTERPRETATION PROGRAM — RIMROCK GEOPHYSICS, INC.

DATA FILE: VANGORDA.SIP

PRINT FILE: C:\DATA\VANGORDA\VANGORDA.OUT RUN DATE  
AND TIME: 11-09-2004 at 10:35

TITLE: SRK - Vangorda Pit - North to South

PROGRAM CONTROL DATA Printer Plot Scales Datum Plane Control Points Plot Control Special  
Control Parameters

Sprds	Elev	Horiz	Time	Point 1	Point 2	Elevations	Trace	Off	L					
Exit	V-Over	m/col	m/row	Elev	X-Loc	Elev	X-Loc	Bottom	BLim	TLim	Print			
									SP	Dip				
4	6	3	1	0.0	0.0	0.0	0.0	0	0	0.5	10.0	0	0	0

## VELOCITY OVERRIDES for VANGORDA.SIP

Layer	Spread 1	Spread 2	Spread 3	Spread 4
	Vv	Vh	Vv	Vh

2	2000	2000	2000	2000	2000	2000	2000	2000
---	------	------	------	------	------	------	------	------

## SHOTPOINT AND GEOPHONE INPUT DATA for VANGORDA.SIP

Spread A, 5 Shotpoints, 24 Geophones, X-Shift = 0.0, X-True = 1, Units: Meters.

SP	Elev	X-Loc	Y-Loc	Depth	UpHole	T	Fudge	T	End	SP
A	1203.8	-64.7	27.8	0.0	0.0	0.0	0.0	0	0	0
B	1197.1	-7.0	16.0	0.0	0.0	0.0	0.0	1		
C	1205.3	58.2	6.8	0.0	0.0	0.0	0.0	0		
D	1205.5	123.0	4.0	0.0	0.0	0.0	0.0	2		
E	1201.9	231.7	-18.5	0.0	0.0	0.0	0.0	0		

## Arrival Times + Fudge T and Layers represented

Geo	Elev	X-Loc	Y-Loc	SPA	SPB	SPC	SPD	SP E
				T-L	T-L	T-L	T-L	T-L
1	1199.1	0.0	15.1	42.1 3	13.0 1	33.4 3	44.1 3	69.1 3
2	1200.2	4.6	14.2	43.5 3	16.0 2	32.9 3	44.5 3	69.0 3
3	1201.1	10.5	13.0	44.8 3	18.5 2	32.6 3	43.5 3	68.8 3
4	1201.9	15.2	12.1	45.9 3	21.1 3	31.9 3	43.3 3	68.5 3
5	1202.6	20.1	11.2	47.1 3	23.1 3	31.1 3	42.9 3	68.5 3
6	1202.9	24.7	10.3	48.4 3	24.8 3	30.4 3	43.0 3	68.1 3
7	1203.5	29.0	9.4	49.6 3	25.8 3	29.0 2	42.3 3	67.8 3
8	1203.9	33.9	8.5	52.0 3	26.5 3	28.0 2	42.3 3	67.1 3
9	1204.3	38.8	7.5	52.0 3	27.4 3	25.3 2	41.8 3	66.5 3
10	1204.8	43.5	6.6	53.9 3	28.6 3	23.3 2	40.1 3	66.1 3
11	1205.0	48.1	5.7	55.8 3	29.6 3	18.8 2	38.6 3	64.6 3
12	1205.1	52.9	4.8	55.8 3	31.0 3	12.9 1	37.1 3	63.5 3
13	1205.3	58.2	3.8	57.6 3	32.3 3	5.3 1	35.5 3	62.4 3
14	1205.5	62.7	2.9	57.6 3	33.3 3	14.1 1	33.6 3	61.3 3
15	1205.6	67.7	1.9	59.4 3	34.0 3	19.3 1	31.3 3	59.6 3
16	1205.3	72.8	0.9	59.4 3	35.1 3	22.9 1	29.8 3	57.5 3
17	1205.7	77.5	0.0	61.3 3	36.1 3	26.8 2	28.1 3	56.5 3
18	1205.8	87.1	0.0	61.3 3	36.8 3	28.9 2	27.1 3	54.6 3
19	1205.7	92.1	0.0	61.9 3	37.5 3	30.1 2	25.5 3	52.9 3
20	1205.7	96.9	0.0	63.1 3	38.4 3	31.3 2	24.0 3	52.5 3
21	1205.5	102.0	0.0	64.3 3	39.0 3	32.9 2	21.9 2	51.8 3
22	1205.5	107.1	0.0	65.5 3	39.6 3	34.3 2	20.0 2	50.0 3

B C 2 7	2521	4.5	0.267	0.420	2	-0.362	4	-0.254	3	0.237	7
C D 21 22	2392	-6.7	0.000	0.000	21	-0.000	22				

Avg = 2489 for 8 Pts

		Spread D Avg Std Err 4 Highest Std Err at geophones										
SPs	Geos	V	TdSP	Overall	Err	Geo	Err	Geo	Err	Geo	Err	Geo
C D	13 16	1892	0.7	0.705	-0.914	15	0.770	16	0.596	13	-0.452	14
C E	15 19	3682	-2.6	0.403	-0.734	18	0.505	19	0.102	15	0.082	16

Avg = 2886 for 9 Pts

Avg of all Hobson-Overton velocities: 2648 for 32 points in Layer 2.

Wtd Avg Velocity computed for Layer 2 = 2577

Override Velocity assigned to Layer 2

Spread	A	B	C	D
-----	-----	-----	-----	-----
2000	2000	2000	2000	

Layer 3 Velocity computed by regression of raw uncorrected arrivals

Spread A											
V	Ti	Geos	<-SP->	Geos	Ti	V	Avg V	Avg Ti	Pts	-----	-----
-----	-----	-----	-----	-----	-----	-----	-----	-----	-----	-----	-----
		A	1 24	29.9	4827		4827	29.9	24		
		B	4 24	18.9	5409		5409	18.9	21		
8545	26.6	1 6	C				8545	26.6	6		
4412	19.6	1 20	D				4412	19.6	20		
5010	25.8	1 24	E				5010	25.8	24		

Avg = 5032 for 95 Pts

Spread B											
V	Ti	Geos	<-SP->	Geos	Ti	V	Avg V	Avg Ti	Pts	-----	-----
-----	-----	-----	-----	-----	-----	-----	-----	-----	-----	-----	-----
		A	1 24	17.9	4953		4953	17.9	24		
		B	8 24	22.9	4556		4556	22.9	17		
4740	26.8	1 19	D				4740	26.8	19		
4089	17.5	1 22	E				4089	17.5	22		

Avg = 4564 for 82 Pts

Spread C											
V	Ti	Geos	<-SP->	Geos	Ti	V	Avg V	Avg Ti	Pts	-----	-----
-----	-----	-----	-----	-----	-----	-----	-----	-----	-----	-----	-----
		A	1 24	21.0	5133		5133	21.0	24		
		B	8 24	22.4	5567		5567	22.4	17		
		C	23 24	13.5	4141		4141	13.5	2		
5145	22.3	1 20	D				5145	22.3	20		
5232	28.1	1 24	E				5232	28.1	24		

Avg = 5214 for 87 Pts

Spread D											
V	Ti	Geos	<-SP->	Geos	Ti	V	Avg V	Avg Ti	Pts	-----	-----
-----	-----	-----	-----	-----	-----	-----	-----	-----	-----	-----	-----
		A	1 17	19.4	5495		5495	19.4	17		

		B	4	21	18.1	5253	5253	18.1	18		
3661	11.3	1	3	C	20	21	18.5	9772	4882	14.9	5
3443	12.0	1	12	D				3443	12.0	12	
4584	15.0	1	14	E				4584	15.0	14	
5726	30.2	1	21	F				5726	30.2	21	

Avg = 4901 for 87 Pts

Avg of all regression velocities: 4924 for 351 points in Layer 3.

Layer 3 Velocity computed by Hobson-Overton method

		Spread A		Avg Std Err		4 Highest Std Err at geophones						
SPs	Geos	V	TdSP	Overall	Err	Geo	Err	Geo	Err	Geo		
A C	1 6	5535	7.4	0.224	-0.309	3	0.267	2	0.265	6	-0.241	4
A D	1 20	4482	8.4	1.388	-2.937	9	2.654	17	2.433	1	1.937	15
A E	1 24	4917	5.3	0.901	1.912	1	1.662	17	-1.625	9	1.520	2
B C	4 6	3724	-5.3	0.051	0.072	5	-0.037	6	-0.034	4		
B D	4 20	4293	-3.5	1.186	-2.221	9	2.033	17	-1.543	10	1.528	16
B E	4 24	4912	-8.0	0.765	1.620	17	1.567	16	-1.429	10	-1.079	9

Avg = 4705 for 91 Pts

		Spread B		Avg Std Err		4 Highest Std Err at geophones						
SPs	Geos	V	TdSP	Overall	Err	Geo	Err	Geo	Err	Geo		
A D	1 19	4864	-10.0	1.283	-2.541	11	-2.146	12	-1.736	10	1.696	19
A E	1 22	4492	-6.0	1.218	-3.368	22	1.953	17	1.866	14	-1.828	21
B D	8 19	4212	-3.6	0.767	-1.231	11	1.180	8	-1.152	12	1.065	16
B E	8 22	4730	2.9	1.381	2.350	16	1.954	15	-1.884	22	1.831	14

Avg = 4599 for 68 Pts

		Spread C		Avg Std Err		4 Highest Std Err at geophones						
SPs	Geos	V	TdSP	Overall	Err	Geo	Err	Geo	Err	Geo		
A D	1 20	4943	-1.2	1.264	3.188	1	2.233	2	-1.707	11	-1.605	10
A E	1 24	5181	-6.6	1.146	-2.334	24	2.048	1	1.781	2	-1.400	8
B D	8 20	4571	-1.2	0.498	1.204	14	-0.535	18	0.515	12	-0.483	11
B E	8 24	5126	-6.5	0.947	-2.288	24	1.582	14	-1.430	8	1.339	13
C E	23 24	12439	-19.1	0.000	0.000	24	0.000	23				

Avg = 5193 for 76 Pts

		Spread D		Avg Std Err		4 Highest Std Err at geophones						
SPs	Geos	V	TdSP	Overall	Err	Geo	Err	Geo	Err	Geo		
A C	1 3	3288	-5.1	0.021	-0.030	2	0.016	3	0.014	1		
A D	1 12	3997	-3.6	0.739	-1.515	1	1.169	6	0.952	8	0.663	5
A E	1 14	4892	0.4	0.958	-2.620	1	1.343	6	1.209	5	0.945	7
A F	1 17	5233	-9.8	1.433	-2.939	1	1.904	7	1.852	6	-1.849	16
B D	4 12	3703	2.0	0.436	-0.810	4	0.794	8	0.487	6	-0.293	10
B E	4 14	4508	2.1	0.282	-0.484	8	-0.347	12	0.346	11	0.337	5
B F	4 21	5786	-11.0	1.555	-3.450	4	-2.820	21	-1.991	20	-1.787	5
C F	20 21	10446	-18.5	0.000	-0.000	20	0.000	21				

Avg = 4921 for 86 Pts

Avg of all Hobson-Overton velocities: 4856 for 321 points in Layer 3.

Wtd Avg Velocity computed for Layer 3 = 4880

Arrival times Td corrected to datum. (Datum Elev = 1207.921 - 0.035x) for VANGORDA.SIP

Spread A		SP A	SP B	SP C	SP D	SP E
----------	--	------	------	------	------	------

Datum Elev .....		1210.2	1208.2	1205.9	1203.6	1199.7
------------------	--	--------	--------	--------	--------	--------

Geo .	X-Loc	Cor T	0.0	15.9	0.8	-2.7	0.0
			--Td--	--Td--	--Td--	--Td--	--Td--
1	1207.9	0.0	12.6	54.7	41.5	46.9	54.0
2	1207.8	4.6	10.8	54.3	42.7	44.5	52.6
3	1207.6	10.5	9.2	54.0	43.6	42.7	50.0
4	1207.4	15.2	7.9	53.8	44.8	40.6	48.4
5	1207.2	20.1	6.6	53.7	45.6	38.5	46.8
6	1207.0	24.7	5.9	54.3	46.6	37.2	46.2
7	1206.9	29.0	4.9	54.5	46.5	34.7	44.4
8	1206.7	33.9	4.0	56.0	46.4	32.9	43.6
9	1206.6	38.8	3.2	55.2	46.5	29.3	42.3
10	1206.4	43.5	2.3	56.2	46.7	26.4	39.6
11	1206.2	48.1	1.8	57.6	47.2	21.4	37.6
12	1206.1	52.9	1.4	57.2	48.2	15.1	35.7
13	1205.9	58.2	0.8	58.4	49.0	6.9	33.6
14	1205.7	62.7	0.3	57.9	49.5	15.2	31.2
15	1205.5	67.7	-0.1	59.3	49.8	20.0	28.5
16	1205.4	72.8	0.1	59.5	51.0	23.8	27.1
17	1205.2	77.5	-0.7	60.6	51.2	26.9	24.6
18	1204.8	87.1	-1.4	59.9	51.3	28.4	23.0
19	1204.7	92.1	-1.5	60.4	51.9	29.4	21.3
20	1204.5	96.9	-1.7	61.4	52.5	30.4	19.5
21	1204.3	102.0	-1.7	62.6	53.2	32.0	17.5
22	1204.1	107.1	-1.9	63.6	53.5	33.2	15.3
23	1204.0	112.2	-2.6	63.5	53.2	33.6	11.5
24	1203.8	117.0	-2.4	64.4	54.0	34.9	9.1

Spread B		SP A	SP B	SP C	SP D	SP E
----------	--	------	------	------	------	------

Datum Elev .....		1208.2	1204.0	1202.0	1199.7	1197.7
------------------	--	--------	--------	--------	--------	--------

Geo .	X-Loc	Cor T	0.0	-2.6	-3.9	-3.2	0.0
			--Td--	--Td--	--Td--	--Td--	--Td--
1	1203.8	117.0	-2.4	40.5	7.9	27.3	45.3
2	1203.6	121.6	-2.5	41.9	11.7	25.9	44.2
3	1203.5	126.3	-2.6	43.3	14.1	23.9	43.2
4	1203.3	131.1	-2.9	44.0	16.0	23.1	42.3
5	1203.1	136.0	-3.0	44.8	19.0	21.2	41.1
6	1203.0	140.9	-3.1	45.3	21.9	20.0	40.3
7	1202.8	145.6	-3.2	45.8	24.0	18.1	39.2
8	1202.6	150.6	-3.4	45.9	25.2	14.6	37.8
9	1202.4	155.6	-3.8	46.1	25.4	10.3	36.3
10	1202.3	160.5	-3.6	47.2	26.8	5.4	36.1
11	1202.1	165.4	-3.9	47.5	27.3	1.2	35.2
12	1201.9	170.3	-4.1	48.8	28.5	1.6	34.1
13	1201.7	175.4	-4.1	50.4	30.4	3.6	32.8
14	1201.6	180.6	-4.2	52.3	32.1	8.4	32.1
15	1201.4	185.3	-4.2	53.1	33.3	11.1	30.0
16	1201.2	190.3	-4.0	54.1	34.5	13.4	28.3
17	1201.0	194.9	-3.9	55.5	34.8	15.1	26.9
18	1200.9	200.0	-3.8	56.3	35.6	17.3	25.9

19	1200.7	204.9	-3.4	58.0	36.8	19.5	25.3	35.2
20	1200.5	209.9	-3.6	58.5	37.6	20.7	24.3	35.0
21	1200.4	214.6	-3.4	59.6	39.1	22.6	22.9	34.9
22	1200.2	219.7	-3.5	59.9	40.5	23.5	20.3	34.5
23	1200.0	224.7	-3.2	61.8	41.7	25.4	16.5	34.2
24	1199.9	228.8	-3.2	62.7	42.2	26.8	13.2	33.3

Spread C                    SP A    SP B    SP C    SP D    SP E

Datum Elev . . . . . 1201.8 1199.9 1197.7 1195.6 1192.3

Geo	X-Loc	Cor T	0.0	-3.1	-0.4	0.2	0.0	
---	---	---	--Td--	--Td--	--Td--	--Td--	--Td--	
1	1199.9	228.8	-3.2	30.4	4.6	25.9	41.8	65.2
2	1199.7	233.6	-3.2	30.7	8.0	25.2	41.1	63.9
3	1199.5	238.6	-2.9	30.6	10.0	24.0	41.0	63.5
4	1199.3	243.6	-2.8	30.5	12.2	22.3	39.8	62.6
5	1199.2	247.9	-2.9	31.4	14.6	21.1	38.9	62.2
6	1199.0	253.2	-2.4	33.4	17.8	20.2	38.8	61.9
7	1198.8	257.4	-2.2	35.2	20.9	19.8	39.1	61.7
8	1198.7	262.6	-2.2	36.3	22.5	19.2	38.6	61.4
9	1198.5	267.7	-2.2	37.2	23.5	17.4	37.5	60.3
10	1198.3	271.9	-2.1	38.4	25.2	16.0	37.2	59.7
11	1198.2	276.2	-1.9	39.6	26.4	13.6	36.8	58.9
12	1198.0	280.8	-1.3	41.6	28.5	11.2	36.0	58.5
13	1197.8	285.7	-0.7	43.1	30.0	7.0	35.4	57.3
14	1197.7	290.2	-0.4	44.5	31.0	3.4	33.7	56.4
15	1197.5	295.2	-0.1	45.9	32.2	8.4	33.4	56.5
16	1197.3	300.2	-0.1	46.8	32.9	12.8	32.4	55.7
17	1197.2	304.8	0.2	47.7	33.6	15.1	31.0	54.7
18	1197.0	309.7	0.3	48.9	34.6	17.2	30.4	53.8
19	1196.8	314.6	0.6	50.0	35.5	19.3	28.8	52.5
20	1196.6	319.9	0.6	50.6	36.4	21.3	27.7	51.5
21	1196.5	325.0	0.9	51.2	37.7	23.1	26.6	50.5
22	1196.3	329.8	1.0	51.6	38.7	23.8	23.3	49.4
23	1196.1	334.8	1.2	52.6	39.6	25.0	21.9	49.6
24	1195.9	339.8	0.8	53.1	39.7	25.8	19.0	49.6

Spread D                    SP A    SP B    SP C    SP D    SP E    SP F

Datum Elev . . . . . 1199.7 1196.1 1194.2 1193.2 1192.3 1190.3

Geo	X-Loc	Cor T	0.0	1.2	1.5	4.3	5.8	0.0	
---	---	---	--Td--	--Td--	--Td--	--Td--	--Td--	--Td--	
1	1195.9	339.8	0.8	37.8	14.9	26.8	40.1	45.0	61.4
2	1195.8	345.0	0.2	39.2	16.3	25.2	37.3	41.9	59.7
3	1195.6	349.7	0.3	40.6	19.4	23.6	36.1	40.7	57.9
4	1195.4	354.2	0.9	41.7	21.9	23.0	35.7	39.8	57.5
5	1195.3	359.3	0.8	43.7	24.0	22.0	34.1	39.1	56.2
6	1195.1	364.1	1.0	45.4	25.6	20.9	32.9	38.7	55.0
7	1194.9	369.0	0.7	46.1	26.7	18.7	31.8	37.8	53.8
8	1194.7	373.8	0.9	47.3	28.5	17.3	30.2	38.0	53.3
9	1194.6	378.7	1.1	47.5	29.4	13.9	29.2	36.4	52.4
10	1194.4	383.9	0.8	47.9	30.0	9.4	27.4	34.6	50.4
11	1194.2	388.6	1.5	49.5	31.5	7.4	26.4	33.6	50.5
12	1194.1	393.1	1.4	49.7	32.1	11.8	24.6	33.0	49.8
13	1193.9	398.6	2.4	51.4	34.3	17.4	24.1	32.5	49.8
14	1193.7	403.0	3.2	52.7	36.2	18.9	22.3	31.9	50.2
15	1193.5	407.8	3.2	54.0	37.0	20.2	19.4	30.9	49.5
16	1193.4	412.6	4.3	55.6	39.0	22.8	16.2	30.9	50.6
17	1193.2	417.3	4.3	57.1	39.8	24.8	14.0	30.4	50.1
18	1193.0	422.2	5.2	59.2	41.5	27.1	16.9	30.8	50.5
19	1192.9	427.1	5.5	60.9	42.2	28.9	22.1	28.7	50.5

20	1192.7	432.0	5.9	61.7	42.5	30.3	28.5	22.6	50.3
21	1192.5	436.9	6.0	63.6	43.1	31.0	30.3	17.9	50.0

Arrival times Tc corrected to top of Layer 2 and Elev of top of Layer 2 for VANGORDA.SIP

Spread A		SP A	SP B	SP C	SP D	SP E
Elev .....		0.0	1191.8	1198.9	1203.2	0.0
Geo .	X-Loc	Cor T	7.6	7.6	9.1	3.2
— .	— —	—Tc—	—Tc—	—Tc—	—Tc—	—Tc—
1	1192.6	0.0	9.3	0.2	0.0	15.0
2	1193.1	4.6	10.1	0.8	-1.7	13.7
3	1193.8	10.5	10.4	1.9	0.5	13.1
4	1194.4	15.2	10.5	2.9	3.1	12.3
5	1194.9	20.1	10.5	4.0	5.0	11.5
6	1195.4	24.7	10.6	5.3	6.6	10.7
7	1195.9	29.0	10.6	6.4	7.6	9.3
8	1196.4	33.9	10.7	8.8	8.2	8.2
9	1196.7	38.8	10.9	8.6	8.9	5.3
10	1197.1	43.5	11.0	10.4	10.0	3.2
11	1198.0	48.1	10.0	13.2	12.0	-0.3
12	1198.9	52.9	8.9	14.4	14.5	0.0
13	1198.9	58.2	9.1	15.9	15.6	0.0
14	1199.5	62.7	8.5	16.6	17.2	0.0
15	1200.1	67.7	7.8	19.1	18.7	0.0
16	1200.7	72.8	7.0	19.8	20.5	0.0
17	1201.3	77.5	6.4	22.4	22.2	11.3
18	1203.1	87.1	3.8	24.9	25.4	16.0
19	1204.0	92.1	2.5	26.9	27.4	18.5
20	1204.6	96.9	1.6	28.9	29.2	20.6
21	1204.0	102.0	2.2	29.6	29.3	21.6
22	1203.6	107.1	2.7	30.3	29.3	22.5
23	1203.4	112.2	3.5	30.0	28.9	22.8
24	1203.2	117.0	3.3	31.0	29.7	24.1
Spread B		SP A	SP B	SP C	SP D	SP E
Elev .....		0.0	1203.3	1199.8	1198.6	0.0
Geo .	X-Loc	Cor T	3.5	3.5	7.1	4.8
— .	— —	—Tc—	—Tc—	—Tc—	—Tc—	—Tc—
1	1203.2	117.0	3.3	18.4	0.0	23.2
2	1203.2	121.6	3.2	20.0	10.2	22.1
3	1203.4	126.3	2.7	21.9	13.1	20.6
4	1203.4	131.1	2.7	22.9	15.2	20.0
5	1202.9	136.0	3.4	23.2	17.7	17.6
6	1202.2	140.9	4.1	23.1	20.0	15.7
7	1201.8	145.6	4.6	23.2	21.7	13.4
8	1201.2	150.6	5.3	22.8	22.5	0.0
9	1200.7	155.6	6.1	22.6	22.3	0.0
10	1200.1	160.5	6.8	22.8	22.8	0.0
11	1199.5	165.4	7.5	22.6	22.7	0.0
12	1200.0	170.3	6.9	24.8	24.9	0.0
13	1200.9	175.4	5.4	27.9	28.2	0.0
14	1201.8	180.6	3.8	31.4	31.6	0.0
15	1202.6	185.3	2.4	33.6	34.1	9.6
16	1202.9	190.3	1.5	35.4	36.1	12.7
17	1203.1	194.9	1.0	37.1	36.8	14.8
18	1203.1	200.0	0.6	38.3	37.9	17.2
19	1201.7	204.9	2.1	38.1	37.3	17.7
20	1200.3	209.9	3.9	37.0	36.4	17.1

21	1199.6	214.6	4.5	37.3	37.1	18.2	20.1	22.4
22	1199.3	219.7	4.8	37.4	38.3	18.9	17.4	21.8
23	1199.4	224.7	4.1	39.7	39.9	21.3	13.9	13.9
24	1199.9	228.8	3.2	41.5	41.4	23.6	0.0	13.9

Spread C			SP A	SP B	SP C	SP D	SP E
Elev . . . . .	0.0	1199.6	1194.9	1191.7	0.0		

Geo .	X-Loc	Cor T	3.6	3.6	4.4	5.3	5.3	
-- .	---	---	--Tc--	--Tc--	--Tc--	--Tc--	--Tc--	
1	1199.5	228.8	3.7	15.9	0.0	21.5	35.8	36.2
2	1198.5	233.6	4.8	15.0	5.9	19.6	34.0	33.8
3	1200.1	238.6	2.0	17.5	10.5	20.9	36.3	35.9
4	1200.2	243.6	1.5	17.7	13.0	19.6	35.6	35.4
5	1200.0	247.9	1.7	18.5	15.3	18.2	34.6	34.9
6	1199.4	253.2	1.8	19.9	18.0	16.8	33.9	34.0
7	1199.0	257.4	2.0	21.3	20.7	16.0	33.8	33.4
8	1199.1	262.6	1.5	23.0	22.7	16.0	33.8	33.6
9	1198.5	267.7	2.1	23.2	23.1	13.4	32.0	31.9
10	1198.0	271.9	2.6	23.9	24.2	11.6	31.2	30.7
11	1197.8	276.2	2.5	25.0	25.4	9.0	30.7	29.9
12	1197.4	280.8	2.2	26.7	27.2	6.3	29.5	29.2
13	1196.1	285.7	3.3	26.4	26.9	0.0	27.1	26.2
14	1194.9	290.2	4.4	26.4	26.6	0.0	24.2	23.9
15	1195.0	295.2	3.8	28.1	28.0	0.0	24.2	24.3
16	1195.1	300.2	3.2	29.6	29.3	5.6	23.8	24.1
17	1195.1	304.8	2.7	30.8	30.3	8.2	22.5	23.3
18	1195.1	309.7	2.4	32.1	31.4	10.5	22.2	22.6
19	1195.2	314.6	1.8	33.6	32.7	12.9	20.9	21.6
20	1195.0	319.9	1.8	34.2	33.6	14.9	19.7	20.7
21	1193.8	325.0	2.8	33.5	33.5	15.4	17.3	18.3
22	1193.4	329.8	3.2	33.4	34.0	15.7	13.6	16.7
23	1192.3	334.8	4.3	33.1	33.8	15.6	10.9	15.6
24	1191.8	339.8	5.2	33.0	33.3	15.8	0.0	15.1

Spread D			SP A	SP B	SP C	SP D	SP E	SP F
Elev . . . . .	0.0	1192.3	1189.9	1187.7	1182.3	0.0		

Geo .	X-Loc	Cor T	4.3	4.3	4.7	3.6	8.7	8.7	
-- .	---	---	--Tc--	--Tc--	--Tc--	--Tc--	--Tc--	--Tc--	
1	1191.8	339.8	5.2	8.2	0.0	14.6	26.1	24.5	24.2
2	1191.3	345.0	6.2	9.2	4.4	12.6	23.0	21.0	22.1
3	1191.5	349.7	5.6	11.2	8.1	11.6	22.3	20.4	20.8
4	1192.5	354.2	3.3	13.9	12.2	12.5	23.5	21.1	22.0
5	1193.4	359.3	1.8	17.6	15.9	13.3	23.6	22.0	22.4
6	1192.7	364.1	2.4	18.4	16.8	11.3	21.5	20.8	20.3
7	1192.1	369.0	3.3	18.6	17.2	8.5	19.9	19.4	18.6
8	1191.6	373.8	3.6	19.3	18.6	6.6	17.8	19.1	17.6
9	1191.4	378.7	3.4	19.5	19.4	3.2	16.8	17.5	16.7
10	1190.6	383.9	4.1	19.5	19.6	0.0	14.6	15.2	14.3
11	1189.9	388.6	4.7	19.7	19.9	0.0	12.2	13.0	13.0
12	1189.2	393.1	5.1	19.6	20.2	0.0	10.1	12.0	12.0
13	1188.3	398.6	5.6	19.8	20.9	3.2	8.1	10.0	10.6
14	1188.4	403.0	4.9	21.1	22.7	4.7	6.3	9.5	10.9
15	1188.5	407.8	4.1	23.2	24.3	6.7	4.2	9.2	11.0
16	1188.7	412.6	2.5	25.3	26.8	9.9	1.5	9.8	12.6
17	1187.7	417.3	3.6	25.6	26.4	10.6	0.0	8.0	10.9
18	1186.9	422.2	3.6	0.0	27.2	12.0	0.0	7.5	10.4
19	1186.0	427.1	4.3	0.0	26.9	12.9	0.0	4.4	9.5
20	1184.4	432.0	6.0	0.0	25.2	12.2	8.6	0.0	7.1
21	1182.9	436.9	7.8	0.0	23.8	11.0	8.6	0.0	5.0

## SRK - Vangorda Pit - North to South

Spread A Points of emergence of refracted rays below target geophones for VANGORDA.SIP

Geo	SP A	SP B	SP C	SP D	SP E
---	-----L	-----L	-----L	-----L	-----L
1	X-Loc -0.4 3	-- 1	1.8 3	1.7 3	1.6 3
	Elev 1192.5	---	1192.3	1193.5	1194.3
2	X-Loc 4.6 3	2.8 2	6.6 3	6.2 3	5.5 3
	Elev 1193.8	1192.9	1193.1	1193.8	1194.8
3	X-Loc 10.6 3	8.8 2	12.6 3	12.2 3	12.0 3
	Elev 1194.7	1193.6	1193.4	1194.5	1195.1
4	X-Loc 15.4 3	15.4 3	17.4 3	17.0 3	16.7 3
	Elev 1195.4	1195.4	1194.0	1194.8	1195.4
5	X-Loc 20.2 3	20.1 3	22.3 3	21.8 3	21.5 3
	Elev 1195.9	1195.4	1193.9	1195.0	1195.7
6	X-Loc 24.6 3	24.1 3	27.2 3	27.1 3	26.6 3
	Elev 1196.3	1195.0	1193.6	1193.8	1195.0
7	X-Loc 28.7 3	28.2 3	32.6 2	31.6 3	31.2 3
	Elev 1196.4	1195.3	1196.4	1194.0	1194.8
8	X-Loc 32.7 3	33.1 3	36.7 2	36.6 3	35.9 3
	Elev 1194.9	1195.7	1196.6	1193.0	1194.5
9	X-Loc 37.7 3	37.6 3	42.4 2	41.7 3	41.1 3
	Elev 1196.3	1196.1	1196.9	1192.6	1194.2
10	X-Loc 41.9 3	42.2 3	47.8 2	46.6 3	46.5 3
	Elev 1195.5	1196.1	1197.9	1193.3	1193.5
11	X-Loc 45.3 3	46.2 3	52.1 2	51.5 3	51.4 3
	Elev 1193.7	1195.3	1198.9	1193.1	1193.3
12	X-Loc 49.8 3	49.8 3	-- 1	56.2 3	56.3 3
	Elev 1193.8	1193.8	--	1193.0	1192.8
13	X-Loc 54.4 3	54.6 3	-- 1	61.9 3	62.2 3
	Elev 1193.0	1193.6	--	1193.6	1192.8
14	X-Loc 59.6 3	59.3 3	-- 1	66.2 3	66.9 3
	Elev 1193.8	1193.3	--	1194.4	1192.7
15	X-Loc 63.7 3	64.0 3	-- 1	70.6 3	71.4 3
	Elev 1192.4	1193.1	--	1195.1	1192.9
16	X-Loc 67.9 3	67.6 3	-- 1	75.6 3	76.1 3
	Elev 1192.4	1191.9	--	1194.3	1192.7
17	X-Loc 71.5 3	71.8 3	76.7 2	80.4 3	81.1 3
	Elev 1191.3	1191.7	1201.1	1194.7	1192.3
18	X-Loc 79.2 3	79.0 3	86.7 2	91.7 3	92.1 3
	Elev 1191.1	1190.8	1203.1	1191.2	1189.8
19	X-Loc 83.1 3	82.8 3	91.7 2	96.6 3	96.9 3
	Elev 1190.3	1189.9	1203.9	1190.6	1189.3
20	X-Loc 87.8 3	87.8 3	96.6 2	101.0 3	101.7 3
	Elev 1189.1	1189.0	1204.6	1190.3	1187.8
21	X-Loc 92.8 3	93.1 3	101.2 2	102.5 2	105.6 3
	Elev 1188.8	1189.4	1204.1	1203.9	1187.4
22	X-Loc 97.1 3	97.9 3	106.3 2	107.7 2	109.1 3
	Elev 1188.8	1190.0	1203.7	1203.6	1188.2
23	X-Loc 102.4 3	103.4 3	111.1 2	113.1 2	113.1 3
	Elev 1189.7	1191.1	1203.4	1203.3	1188.3
24	X-Loc 105.7 3	106.9 3	116.1 2	-- 1	118.4 3
	Elev 1189.6	1191.1	1203.2	--	1186.8

Spread A Points of entry of refracted rays below source shotpoints:

L=2	Right	X-Loc	--	-4.5	59.8	--	--
		Elev	--	1192.1	1198.8	--	--
L=2	Left	X-Loc	--	--	55.7	122.4	--
		Elev	--	--	1199.0	1203.2	--

L=3	Right	X-Loc	-5.8	-5.8	---	---	---
		Elev	1191.9*	1191.9	---	---	---
L=3	Left	X-Loc	---	---	54.0	111.0	111.0
		Elev	---	---	1192.4	1187.8	1187.8*

## SRK - Vangorda Pit - North to South

## Spread B Points of emergence of refracted rays below target geophones for VANGORDA.SIP

Geo	SP A	SP B	SP C	SP D	SP E
1	X-Loc 103.1 3	— 1	117.8 2	118.9 3	119.1 3
	Elev 1185.1	—	1203.2	1182.0	1179.2
2	X-Loc 105.8 3	120.7 2	122.6 2	124.8 3	125.1 3
	Elev 1184.5	1203.2	1203.2	1180.7	1177.9
3	X-Loc 108.3 3	125.7 2	126.9 2	149.2 3	151.3 3
	Elev 1183.4	1203.4	1203.4	1180.3	1178.1
4	X-Loc 110.5 3	130.3 2	131.6 2	151.6 3	153.0 3
	Elev 1183.4	1203.4	1203.4	1179.9	1178.3
5	X-Loc 114.9 3	134.9 2	136.5 2	154.7 3	155.7 3
	Elev 1182.7	1203.0	1202.8	1180.8	1179.7
6	X-Loc 123.1 3	139.5 2	141.7 2	156.9 3	157.2 3
	Elev 1182.8	1202.4	1202.1	1180.9	1180.4
7	X-Loc 129.7 3	144.2 2	146.3 2	158.6 3	158.7 3
	Elev 1182.6	1201.9	1201.7	1181.3	1181.2
8	X-Loc 148.0 3	148.2 3	— 1	161.4 3	161.0 3
	Elev 1184.4	1185.3	—	1182.3	1183.0
9	X-Loc 152.9 3	153.0 3	— 1	163.7 3	163.1 3
	Elev 1186.2	1187.2	—	1183.1	1184.4
10	X-Loc 157.1 3	157.2 3	— 1	165.8 3	165.0 3
	Elev 1186.9	1187.5	—	1182.7	1185.2
11	X-Loc 160.5 3	160.7 3	— 1	168.8 3	168.3 3
	Elev 1188.0	1188.5	—	1182.6	1185.2
12	X-Loc 164.1 3	164.4 3	— 1	173.7 3	173.3 3
	Elev 1187.2	1187.7	—	1181.3	1184.2
13	X-Loc 165.3 3	165.5 3	— 1	180.8 3	180.1 3
	Elev 1185.4	1185.7	—	1179.3	1182.6
14	X-Loc 166.5 3	166.8 3	— 1	187.8 3	186.7 3
	Elev 1183.3	1183.7	—	1177.1	1181.2
15	X-Loc 169.2 3	169.2 3	185.0 2	200.2 3	198.5 3
	Elev 1182.0	1182.1	1202.6	1176.8	1179.8
16	X-Loc 173.8 3	173.7 3	190.0 2	203.9 3	202.6 3
	Elev 1180.6	1180.5	1202.9	1177.0	1179.6
17	X-Loc 177.4 3	178.1 3	194.6 2	206.8 3	205.9 3
	Elev 1179.3	1180.2	1203.1	1177.2	1179.2
18	X-Loc 184.1 3	184.8 3	199.9 2	211.4 3	211.0 3
	Elev 1178.4	1179.5	1203.1	1176.9	1178.0
19	X-Loc 190.3 3	191.2 3	204.0 2	219.7 3	219.2 3
	Elev 1178.3	1179.9	1201.9	1178.1	1178.9
20	X-Loc 201.2 3	201.7 3	208.1 2	210.6 2	226.8 3
	Elev 1179.8	1181.1	1200.7	1200.1	1180.3
21	X-Loc 205.2 3	205.6 3	213.0 2	215.7 2	232.3 3
	Elev 1180.4	1181.2	1199.7	1199.4	1180.4
22	X-Loc 210.7 3	210.5 3	218.3 2	220.8 2	236.2 3
	Elev 1181.3	1181.0	1199.3	1199.2	1179.9
23	X-Loc 218.9 3	219.0 3	223.5 2	226.4 2	226.4 2
	Elev 1180.4	1180.8	1199.1	1199.5	1199.5
24	X-Loc 226.0 3	226.1 3	228.5 2	— 1	228.9 2
	Elev 1180.9	1181.6	1199.9	—	1199.9

Spread B Points of entry of refracted rays below source shotpoints:

L=2	Right	X-Loc	---	113.2	170.5	—	—
	Elev	—	1203.3	1200.0	—	—	
L=2	Left	X-Loc	---	—	166.8	232.2	232.2
	Elev	—	—	1199.4	1196.9	1196.9*	
L=3	Right	X-Loc	115.1	115.1	—	—	—
	Elev	1187.2*	1187.2	—	—	—	
L=3	Left	X-Loc	---	—	229.5	229.5	—
	Elev	—	—	—	1180.2	1180.2*	—

## SRK - Vangorda Pit - North to South

Spread C Points of emergence of refracted rays below target geophones for VANGORDA.SIP

Geo		SP A	SP B	SP C	SP D	SP E
---		—	—	—	—	—
1	X-Loc	225.7 3	— 1	228.9 2	237.2 3	236.6 3
	Elev	1179.1	—	1199.9	1184.7	1185.7
2	X-Loc	232.4 3	231.4 2	235.9 2	239.2 3	238.6 3
	Elev	1183.8	1199.1	1199.2	1184.5	1186.3
3	X-Loc	234.8 3	238.6 2	239.1 2	244.2 3	243.6 3
	Elev	1183.4	1200.2	1200.2	1181.8	1183.8
4	X-Loc	238.3 3	243.2 2	243.9 2	248.3 3	247.9 3
	Elev	1184.5	1200.2	1200.2	1181.2	1182.9
5	X-Loc	239.5 3	247.4 2	248.2 2	252.5 3	252.2 3
	Elev	1184.4	1200.0	1200.0	1180.8	1182.0
6	X-Loc	242.9 3	252.6 2	253.6 2	257.9 3	257.6 3
	Elev	1183.7	1199.5	1199.4	1179.6	1181.0
7	X-Loc	245.7 3	256.7 2	258.0 2	262.5 3	262.1 3
	Elev	1182.7	1199.0	1199.0	1178.1	1180.0
8	X-Loc	250.3 3	250.4 3	262.9 2	269.0 3	268.5 3
	Elev	1181.8	1182.0	1199.2	1176.4	1178.1
9	X-Loc	255.6 3	255.7 3	268.1 2	276.5 3	275.8 3
	Elev	1181.8	1181.9	1198.4	1176.3	1178.0
10	X-Loc	259.7 3	259.4 3	272.5 2	283.9 3	282.8 3
	Elev	1181.4	1181.0	1197.9	1176.2	1178.2
11	X-Loc	264.1 3	263.8 3	276.7 2	287.3 3	286.0 3
	Elev	1180.6	1180.2	1197.8	1175.7	1178.2
12	X-Loc	268.7 3	268.3 3	280.9 2	291.2 3	290.3 3
	Elev	1179.1	1178.6	1197.4	1175.9	1177.8
13	X-Loc	276.2 3	276.0 3	— 1	292.8 3	291.9 3
	Elev	1179.1	1178.5	—	1176.6	1179.2
14	X-Loc	283.8 3	283.7 3	— 1	295.9 3	295.3 3
	Elev	1179.8	1179.6	—	1178.2	1180.0
15	X-Loc	289.1 3	289.1 3	— 1	302.3 3	301.8 3
	Elev	1179.4	1179.5	—	1176.7	1178.1
16	X-Loc	291.9 3	292.0 3	299.5 2	308.9 3	308.4 3
	Elev	1179.1	1179.4	1195.1	1176.1	1177.2
17	X-Loc	295.5 3	295.8 3	304.1 2	314.3 3	313.9 3
	Elev	1178.8	1179.3	1195.1	1176.5	1177.1
18	X-Loc	298.6 3	299.1 3	309.1 2	323.5 3	322.7 3
	Elev	1178.2	1179.0	1195.1	1176.5	1177.6
19	X-Loc	306.2 3	306.7 3	314.2 2	327.0 3	326.5 3
	Elev	1177.4	1178.4	1195.2	1177.1	1177.9
20	X-Loc	312.8 3	313.1 3	319.4 2	336.0 3	335.4 3
	Elev	1177.9	1178.5	1195.1	1179.0	1179.6
21	X-Loc	321.4 3	321.4 3	323.8 2	325.6 2	337.1 3
	Elev	1179.8	1179.7	1194.0	1193.7	1180.3
22	X-Loc	326.4 3	326.2 3	328.8 2	330.1 2	337.6 3
	Elev	1181.3	1180.5	1193.5	1193.4	1180.5
23	X-Loc	333.8 3	333.8 3	334.1 3	335.5 2	341.7 3
	Elev	1183.4	1182.7	1187.9	1192.2	1180.2

24	X-Loc	336.7 3	336.6 3	338.2 3	— 1	345.9 3
	Elev	1184.3	1184.0	1188.7	—	1179.9

## Spread C Points of entry of refracted rays below source shotpoints:

L=2	Right	X-Loc	—	228.2	291.7	—	—
		Elev	—	1199.9	1194.6	—	—
L=2	Left	X-Loc	—	—	288.0	349.6	—
		Elev	—	—	1195.2	1191.4	—
L=3	Right	X-Loc	236.9	236.9	293.8	—	—
		Elev	1184.3*	1184.3	1184.9	—	—
L=3	Left	X-Loc	—	—	—	345.2	345.2
		Elev	—	—	1180.1	1180.1*	

## SRK - Vangorda Pit - North to South

## Spread D Points of emergence of refracted rays below target geophones for VANGORDA.SIP

Geo	SP A		SP B		SP C		SP D		SP E		SP F	
	—	—	—	—	—	—	—	—	—	—	—	—
1	X-Loc	336.7 3	— 1	343.2 3	345.8 3	343.8 3	343.6 3					
	Elev	1184.3	—	1185.5	1180.4	1184.4	1184.8					
2	X-Loc	341.6 3	342.8 2	348.2 3	350.0 3	348.0 3	348.5 3					
	Elev	1184.9	1191.2	1186.5	1182.6	1186.9	1185.8					
3	X-Loc	346.0 3	348.7 2	351.7 3	352.5 3	351.6 3	351.7 3					
	Elev	1183.9	1191.3	1186.2	1182.1	1186.3	1185.8					
4	X-Loc	348.7 3	349.3 3	355.5 2	357.9 3	356.7 3	356.9 3					
	Elev	1182.5	1183.5	1192.8	1179.8	1184.6	1183.5					
5	X-Loc	349.3 3	350.0 3	359.6 2	366.6 3	364.8 3	365.0 3					
	Elev	1180.3	1181.2	1193.5	1178.6	1182.5	1182.1					
6	X-Loc	354.4 3	355.1 3	364.6 2	372.6 3	370.7 3	370.4 3					
	Elev	1179.2	1180.2	1192.6	1179.6	1182.6	1183.1					
7	X-Loc	360.3 3	360.7 3	369.7 2	377.0 3	375.2 3	374.6 3					
	Elev	1179.3	1180.0	1192.0	1180.4	1183.2	1184.0					
8	X-Loc	368.0 3	368.0 3	374.7 2	380.8 3	380.2 3	379.2 3					
	Elev	1179.1	1179.2	1191.5	1181.7	1182.5	1184.1					
9	X-Loc	375.5 3	375.3 3	379.2 2	385.1 3	384.1 3	383.6 3					
	Elev	1180.6	1179.9	1191.4	1182.1	1183.5	1184.3					
10	X-Loc	381.1 3	380.8 3	— 1	388.5 3	387.6 3	386.9 3					
	Elev	1182.2	1181.3	—	1183.6	1185.1	1186.1					
11	X-Loc	385.7 3	385.4 3	— 1	390.9 3	390.4 3	390.4 3					
	Elev	1182.5	1181.6	—	1184.2	1185.6	1185.5					
12	X-Loc	389.3 3	388.6 3	— 1	394.1 3	394.1 3	394.1 3					
	Elev	1183.9	1182.5	—	1185.6	1185.7	1185.7					
13	X-Loc	394.7 3	393.5 3	396.6 2	399.1 2	399.2 3	399.3 3					
	Elev	1183.7	1181.8	1188.7	1188.2	1185.2	1184.6					
14	X-Loc	398.1 3	396.2 3	400.5 2	405.6 2	403.8 3	404.1 3					
	Elev	1182.9	1180.4	1187.9	1188.0	1183.7	1182.2					
15	X-Loc	401.3 3	399.7 3	407.6 2	408.9 2	408.9 2	408.8 3					
	Elev	1181.8	1180.0	1188.6	1188.6	1188.6	1180.8					
16	X-Loc	404.8 3	402.8 3	412.0 2	412.8 2	412.8 2	415.9 3					
	Elev	1180.3	1178.0	1188.7	1188.7	1188.7	1177.1					
17	X-Loc	408.8 3	407.5 3	415.8 2	— 1	417.9 2	422.2 3					
	Elev	1179.7	1178.2	1188.0	—	1187.5	1177.2					
18	X-Loc	— 0	414.9 3	420.9 2	— 1	422.7 2	429.6 3					
	Elev	—	1176.9	1187.1	—	1186.8	1176.8					
19	X-Loc	— 0	423.8 3	425.6 2	— 1	427.2 2	433.8 3					
	Elev	—	1177.8	1186.4	—	1186.1	1176.7					
20	X-Loc	— 0	429.8 3	430.0 3	429.3 2	— 1	436.6 3					
	Elev	—	1180.2	1180.9	1185.4	—	1177.5					
21	X-Loc	— 0	435.2 3	435.4 3	433.1 2	— 1	438.6 3					

Elev	—	1182.4	1183.0	1184.0	—	1178.0
------	---	--------	--------	--------	---	--------

## Spread D Points of entry of refracted rays below source shotpoints:

L=2 Right X-Loc	—	335.5	389.3	417.9	—	---
Elev	—	1192.2	1189.8	1187.5	—	---
L=2 Left X-Loc	—	—	386.9	415.8	438.9	—
Elev	—	—	1190.2	1188.0	1182.3	—
L=3 Right X-Loc	340.8	340.8	390.1	—	—	—
Elev	1181.2*	1181.2	1186.3	—	—	—
L=3 Left X-Loc	—	—	386.9	408.1	440.0	440.0
Elev	—	—	1186.5	1178.9	1181.8	1181.8*

## SRK - Vangorda Pit - North to South

## Spread A Depth and Elev of layers directly beneath SPs and Geos for VANGORDA.SIP

SP	Surface		Layer 2		Layer 3	
	X-Loc	Elev	Depth	Elev	Depth	Elev
B	-7.0	1197.1	5.3	1191.8	5.3	1191.8
C	58.2	1205.3	6.4	1198.9	12.2	1193.1
D	123.0	1205.5	2.3	1203.2	23.7	1181.8
			Geo			
1	0.0	1199.1	6.5	1192.6	6.5	1192.6
2	4.6	1200.2	7.1	1193.1	7.1	1193.1
3	10.5	1201.1	7.3	1193.8	7.3	1193.8
4	15.2	1201.9	7.5	1194.4	7.5	1194.4
5	20.1	1202.6	7.7	1194.9	7.7	1194.9
6	24.7	1202.9	7.5	1195.4	7.9	1195.0
7	29.0	1203.5	7.6	1195.9	8.5	1195.0
8	33.9	1203.9	7.5	1196.4	9.1	1194.8
9	38.8	1204.3	7.6	1196.7	9.6	1194.7
10	43.5	1204.8	7.7	1197.1	10.5	1194.3
11	48.1	1205.0	7.0	1198.0	11.2	1193.8
12	52.9	1205.1	6.2	1198.9	11.8	1193.3
13	58.2	1205.3	6.4	1198.9	12.2	1193.1
14	62.7	1205.5	6.0	1199.5	12.5	1193.0
15	67.7	1205.6	5.5	1200.1	12.7	1192.9
16	72.8	1205.3	4.6	1200.7	12.7	1192.6
17	77.5	1205.7	4.4	1201.3	13.6	1192.1
18	87.1	1205.8	2.7	1203.1	15.3	1190.5
19	92.1	1205.7	1.7	1204.0	15.9	1189.8
20	96.9	1205.7	1.1	1204.6	16.4	1189.3
21	102.0	1205.5	1.5	1204.0	17.0	1188.5
22	107.1	1205.5	1.9	1203.6	18.2	1187.3
23	112.2	1205.8	2.4	1203.4	20.3	1185.5
24	117.0	1205.5	2.3	1203.2	21.9	1183.6

## SRK - Vangorda Pit - North to South

## Spread B Depth and Elev of layers directly beneath SPs and Geos for VANGORDA.SIP

SP	Surface		Layer 2		Layer 3	
	X-Loc	Elev	Depth	Elev	Depth	Elev
B	112.4	1205.8	2.5	1203.3	20.4	1185.4
C	167.8	1204.7	4.9	1199.8	21.4	1183.3

D	233.7	1201.9	3.3	1198.6	19.2	1182.7
<b>Geo</b>						
1	117.0	1205.5	2.3	1203.2	21.9	1183.6
2	121.6	1205.4	2.2	1203.2	23.3	1182.1
3	126.3	1205.3	1.9	1203.4	24.1	1181.2
4	131.1	1205.3	1.9	1203.4	22.7	1182.6
5	136.0	1205.2	2.3	1202.9	22.4	1182.8
6	140.9	1205.1	2.9	1202.2	22.1	1183.0
7	145.6	1205.0	3.2	1201.8	21.8	1183.2
8	150.6	1205.0	3.8	1201.2	22.5	1182.5
9	155.6	1205.1	4.4	1200.7	22.1	1183.0
10	160.5	1204.8	4.7	1200.1	21.0	1183.8
11	165.4	1204.8	5.3	1199.5	20.9	1183.9
12	170.3	1204.8	4.8	1200.0	22.1	1182.7
13	175.4	1204.6	3.7	1200.9	23.3	1181.3
14	180.6	1204.5	2.7	1201.8	24.4	1180.1
15	185.3	1204.3	1.7	1202.6	25.0	1179.3
16	190.3	1204.0	1.1	1202.9	24.8	1179.2
17	194.9	1203.8	0.7	1203.1	24.6	1179.2
18	200.0	1203.5	0.4	1203.1	24.4	1179.1
19	204.9	1203.1	1.4	1201.7	23.9	1179.2
20	209.9	1203.0	2.7	1200.3	23.6	1179.4
21	214.6	1202.7	3.1	1199.6	23.3	1179.4
22	219.7	1202.6	3.3	1199.3	22.8	1179.8
23	224.7	1202.2	2.8	1199.4	21.7	1180.5
24	228.8	1202.1	2.2	1199.9	20.7	1181.4

## SRK - Vangorda Pit - North to South

Spread C Depth and Elev of layers directly beneath SPs and Geos for VANGORDA.SIP

SP	Surface		Layer 2		Layer 3	
	X-Loc	Elev	Depth	Elev	Depth	Elev
B	226.8	1202.1	2.5	1199.6	21.2	1180.9
C	290.2	1198.0	3.1	1194.9	19.3	1178.7
D	350.6	1195.4	3.7	1191.7	12.5	1182.9
<b>Geo</b>						
1	228.8	1202.1	2.6	1199.5	20.7	1181.4
2	233.6	1201.9	3.4	1198.5	19.2	1182.7
3	238.6	1201.5	1.4	1200.1	17.8	1183.7
4	243.6	1201.3	1.1	1200.2	18.1	1183.2
5	247.9	1201.2	1.2	1200.0	18.7	1182.5
6	253.2	1200.7	1.3	1199.4	19.3	1181.4
7	257.4	1200.4	1.4	1199.0	19.6	1180.8
8	262.6	1200.2	1.1	1199.1	20.4	1179.8
9	267.7	1200.0	1.5	1198.5	21.1	1178.9
10	271.9	1199.8	1.8	1198.0	21.7	1178.1
11	276.2	1199.5	1.7	1197.8	21.4	1178.1
12	280.8	1198.9	1.5	1197.4	20.7	1178.2
13	285.7	1198.3	2.2	1196.1	19.9	1178.4
14	290.2	1198.0	3.1	1194.9	19.3	1178.7
15	295.2	1197.6	2.6	1195.0	18.9	1178.7
16	300.2	1197.4	2.3	1195.1	19.2	1178.2
17	304.8	1197.0	1.9	1195.1	19.2	1177.8
18	309.7	1196.8	1.7	1195.1	19.4	1177.4
19	314.6	1196.4	1.2	1195.2	18.7	1177.7
20	319.9	1196.2	1.2	1195.0	18.0	1178.2
21	325.0	1195.8	2.0	1193.8	16.6	1179.2

22	329.8	1195.6	2.2	1193.4	14.5	1181.1
23	334.8	1195.3	3.0	1192.3	13.0	1182.3
24	339.8	1195.4	3.6	1191.8	12.5	1182.9

## SRK - Vangorda Pit - North to South

## Spread D Depth and Elev of layers directly beneath SPs and Geos for VANGORDA.SIP

SP	Surface		Layer 2		Layer 3	
	X-Loc	Elev	Depth	Elev	Depth	Elev
B	334.8	1195.3	3.0	1192.3	13.0	1182.3
C	388.6	1193.2	3.3	1189.9	9.3	1183.9
D	417.3	1190.2	2.5	1187.7	12.6	1177.6
E	441.9	1188.3	6.0	1182.3	10.9	1177.4
			Geo			
1	339.8	1195.4	3.6	1191.8	12.5	1182.9
2	345.0	1195.6	4.3	1191.3	12.3	1183.3
3	349.7	1195.4	3.9	1191.5	12.4	1183.0
4	354.2	1194.8	2.3	1192.5	12.4	1182.4
5	359.3	1194.7	1.3	1193.4	13.5	1181.2
6	364.1	1194.4	1.7	1192.7	13.8	1180.6
7	369.0	1194.4	2.3	1192.1	13.5	1180.9
8	373.8	1194.1	2.5	1191.6	12.5	1181.6
9	378.7	1193.8	2.4	1191.4	11.4	1182.4
10	383.9	1193.8	3.2	1190.6	10.4	1183.4
11	388.6	1193.2	3.3	1189.9	9.3	1183.9
12	393.1	1193.1	3.9	1189.2	9.4	1183.7
13	398.6	1192.2	3.9	1188.3	9.6	1182.6
14	403.0	1191.5	3.1	1188.4	10.1	1181.4
15	407.8	1191.3	2.8	1188.5	11.3	1180.0
16	412.6	1190.4	1.7	1188.7	11.9	1178.5
17	417.3	1190.2	2.5	1187.7	12.6	1177.6
18	422.2	1189.4	2.5	1186.9	11.6	1177.8
19	427.1	1189.0	3.0	1186.0	10.4	1178.6
20	432.0	1188.6	4.2	1184.4	9.3	1179.3
21	436.9	1188.3	5.4	1182.9	9.9	1178.4

## VANGORDA.SIP

## Velocities used, Spread A

	Layer 1	Layer 2	Layer 3
	-----	-----	-----
Vertical	698	2000	
Horizontal		2000	4880

## Velocities used, Spread B

	Layer 1	Layer 2	Layer 3
	-----	-----	-----
Vertical	698	2000	
Horizontal		2000	4880

## Velocities used, Spread C

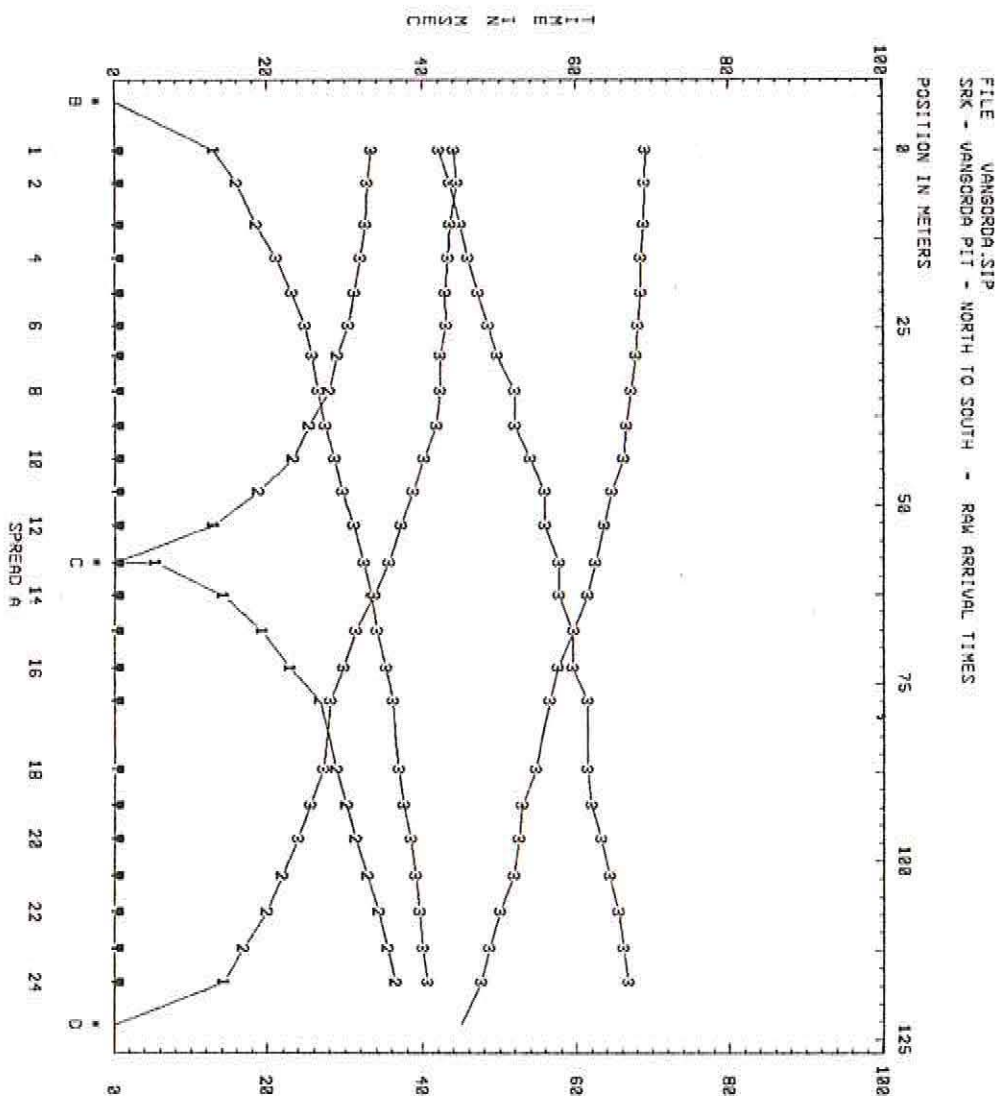
	Layer 1	Layer 2	Layer 3
	-----	-----	-----
Vertical	698	2000	

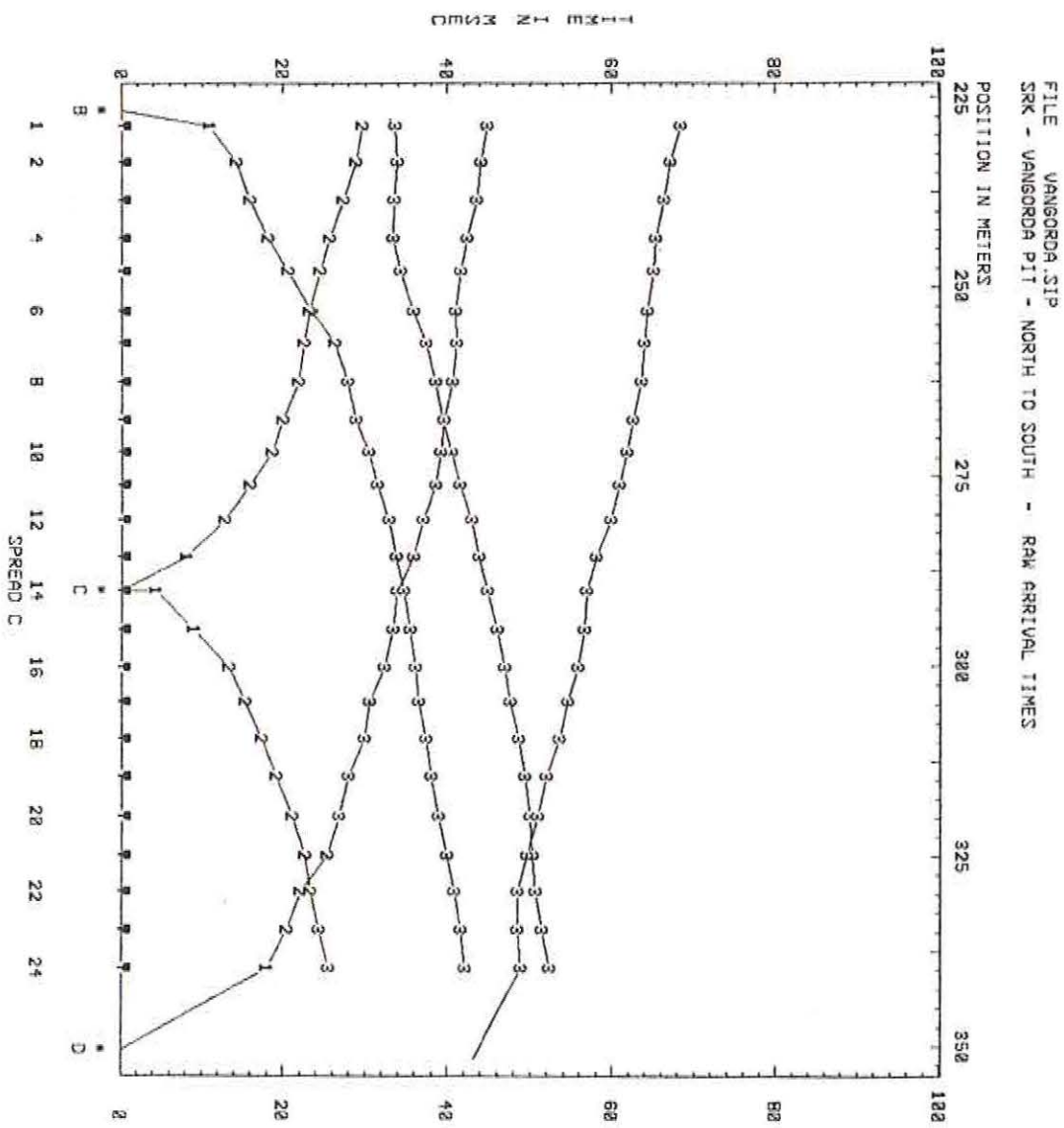
AURORA GEOSCIENCES LTD.

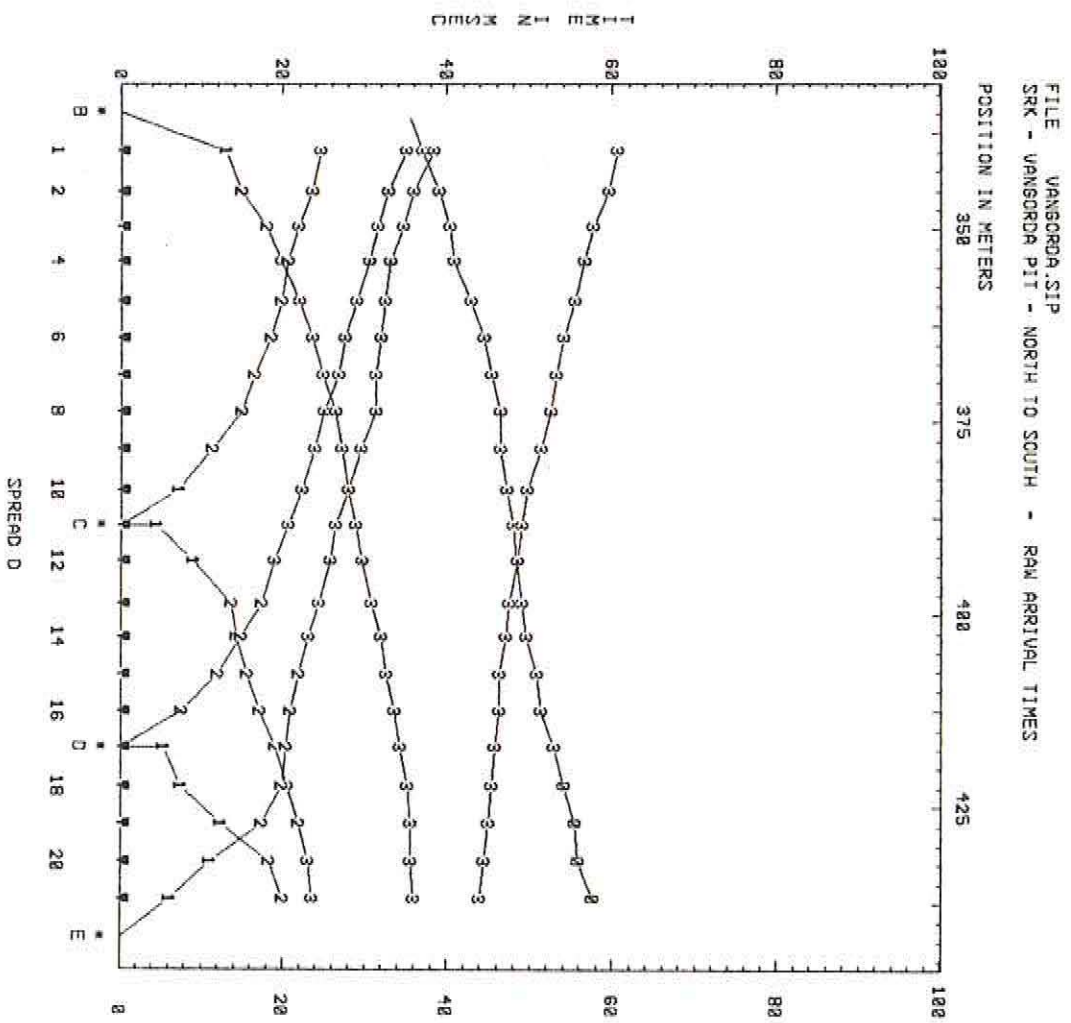
Horizontal                  2000                  4880

Velocities used, Spread D

	Layer 1	Layer 2	Layer 3
Vertical	698	2000	2000
Horizontal		2000	4880

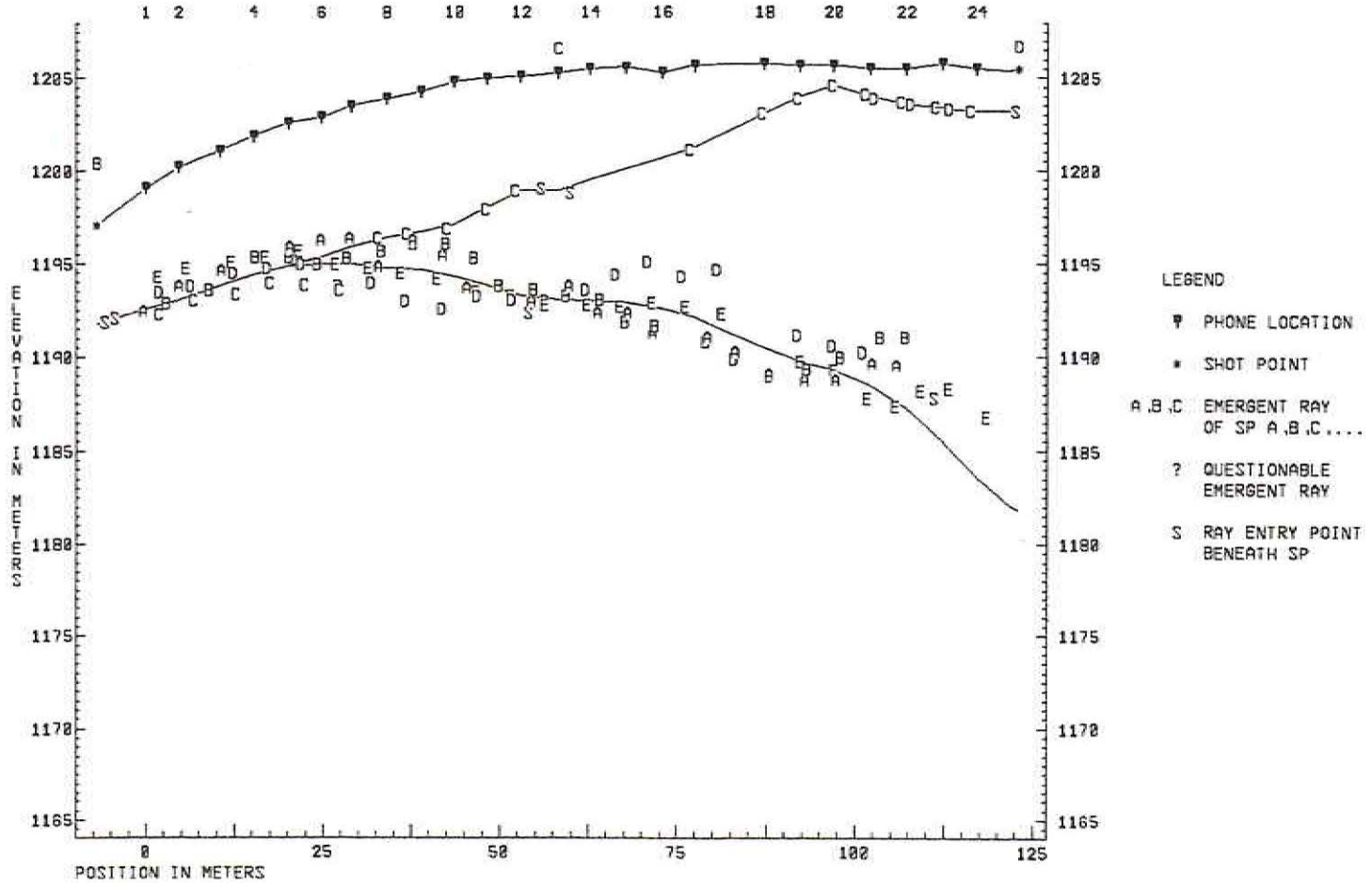






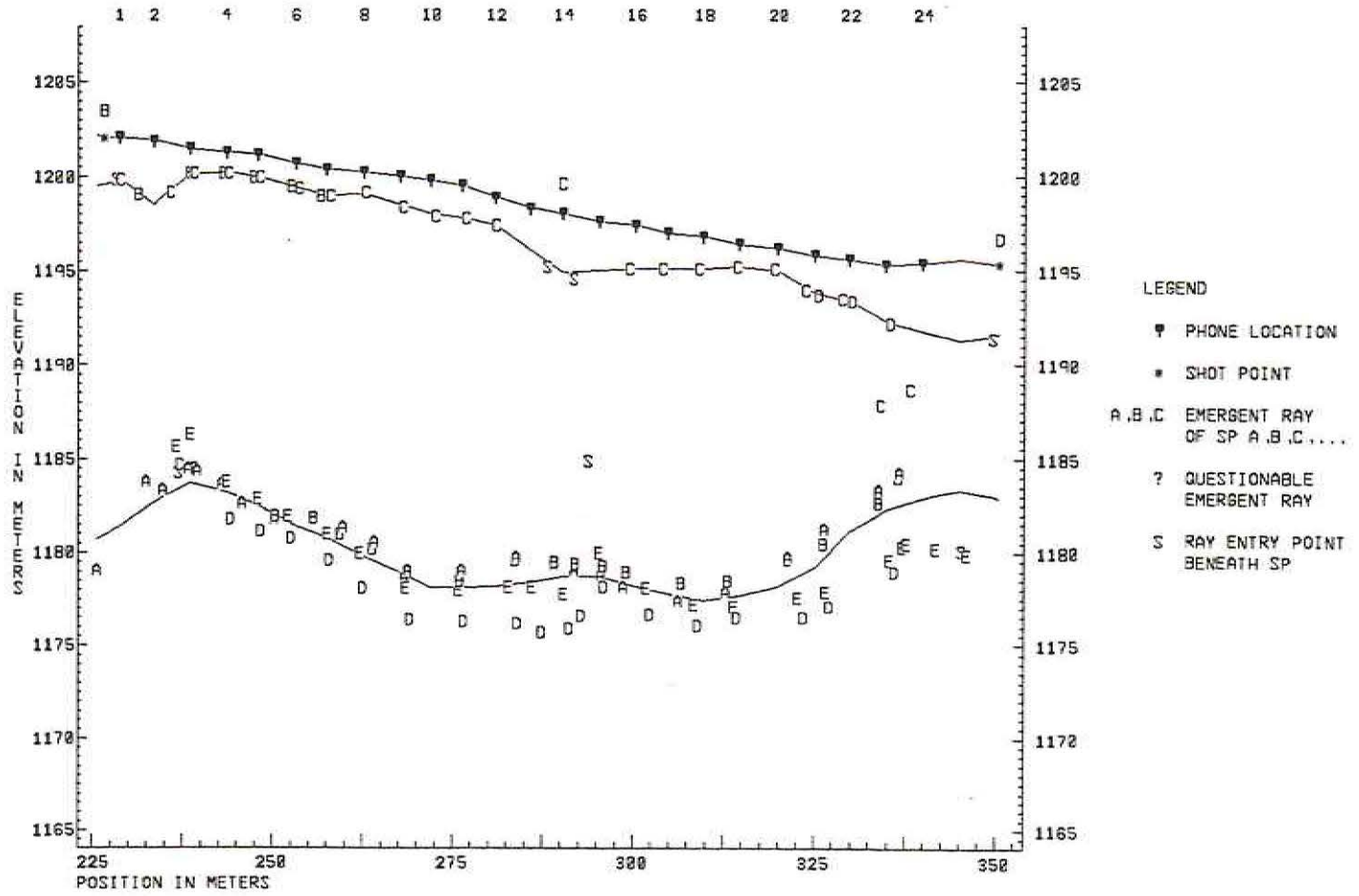
FILE VANGORDA.SIP  
SRK - VANGORDA PIT - NORTH TO SOUTH

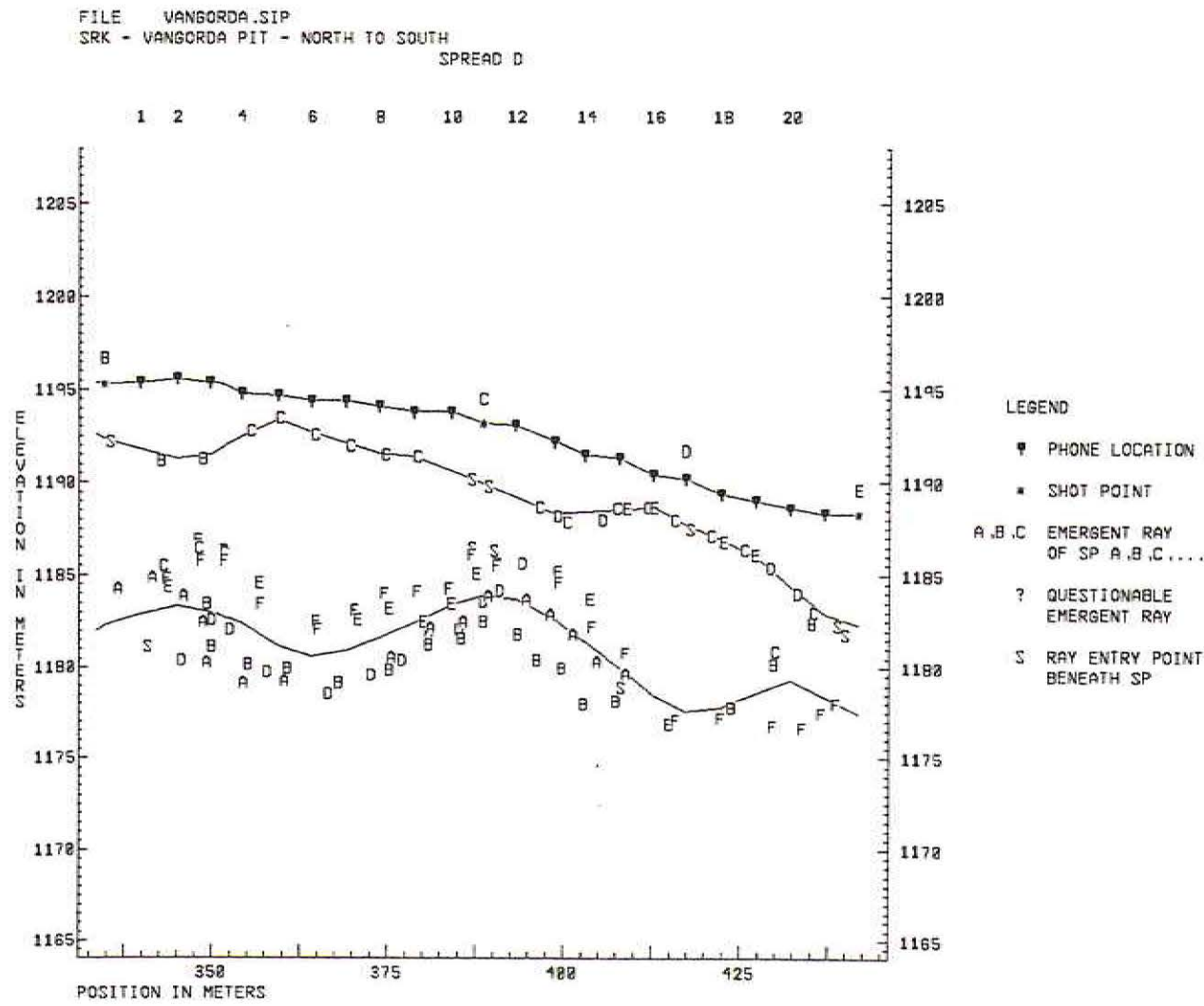
## SPREAD A



FILE VANGORDA.SIP  
SRK - VANGORDA PIT - NORTH TO SOUTH

SPREAD C







**LINE SL-3 - NORTH FORK OF ROSE CREEK / FARO ROCK DUMP**

SIPT2 V-4.1 — SEISMIC REFRACTION INTERPRETATION PROGRAM --- RIMROCK  
GEOPHYSICS, INC.

DATA FILE: SPREAD1.SIP

PRINT FILE: C:\DATA\SRKROCK\SPREAD1\SPREAD1. RUN DATE AND  
TIME: 10-23-2004 at 15:51

TITLE: Faro - SRK - Rock Dump Line - Spread 1 - West to East

PROGRAM CONTROL DATA			Printer Plot Scales			Datum Plane Control Points			Plot Control			Special					
			Control Parameters														
Sprds	Exit	Layers	Elev	Horiz	Time	Point 1	Point 2	Elevations	Trace	Off	L	BLim	TLim	Print			
			V-Over	m/col	m/row	ms/col	Elev	X-Loc	Elev	X-Loc	Top	Bottom					
							SP	Dip									
1	6	3	0	0.0	0.0	0.0	0.0	0.0	0.0	0.0	0	0	0.5	10.0	0	0	0

## SHOTPOINT AND GEOPHONE INPUT DATA for SPREAD1.SIP

Spread A, 5 Shotpoints, 24 Geophones, X-Shift = 0.0, X-True = 1, Units: Meters.

SP	Elev	X-Loc	Y-Loc	Depth	UpHole	T	Fudge	T	End	SP
A	1097.9	-119.5	0.0	0.0	0.0	0.0	0.0	0.0	0	
B	1091.6	-4.1	0.0	0.0	0.0	0.0	0.0	0.0	1	
C	1091.8	57.6	5.0	0.0	0.0	0.0	0.0	0.0	0	
D	1092.4	119.8	0.0	0.0	0.0	0.0	0.0	0.0	2	
E	1086.4	196.8	0.0	0.0	0.0	0.0	0.0	0.0	0	

Arrival Times + Fudge T and Layers represented

Geo	Elev	X-Loc	Y-Loc	SP A	SP B	SP C	SP D	SP E
-----	------	-------	-------	------	------	------	------	------

			T-L	T-L	T-L	T-L	T-L	T-L	
1	1092.0	0.0	51.5	3	15.5	1	65.5	2	
2	1091.8	5.2	0.0	52.0	3	30.0	1	62.5	2
3	1091.7	10.0	0.0	52.5	3	35.6	2	57.6	2
4	1091.3	15.3	0.0	53.5	3	40.4	2	54.0	2
5	1090.9	20.3	0.0	54.5	3	42.8	2	50.1	2
6	1091.1	25.2	0.0	57.3	3	47.9	2	49.1	2
7	1091.4	30.0	0.0	58.8	3	50.6	2	48.0	2
8	1091.2	35.2	0.0	61.9	3	55.0	2	45.5	2
9	1091.4	40.3	0.0	62.0	3	57.6	2	39.6	1
10	1091.2	45.2	0.0	62.5	3	56.8	2	32.1	1
11	1091.6	50.3	0.0	64.1	3	58.5	2	22.5	1
12	1091.8	55.3	0.0	65.0	3	59.9	3	10.4	1
13	1091.8	59.9	0.0	65.8	3	60.8	3	2.8	1
14	1091.8	65.1	0.0	66.1	3	62.9	3	9.3	2
15	1092.1	70.1	0.0	67.8	3	64.6	3	13.3	2
16	1091.8	74.5	0.0	70.0	3	66.0	3	17.6	2
17	1091.8	80.0	0.0	71.0	3	66.4	3	22.3	2
18	1091.9	85.1	0.0	72.1	3	68.1	3	30.0	2
19	1092.2	90.0	0.0	75.1	3	71.1	3	35.3	2
20	1092.1	95.0	0.0	75.4	3	71.4	3	41.0	2
21	1092.4	100.0	0.0	77.8	3	75.0	3	44.5	2
22	1092.2	105.0	0.0	81.8	3	76.1	3	50.6	2
23	1092.8	110.0	0.0	81.6	3	79.3	3	59.0	3
24	1092.4	114.8	0.0	83.6	3	80.6	3	61.1	3

## Layer 1 Velocity from direct arrivals

Spread A	SP	Geo	DD	V	Avg V
	B	1	4.1	266	
	B	2	9.3	310	
				288	
	C	9	18.0	455	
	C	10	13.4	417	
	C	11	8.9	393	
	C	12	5.5	529	
	C	13	5.5	1966	
				752	
	D	23	9.8	472	
	D	24	5.0	562	
				517	

Wtd Avg Velocity computed for Layer 1 = 597

## Layer 2 Velocity computed by regression of raw uncorrected arrivals

Spread A								
V	Ti	Geos	<-SP->	Geos	Ti	V	Avg V	Avg Ti
		B	3	11	29.2	1695	1695	29.2
1722	30.6	1	8	C	14	22	1176	9
					-1.2	917	1176	14.7
1809	17.1	5	22	D			1809	18
							1809	17.1
1853	30.9	23	24	E			1853	2
							1853	30.9
Avg = 1494 for 46 Pts								

## Layer 2 Velocity computed by Hobson-Overton method

Spread A	Avg	Std Err	4 Highest Std Err at geophones
SPs	Geos	V	TdSP Overall Err Geo Err Geo Err Geo Err Geo

AURORA GEOSCIENCES LTD.

B C 3 8	1638	-0.1	0.918	-1.273	3	1.044	6	-0.978	7	0.895	5
B D 5 11	2123	9.8	1.305	1.928	8	1.823	9	-1.434	5	-1.301	11
C D 14 22	1248	-1.3	1.195	2.076	19	-1.375	21	-1.357	22	1.308	20

Avg = 1633 for 22 Pts

---

Wtd Avg Velocity computed for Layer 2 = 1562

---

Layer 3 Velocity computed by regression of raw uncorrected arrivals

Spread A											
V	Ti	Geos	<-SP->	Geos	Ti	V	Avg V	Avg Ti	Pts		
			A	1 24	16.6	3590	3590	16.6	24		
			B	12 24	38.4	2871	2871	38.4	13		
			C	23 24	35.8	2273	2273	35.8	2		
2008	19.4	1 4	D			2008	2008	19.4	4		
3034	52.2	1 22	E			3034	3034	52.2	22		

Avg = 3047 for 65 Pts

Layer 3 Velocity computed by Hobson-Overton method

Spread A											
SPs	Geos	V	TdSP	Avg Std Err		4 Highest Std Err at geophones					
				Overall	Err	Geo	Err	Geo	Err	Geo	Err
A D 1 4	3194	-27.6	0.379	-0.631	2	0.325	1	0.264	3	0.042	4
A E 1 22	3329	-43.7	2.531	4.650	22	-4.229	12	-4.112	14	-3.832	11
B E 12 22	2608	-10.5	0.943	1.647	19	1.420	16	1.198	15	-1.103	18

Avg = 3100 for 37 Pts

---

Wtd Avg Velocity computed for Layer 3 = 3075

---

Arrival times Td corrected to datum. (Datum Elev = 1091.230 + 0.010x) for SPREAD1.SIP

Spread A		SPA	SPB	SP C	SP D	SP E
Datum Elev .....		1090.1	1091.2	1091.8	1092.4	1093.1
Geo .	X-Loc	Cor T	0.0	-0.7	-0.0	-0.0
-- .	--	--	-Td-	-Td-	-Td-	-Td-
1 1091.2	0.0	-1.3	50.2	13.5	64.2	77.5
2 1091.3	5.2	-0.9	51.1	28.4	61.6	76.1
3 1091.3	10.0	-0.6	51.9	34.3	56.9	72.9
4 1091.4	15.3	0.1	53.6	39.8	54.1	71.6
5 1091.4	20.3	0.9	55.4	43.0	50.9	70.6
6 1091.5	25.2	0.6	57.9	47.8	49.7	69.2
7 1091.5	30.0	0.2	59.0	50.1	48.2	67.4
8 1091.6	35.2	0.6	62.5	54.9	46.1	65.2
9 1091.6	40.3	0.4	62.4	57.3	39.9	62.8
10 1091.7	45.2	0.8	63.3	56.9	32.8	60.6
11 1091.7	50.3	0.2	64.3	58.0	22.6	57.2
12 1091.8	55.3	-0.1	64.9	59.1	10.3	53.2
13 1091.8	59.9	0.0	65.8	60.1	2.8	49.3
14 1091.9	65.1	0.1	66.2	62.3	9.4	47.5
15 1091.9	70.1	-0.3	67.5	63.6	12.9	43.6
16 1091.9	74.5	0.2	70.2	65.6	17.8	42.5

17	1092.0	80.0	0.3	71.3	66.0	22.6	37.1	90.3
18	1092.0	85.1	0.2	72.3	67.7	30.2	35.8	88.6
19	1092.1	90.0	-0.2	74.9	70.2	35.1	31.9	84.7
20	1092.1	95.0	0.1	75.5	70.8	41.0	30.6	83.2
21	1092.2	100.0	-0.4	77.4	74.0	44.1	28.4	82.4
22	1092.2	105.0	0.1	81.9	75.5	50.6	26.9	81.1
23	1092.3	110.0	-0.9	80.7	77.7	58.1	19.9	77.0
24	1092.3	114.8	-0.1	83.5	79.8	60.9	8.7	75.2

Arrival times Tc corrected to top of Layer 2 and Elev of top of Layer 2 for SPREAD1.SIP

Spread A		SP A	SP B	SP C	SP D	SP E		
Elev .....		0.0	1082.9	1088.8	1086.6	0.0		
Geo	X-Loc	Cor T	14.6	14.6	5.0	9.7		
—	—	—Tc—	—Tc—	—Tc—	—Tc—	—Tc—		
1	1083.2	0.0	14.7	18.3	0.0	45.9	54.4	53.3
2	1083.7	5.2	13.5	20.0	0.0	44.0	53.7	52.7
3	1083.9	10.0	13.1	20.9	8.0	39.6	50.8	51.4
4	1084.3	15.3	11.8	23.2	14.1	37.3	50.0	51.4
5	1085.1	20.3	9.7	26.3	18.5	35.4	50.3	52.5
6	1085.6	25.2	9.2	29.6	24.1	34.9	49.6	52.6
7	1085.4	30.0	10.1	30.2	25.9	32.9	47.4	51.2
8	1085.6	35.2	9.6	33.8	30.8	30.9	45.2	50.7
9	1085.9	40.3	9.2	34.4	33.9	0.0	43.6	50.0
10	1087.1	45.2	7.0	37.1	35.3	0.0	43.2	52.2
11	1087.1	50.3	7.6	38.1	36.4	0.0	39.8	50.2
12	1088.3	55.3	5.7	40.8	39.6	0.0	37.8	50.4
13	1089.4	59.9	4.0	43.3	42.2	0.0	35.5	48.6
14	1089.6	65.1	3.8	43.8	44.6	0.6	34.0	47.4
15	1089.1	70.1	5.0	44.3	45.0	3.3	29.2	42.3
16	1088.2	74.5	6.0	45.5	45.4	6.6	26.5	39.1
17	1087.0	80.0	8.0	44.5	43.9	9.4	19.1	35.2
18	1086.1	85.1	9.7	44.0	43.9	15.4	16.2	31.9
19	1085.4	90.0	11.4	45.2	45.1	18.9	11.0	26.7
20	1084.7	95.0	12.3	44.6	44.5	23.7	8.5	24.0
21	1085.1	100.0	11.8	47.5	48.6	27.7	7.2	24.2
22	1085.5	105.0	11.3	52.1	50.3	34.4	5.9	22.9
23	1086.6	110.0	10.5	52.6	54.3	43.6	0.0	2.3
24	1086.9	114.8	9.1	56.0	56.9	47.0	0.0	1.0

Faro - SRK - Rock Dump Line - Spread 1 - West to East

Spread A Points of emergence of refracted rays below target geophones for SPREAD1.SIP

Geo	SP A	SP B	SP C	SP D	SP E	
—	—L	—L	—L	—L	—L	
1	X-Loc -13.2	3	— 1	5.2	2 9.9	3 8.9
	Elev 1068.1	—	1084.0	1070.6	1072.2	
2	X-Loc -8.2	3	— 1	8.4	2 14.5	3 13.6
	Elev 1068.2	—	1083.9	1069.9	1071.6	
3	X-Loc -4.2	3	6.7	2 13.1	2 17.0	3 17.0
	Elev 1068.3	1083.9	1083.9	1071.1	1071.3	
4	X-Loc 9.1	3	12.1	2 19.5	2 21.2	3 21.4
	Elev 1068.4	1083.9	1085.0	1070.2	1069.6	
5	X-Loc 8.6	3	19.6	2 23.2	2 23.2	2 26.6
	Elev 1067.4	1085.1	1085.6	1085.6	1067.3	
6	X-Loc 12.0	3	23.6	2 26.9	2 26.9	2 32.2
	Elev 1066.0	1085.6	1085.6	1085.6	1065.4	
7	X-Loc 14.8	3	26.9	2 32.3	2 32.3	2 40.0
	Elev 1066.5	1085.6	1085.2	1085.2	1064.1	

8	X-Loc	15.6 3	32.5 2	38.4 2	38.4 2	48.0 3
	Elev	1064.9	1085.2	1085.5	1085.5	1062.5
9	X-Loc	20.1 3	38.6 2	— 1	44.0 2	54.8 3
	Elev	1066.1	1085.5	—	1086.9	1061.5
10	X-Loc	23.7 3	44.8 2	— 1	46.7 2	65.7 3
	Elev	1065.4	1087.1	—	1087.2	1059.0
11	X-Loc	27.9 3	48.2 2	— 1	52.1 2	72.5 3
	Elev	1065.6	1087.1	—	1087.0	1059.4
12	X-Loc	36.1 3	36.8 3	— 1	58.4 2	74.2 3
	Elev	1064.3	1065.1	—	1089.1	1058.7
13	X-Loc	41.1 3	41.6 3	— 1	60.4 2	76.7 3
	Elev	1063.4	1064.1	—	1090.0	1059.7
14	X-Loc	47.3 3	46.7 3	63.9 2	65.9 2	97.0 3
	Elev	1064.2	1063.3	1089.6	1089.5	1062.3
15	X-Loc	53.0 3	52.4 3	68.8 2	70.6 2	96.1 3
	Elev	1064.7	1063.9	1089.3	1089.1	1064.9
16	X-Loc	58.7 3	58.6 3	72.3 2	75.2 2	90.5 3
	Elev	1064.3	1064.1	1088.7	1088.0	1064.8
17	X-Loc	69.0 3	69.2 3	77.1 2	81.1 2	98.4 3
	Elev	1066.5	1066.9	1087.6	1086.8	1067.0
18	X-Loc	73.4 3	73.3 3	81.8 2	86.6 2	101.3 3
	Elev	1068.1	1068.0	1086.7	1085.9	1068.3
19	X-Loc	76.5 3	76.5 3	86.3 2	91.8 2	100.6 3
	Elev	1068.0	1067.9	1085.9	1085.1	1071.3
20	X-Loc	89.7 3	89.7 3	91.0 2	97.3 2	105.1 3
	Elev	1071.5	1071.4	1085.3	1084.5	1071.2
21	X-Loc	93.9 3	93.5 3	95.8 2	105.1 2	107.3 3
	Elev	1071.6	1070.4	1084.6	1085.5	1070.3
22	X-Loc	98.7 3	99.2 3	104.0 2	109.1 2	121.2 3
	Elev	1069.3	1070.7	1085.2	1086.5	1068.1
23	X-Loc	103.1 3	102.4 3	101.1 3	— 1	113.1 2
	Elev	1071.1	1069.4	1066.4	—	1087.0
24	X-Loc	103.9 3	103.4 3	101.1 3	— 1	116.5 2
	Elev	1069.6	1068.6	1064.8	—	1087.0

Spread A Points of entry of refracted rays below source shotpoints:

L=2	Right	X-Loc	—	3.1	59.3	—	—
	Elev	—	1083.3	1089.7	—	—	—
L=2	Left	X-Loc	—	—	57.8	117.1	117.3
	Elev	—	—	1088.7	1087.0	1087.0?	—
L=3	Right	X-Loc	7.9	7.9	75.3	—	—
	Elev	1069.5*	1069.5	1060.3	—	—	—
L=3	Left	X-Loc	—	—	—	104.8	104.8
	Elev	—	—	—	1069.0	1069.0*	—

#### Faro - SRK - Rock Dump Line - Spread 1 - West to East

Spread A Depth and Elev of layers directly beneath SPs and Geos for SPREAD1.SIP

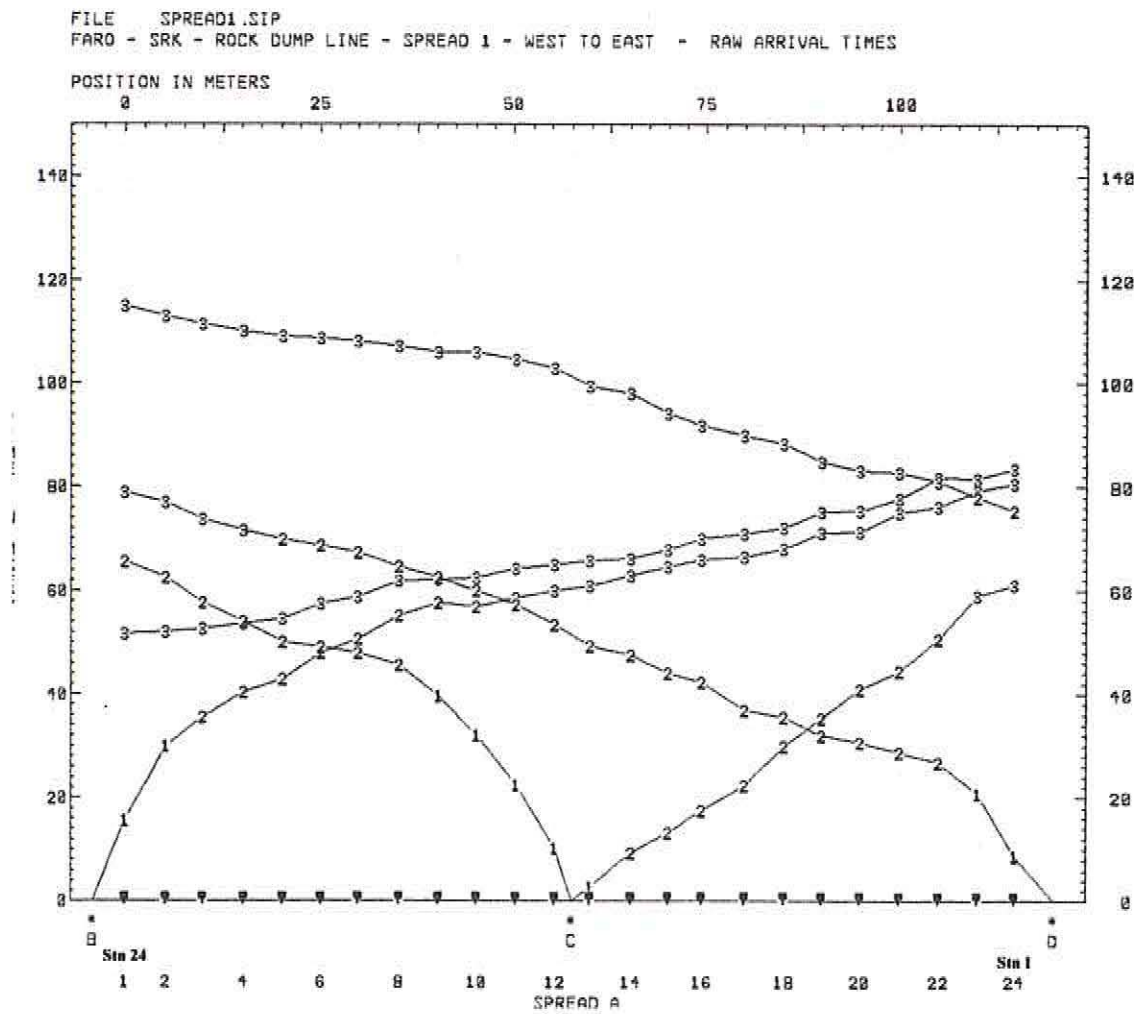
SP	Surface		Layer 2		Layer 3	
	X-Loc	Elev	Depth	Elev	Depth	Elev
B	-4.1	1091.6	8.7	1082.9	23.3	1068.3
C	57.6	1091.8	3.0	1088.8	28.0	1063.8
D	119.8	1092.4	5.1	1087.3	24.1	1068.3
			Geo		—	—
1	0.0	1092.0	8.8	1083.2	23.2	1068.8
2	5.2	1091.8	8.1	1083.7	22.4	1069.4
3	10.0	1091.7	7.8	1083.9	22.5	1069.2

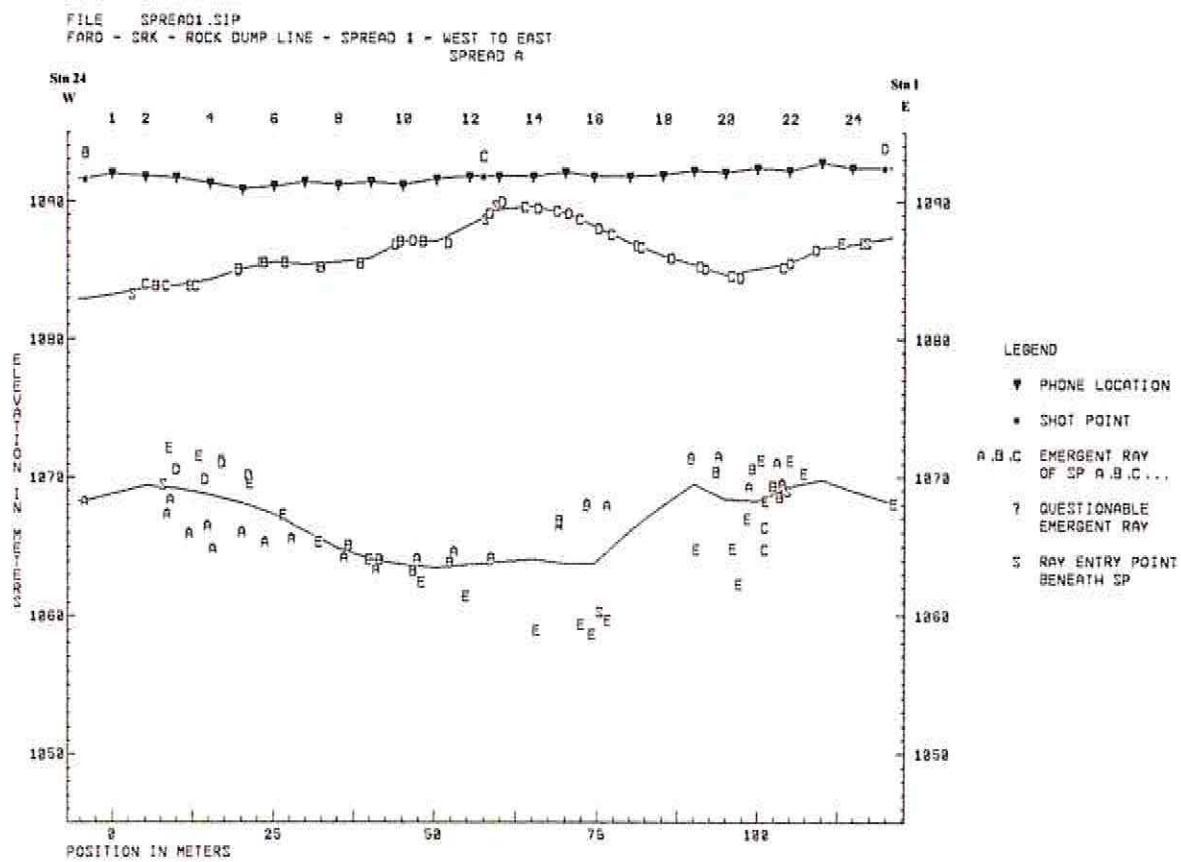
4	15.3	1091.3	7.0	1084.3	22.6	1068.7
5	20.3	1090.9	5.8	1085.1	22.8	1068.1
6	25.2	1091.1	5.5	1085.6	23.8	1067.3
7	30.0	1091.4	6.0	1085.4	25.3	1066.1
8	35.2	1091.2	5.6	1085.6	26.3	1064.9
9	40.3	1091.4	5.5	1085.9	27.3	1064.1
10	45.2	1091.2	4.1	1087.1	27.5	1063.7
11	50.3	1091.6	4.5	1087.1	28.1	1063.5
12	55.3	1091.8	3.5	1088.3	28.1	1063.7
13	59.9	1091.8	2.4	1089.4	27.9	1063.9
14	65.1	1091.8	2.3	1089.6	27.7	1064.1
15	70.1	1092.1	3.0	1089.1	28.3	1063.8
16	74.5	1091.8	3.6	1088.2	28.0	1063.8
17	80.0	1091.8	4.8	1087.0	25.7	1066.1
18	85.1	1091.9	5.8	1086.1	24.0	1067.9
19	90.0	1092.2	6.8	1085.4	22.7	1069.5
20	95.0	1092.1	7.4	1084.7	23.7	1068.4
21	100.0	1092.4	7.3	1085.1	24.1	1068.3
22	105.0	1092.2	6.7	1085.5	22.9	1069.3
23	110.0	1092.8	6.2	1086.6	23.0	1069.8
24	114.8	1092.4	5.5	1086.9	23.4	1069.0

## SPREAD1.SIP

## Velocities used, Spread A

	Layer 1	Layer 2	Layer 3
Vertical	597	1562	3075
Horizontal			





SIPT2 V-4.1 -- SEISMIC REFRACTION INTERPRETATION PROGRAM --- RIMROCK  
 GEOPHYSICS, INC.

DATA FILE: SPREAD2.SIP

PRINT FILE: C:\DATA\SRKROCK\SPREAD2\SPREAD2. RUN DATE AND

TIME: 10-23-2004 at 15:52

TITLE: Faro - SRK - Rock pile - Spread 2 - East to West

PROGRAM CONTROL DATA      Printer Plot Scales      Datum Plane Control Points      Plot Control      Special  
Control Parameters

Sprrds	Exit	Layers	V-Over	m/col	Horiz	Time	Point 1	Point 2	Elevations	Trace	Off	L					
							Elev	X-Loc	Elev	X-Loc	Top	Bottom	BLim	TLim	Print		
							SP	Dip									
1	6	3	1	0.0	0.0	0.0	0.0	0.0	0.0	0.0	0	0	0.5	10.0	0	0	0

## VELOCITY OVERRIDES for SPREAD2.SIP

## Spread 1

Layer Vv Vh

2 1500 1500

## SHOTPOINT AND GEOPHONE INPUT DATA for SPREAD2.SIP

Spread A, 5 Shotpoints, 24 Geophones, X-Shift = 0.0, X-True = 1, Units: Meters.

SP	Elev	X-Loc	Y-Loc	Depth	UpHole	T	Fudge	T	End	SP
A	1086.4	-196.8	0.0	0.0	0.0	0.0	0.0	0.0	0	0
B	1091.8	-4.8	0.0	0.0	0.0	0.0	0.0	0.0	1	
C	1091.0	56.9	1.0	0.0	0.0	0.0	0.0	0.0	0	
D	1098.0	119.5	0.0	0.0	0.0	0.0	0.0	0.0	2	
E	1106.0	164.5	0.0	0.0	0.0	0.0	10.0	0.0	0	

Arrival Times + Fudge T and Layers represented

Geo	Elev	X-Loc	Y-Loc	SP A		SP B		SP C		SP D		SP E	
				T-L	L	T-L	L	T-L	L	T-L	L		
1	1092.0	0.0	0.0	81.0	3	18.9	1	51.0	3	69.5	3	82.6	3
2	1091.6	4.1	0.0	82.3	3	26.6	1	48.9	3	68.6	3	82.1	3
3	1091.2	9.1	0.0	82.5	3	29.0	2	44.9	2	66.0	3	78.5	3
4	1090.8	14.3	0.0	83.3	3	33.0	2	41.9	2	63.8	3	77.1	3
5	1090.8	18.1	0.0	86.3	3	38.0	2	37.4	2	61.8	3	72.9	3
6	1090.4	24.1	0.0	87.9	3	41.5	2	35.3	2	60.4	3	71.6	3
7	1090.2	29.4	0.0	92.4	3	45.4	2	34.8	2	58.5	3	70.8	3
8	1090.5	34.2	0.0	93.0	3	47.5	2	33.0	2	60.0	3	68.5	3
9	1090.0	39.4	0.0	94.9	3	52.4	2	31.3	2	60.8	3	69.4	3
10	1089.9	44.3	0.0	95.8	3	54.1	3	28.1	2	60.0	3	69.4	3
11	1091.0	49.4	0.0	97.3	3	55.0	3	20.8	1	54.1	3	67.4	3
12	1091.0	54.0	0.0	97.6	3	57.1	3	10.6	1	49.8	3	62.3	3
13	1091.1	59.7	0.0	96.8	3	59.0	3	7.1	1	47.1	3	57.9	3
14	1091.5	64.2	0.0	99.0	3	59.0	3	15.9	1	45.8	3	57.3	3
15	1092.1	69.3	0.0	99.6	3	61.1	3	17.6	2	46.3	3	57.6	3
16	1092.3	74.3	0.0	101.6	3	61.1	3	19.4	2	49.8	3	59.8	3
17	1092.7	79.3	0.0	105.1	3	63.4	3	26.4	2	51.0	3	62.9	3
18	1093.3	84.4	0.0	108.4	3	65.5	3	36.1	2	50.1	3	61.6	3
19	1094.3	89.4	0.0	110.5	3	68.6	3	41.0	2	48.4	3	61.4	3
20	1095.1	94.3	0.0	111.3	3	70.9	3	44.0	2	41.9	2	57.1	3
21	1096.0	99.7	0.0	112.9	3	73.0	3	48.4	2	35.3	2	54.9	3
22	1096.1	104.4	0.0	113.1	3	73.5	3	51.5	2	31.3	2	55.4	3
23	1097.5	109.2	0.0	115.3	3	76.5	3	54.1	3	23.4	2	53.1	2
24	1097.9	114.5	0.0	118.3	3	77.9	3	55.4	3	8.9	2	49.6	2

Layer 1 Velocity from direct arrivals

Spread A	SP	Geo	DD	V	Avg V
	B	1	4.8	254	
	B	2	8.9	335	
				294	
	C	11	7.6	364	
	C	12	3.1	289	
	C	13	3.0	419	
	C	14	7.4	464	
				384	

Wtd Avg Velocity computed for Layer 1 = 354

Layer 2 Velocity computed by regression of raw uncorrected arrivals

Spread A									
V	Ti	Geos	<-SP->	Geos	Ti	V	Avg V	Avg Ti	Pts
		B	3 9	19.3	1337		1337	19.3	7
2317	22.8	3 10	C	15 22	4.4	967	1365	13.6	16
		645	4.6	20 24	D		645	4.6	5
		1514	16.1	23 24	E		1514	16.1	2
							Avg = 1152	for 30 Pts	

Layer 2 Velocity computed by Hobson-Overton method

Spread A									
SPs	Geos	Avg	Std Err	4 Highest	Std Err at geophones	Geos	Err Geo	Err Geo	Err Geo
B	C	3 9	1700	6.3	1.998	3.609	5	-2.301	3
						2.148	6	-1.425	4
C	D	20 22	1117	-8.5	0.589	0.832	21	-0.448	22
						-0.384	20		
						Avg = 1525	for 10 Pts		

Wtd Avg Velocity computed for Layer 2 = 1302

Override Velocity assigned to Layer 2

Spread	A
	1500

Layer 3 Velocity computed by regression of raw uncorrected arrivals

Spread A									
V	Ti	Geos	<-SP->	Geos	Ti	V	Avg V	Avg Ti	Pts
		A	1 24	18.1	3153		3153	18.1	24
		B	10 24	35.8	2875		2875	35.8	15
1955	21.9	1 2	C	23 24	41.2	4084	2644	31.5	4
							3942	37.2	19
3942	37.2	1 19	D						
							4024	38.1	22
							Avg = 3410	for 84 Pts	

Layer 3 Velocity computed by Hobson-Overton method

Spread A									
SPs	Geos	Avg	Std Err	4 Highest	Std Err at geophones	Geos	Err Geo	Err Geo	Err Geo

	A	C	1	2	2409	-28.1	0.000	0.000	1	-0.000	2		
A D	1	19	3564	-8.4	2.502	4.277	12	4.176	7	3.952	14	-3.638	17
A E	1	22	3559	-7.3	2.697	4.131	14	3.865	13	-3.863	17	3.758	8
B D	10	19	4575	6.1	3.515	-6.188	10	4.878	13	4.208	14	3.571	15
B E	10	22	4077	5.7	3.246	5.527	13	-4.694	17	3.917	14	-3.805	18

Avg = 3782 for 66 Pts

---

Wtd Avg Velocity computed for Layer 3 = 3637

---

Arrival times Td corrected to datum. (Datum Elev = 1089.320 + 0.055x) for SPREAD2.SIP

Spread A		SP A	SP B	SP C	SP D	SP E		
Datum Elev	.....	1078.4	1089.1	1092.5	1095.9	1098.4		
Geo	.	X-Loc	Cor T	0.0	-7.8	4.2	-5.8	0.0
---	---	---	---	--Td--	--Td--	--Td--	--Td--	--Td--
1	1089.3	0.0	-7.6	73.4	3.6	47.6	56.1	75.0
2	1089.5	4.1	-5.8	76.5	13.1	47.3	57.0	76.3
3	1089.8	9.1	-3.9	78.6	17.4	45.2	56.3	74.6
4	1090.1	14.3	-1.9	81.4	23.3	44.1	56.1	75.2
5	1090.3	18.1	-1.3	85.0	28.9	40.2	54.7	71.6
6	1090.7	24.1	0.7	88.6	34.5	40.2	55.3	72.3
7	1091.0	29.4	2.1	94.5	39.8	41.1	54.8	72.9
8	1091.2	34.2	2.0	95.0	41.8	39.2	56.2	70.5
9	1091.5	39.4	4.3	99.2	48.9	39.7	59.3	73.7
10	1091.8	44.3	5.3	101.1	51.6	37.6	59.5	74.7
11	1092.1	49.4	3.0	100.3	50.2	28.0	51.3	70.4
12	1092.3	54.0	3.7	101.3	53.1	18.5	47.7	66.0
13	1092.6	59.7	4.3	101.1	55.6	15.6	45.6	62.2
14	1092.9	64.2	3.9	102.9	55.1	24.0	43.9	61.2
15	1093.2	69.3	3.0	102.6	56.4	24.8	43.5	60.6
16	1093.4	74.3	3.2	104.8	56.6	26.8	47.2	63.0
17	1093.7	79.3	2.9	108.0	58.5	33.4	48.1	65.8
18	1094.0	84.4	2.0	110.4	59.7	42.2	46.3	63.6
19	1094.3	89.4	-0.1	110.4	60.8	45.1	42.6	61.3
20	1094.6	94.3	-1.5	109.8	61.6	46.6	34.6	55.6
21	1094.9	99.7	-3.2	109.7	62.0	49.3	26.3	51.7
22	1095.1	104.4	-2.8	110.3	63.0	52.9	22.7	52.6
23	1095.4	109.2	-6.0	109.3	62.8	52.3	11.6	47.1
24	1095.7	114.5	-6.3	112.0	63.9	53.3	-3.2	43.3

Arrival times Tc corrected to top of Layer 2 and Elev of top of Layer 2 for SPREAD2.SIP

Spread A		SP A	SP B	SP C	SP D	SP E		
Elev	.....	0.0	1090.2	1088.2	1096.8	0.0		
Geo	.	X-Loc	Cor T	4.5	4.5	7.9	3.3	3.3
---	---	---	---	--Tc--	--Tc--	--Tc--	--Tc--	--Tc--
1	1089.9	0.0	5.8	30.2	0.0	37.2	60.4	62.0
2	1089.8	4.1	5.2	32.2	0.0	35.8	60.2	62.1
3	1089.7	9.1	4.3	33.2	20.2	32.7	58.4	59.4
4	1089.1	14.3	4.8	33.5	23.7	29.2	55.8	57.5
5	1088.7	18.1	6.0	35.3	27.5	23.5	52.6	52.1
6	1088.2	24.1	6.3	36.6	30.7	21.1	50.9	50.5
7	1087.6	29.4	7.5	40.0	33.4	19.4	47.8	48.5
8	1087.5	34.2	8.5	39.5	34.4	16.6	48.2	45.2

9	1086.8	39.4	9.0	40.9	38.9	14.4	48.6	45.6
10	1087.0	44.3	8.1	42.7	41.5	12.1	48.7	46.5
11	1087.5	49.4	8.5	43.8	41.9	0.0	42.3	44.1
12	1087.8	54.0	9.0	43.7	43.6	0.0	37.6	38.5
13	1088.6	59.7	7.2	44.6	47.3	0.0	36.7	35.9
14	1089.1	64.2	6.9	47.1	47.5	0.0	35.6	35.6
15	1089.7	69.3	6.6	48.0	49.9	3.0	36.4	36.2
16	1089.9	74.3	6.7	49.9	49.9	4.8	39.9	38.3
17	1089.0	79.3	10.3	49.8	48.5	8.2	37.4	37.8
18	1088.4	84.4	13.9	49.5	47.1	14.3	32.9	32.9
19	1088.3	89.4	17.0	48.5	47.0	16.1	28.1	29.6
20	1088.6	94.3	18.4	47.9	47.9	17.6	20.2	23.9
21	1089.3	99.7	18.8	49.1	49.7	21.7	13.2	21.3
22	1090.7	104.4	15.1	53.0	53.8	28.5	12.9	25.5
23	1093.8	109.2	10.6	59.7	61.4	35.6	9.6	4.1
24	1096.4	114.5	4.3	69.0	69.1	43.2	1.4	6.9

## Faro - SRK - Rock pile - Spread 2 - East to West

Spread A Points of emergence of refracted rays below target geophones for SPREAD2.SIP

Geo	SP A	SP B	SP C	SP D	SP E
	-L	-L	-L	-L	-L
1	X-Loc -10.6 3	-- 1	6.9 3	8.7 3	9.4 3
	Elev 1065.7	---	1070.8	1065.7	1063.8
2	X-Loc -6.6 3	-- 1	9.6 3	11.3 3	12.0 3
	Elev 1065.1	---	1070.8	1064.8	1062.5
3	X-Loc -1.3 3	8.8 2	9.3 2	18.1 3	18.6 3
	Elev 1065.6	1089.7	1089.7	1064.5	1063.1
4	X-Loc 4.5 3	13.7 2	14.5 2	22.0 3	22.7 3
	Elev 1066.1	1089.2	1089.1	1065.1	1063.0
5	X-Loc 6.6 3	17.4 2	18.4 2	34.2 3	34.5 3
	Elev 1065.0	1088.8	1088.7	1067.4	1067.1
6	X-Loc 9.7 3	23.4 2	24.3 2	38.6 3	38.9 3
	Elev 1065.2	1088.3	1088.2	1067.5	1067.1
7	X-Loc 14.4 3	28.4 2	30.1 2	42.2 3	43.0 3
	Elev 1062.9	1087.6	1087.5	1068.7	1067.4
8	X-Loc 19.9 3	33.5 2	34.4 2	44.7 3	43.8 3
	Elev 1064.1	1087.5	1087.5	1067.3	1069.1
9	X-Loc 34.2 3	38.1 2	40.4 2	49.9 3	49.1 3
	Elev 1064.3	1086.9	1086.7	1065.1	1066.8
10	X-Loc 38.8 3	39.1 3	45.1 2	59.3 3	58.6 3
	Elev 1064.6	1065.8	1087.1	1064.7	1065.8
11	X-Loc 43.7 3	44.2 3	-- 1	65.3 3	67.2 3
	Elev 1066.7	1068.4	--	1071.7	1069.8
12	X-Loc 45.6 3	45.7 3	-- 1	66.5 3	67.7 3
	Elev 1066.7	1067.0	--	1073.5	1072.1
13	X-Loc 50.1 3	49.2 3	-- 1	70.3 3	70.3 3
	Elev 1067.6	1065.7	--	1073.4	1073.4
14	X-Loc 58.6 3	58.5 3	-- 1	73.8 3	74.1 3
	Elev 1067.2	1067.1	--	1073.6	1072.9
15	X-Loc 67.6 3	67.5 3	69.0 2	78.3 3	78.5 3
	Elev 1069.8	1068.5	1089.7	1072.3	1071.8
16	X-Loc 70.5 3	70.6 3	73.9 2	83.1 3	82.8 3
	Elev 1069.6	1069.9	1090.0	1068.5	1069.1
17	X-Loc 73.4 3	73.7 3	77.7 2	91.7 3	92.3 3
	Elev 1070.2	1071.4	1089.3	1069.2	1068.3
18	X-Loc 76.4 3	77.3 3	82.3 2	96.6 3	97.0 3
	Elev 1071.2	1073.4	1088.5	1071.9	1071.3
19	X-Loc 81.0 3	81.7 3	88.0 2	98.8 3	100.0 3
	Elev 1073.3	1074.7	1088.2	1074.8	1072.9
20	X-Loc 90.0 3	90.1 3	93.0 2	97.0 2	102.6 3

	Elev	1075.3	1075.5	1088.4	1088.9	1076.9
21	X-Loc	97.6 3	97.6 3	99.2 2	102.7 2	111.3 3
	Elev	1076.4	1076.2	1089.2	1090.0	1080.3
22	X-Loc	100.3 3	100.2 3	104.3 2	107.3 2	122.3 3
	Elev	1075.4	1074.9	1090.4	1092.6	1067.6
23	X-Loc	102.5 3	102.1 3	103.5 3	111.2 2	111.2 2
	Elev	1072.4	1071.2	1075.1	1095.0	1095.0
24	X-Loc	112.7 3	112.8 3	113.0 3	114.9 2	114.9 2
	Elev	1070.2	1070.4	1074.1	1096.6	1096.6

Spread A Points of entry of refracted rays below source shotpoints:

L=2	Right	X-Loc	---	-4.5	58.2	---	---
		Elev	---	1090.1	1088.4	---	---
L=2	Left	X-Loc	---	---	56.8	119.6	119.6
		Elev	---	---	1088.1	1096.9	1096.9*
L=3	Right	X-Loc	7.0	7.0	70.9	---	---
		Elev	1066.2*	1066.2	1069.5	---	---
L=3	Left	X-Loc	---	---	50.0	114.4	114.4
		Elev	---	---	1072.2	1078.0	1078.0*

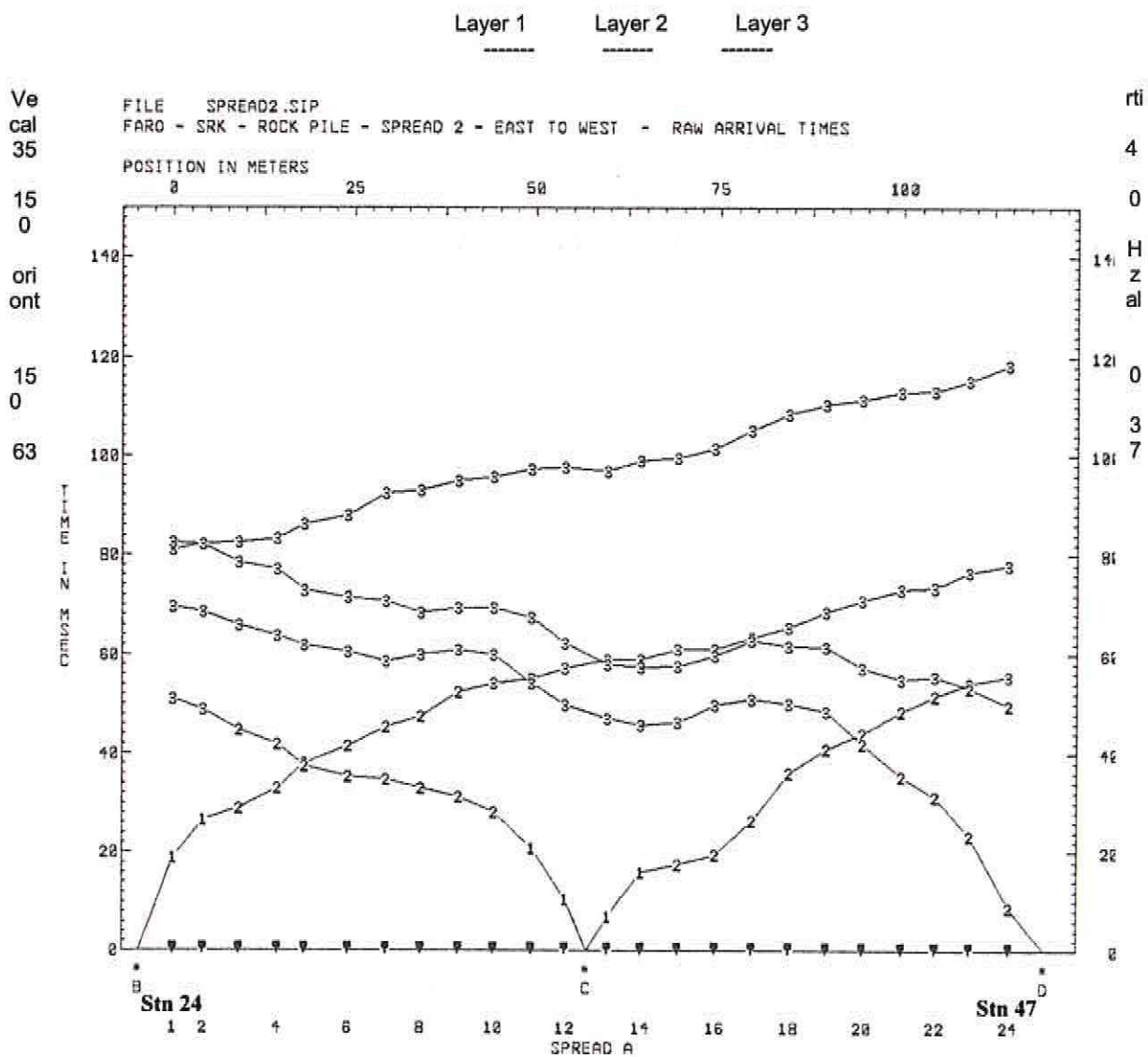
#### Faro - SRK - Rock pile - Spread 2 - East to West

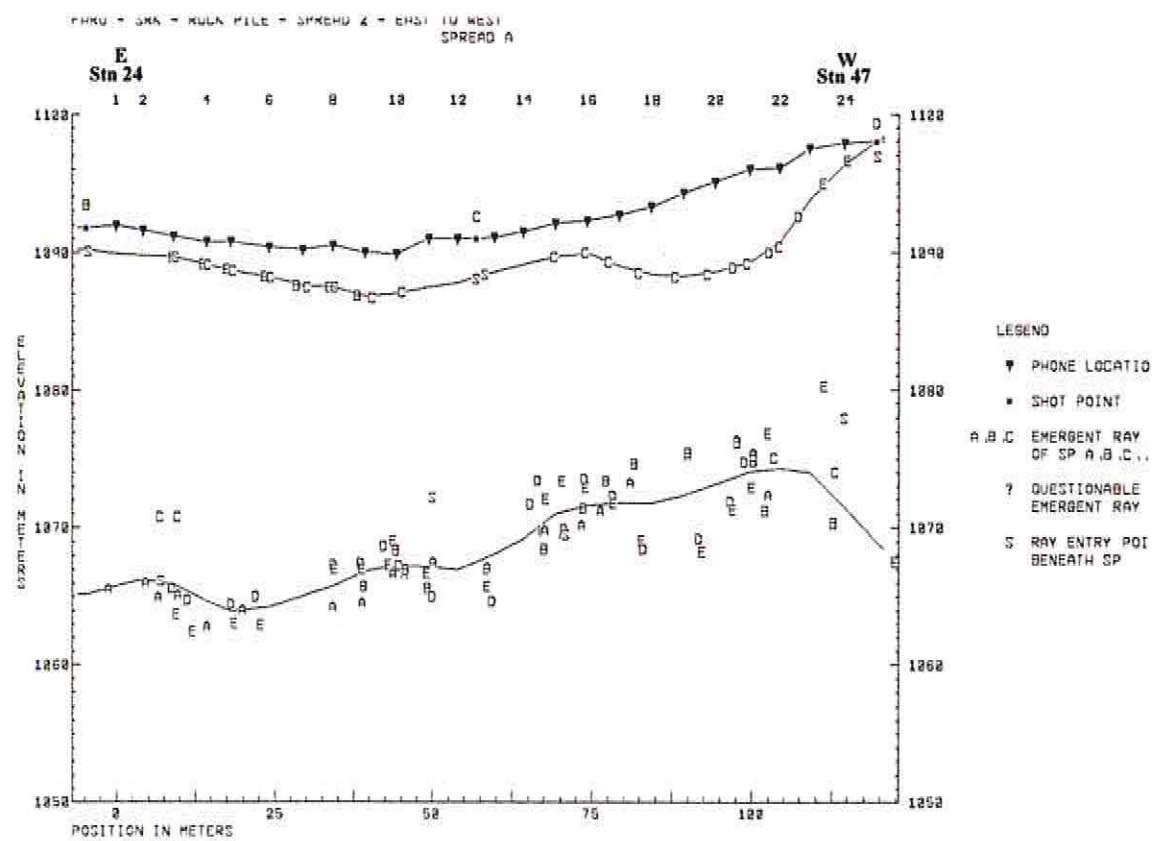
Spread A Depth and Elev of layers directly beneath SPs and Geos for SPREAD2.SIP

SP	Surface		Layer 2		Layer 3	
	X-Loc	Elev	Depth	Elev	Depth	Elev
B	-4.8	1091.8	1.6	1090.2	26.6	1065.2
C	56.9	1091.0	2.8	1088.2	23.4	1067.6
D	119.5	1098.0	0.0	1098.0	29.0	1069.0
				Geo		
1	0.0	1092.0	2.1	1089.9	26.2	1065.8
2	4.1	1091.6	1.8	1089.8	25.3	1066.3
3	9.1	1091.2	1.5	1089.7	25.3	1065.9
4	14.3	1090.8	1.7	1089.1	26.1	1064.7
5	18.1	1090.8	2.1	1088.7	26.8	1064.0
6	24.1	1090.4	2.2	1088.2	26.1	1064.3
7	29.4	1090.2	2.6	1087.6	25.1	1065.1
8	34.2	1090.5	3.0	1087.5	24.7	1065.8
9	39.4	1090.0	3.2	1086.8	23.1	1066.9
10	44.3	1089.9	2.9	1087.0	22.6	1067.3
11	49.4	1091.0	3.5	1087.5	23.8	1067.2
12	54.0	1091.0	3.2	1087.8	24.0	1067.0
13	59.7	1091.1	2.5	1088.6	23.0	1068.1
14	64.2	1091.5	2.4	1089.1	22.3	1069.2
15	69.3	1092.1	2.4	1089.7	21.1	1071.0
16	74.3	1092.3	2.4	1089.9	20.7	1071.6
17	79.3	1092.7	3.7	1089.0	20.9	1071.8
18	84.4	1093.3	4.9	1088.4	21.5	1071.8
19	89.4	1094.3	6.0	1088.3	22.1	1072.3
20	94.3	1095.1	6.5	1088.6	21.9	1073.2
21	99.7	1096.0	6.7	1089.3	21.9	1074.1
22	104.4	1096.1	5.4	1090.7	21.8	1074.3
23	109.2	1097.5	3.7	1093.8	23.5	1074.0
24	114.5	1097.9	1.5	1096.4	26.5	1071.4

SPREAD2.SIP

## Velocities used, Spread A





SIPT2 V-4.1 — SEISMIC REFRACTION INTERPRETATION PROGRAM --- RIMROCK  
GEOPHYSICS, INC.

DATA FILE: SPREAD3.SIP

PRINT FILE: C:\DATA\SRKROCK\SPREAD3\SPREAD3. RUN DATE AND  
TIME: 10-23-2004 at 15:59

TITLE: Faro - SRK - Rock dump - Spread 3 - East to West

PROGRAM CONTROL DATA		Printer	Plot	Scales	Datum	Plane	Control Points	Plot Control	Special	
		Control Parameters								
Spuds	Exit	Layers	V-Over	Horiz	Time	Point 1	Point 2	Elevations	Trace Off L	
			m/col	m/row	ms/col	Elev	X-Loc	Elev X-Loc Top Bottom	BLim TLim Print	
								SP Dip		
1	6	3	0	0.0	0.0	0.0	0.0	0.0 0 0 0.0	0.5 10.0 0 0 0 0	

## SHOTPOINT AND GEOPHONE INPUT DATA for SPREAD3.SIP

Spread A, 5 Shotpoints, 24 Geophones, X-Shift = 0.0, X-True = 1, Units: Meters.

SP	Elev	X-Loc	Y-Loc	Depth	UpHole	T	Fudge	T	End	SP
A	1100.4	-50.6	0.0	0.0	0.0	0.0	0.0	0.0	0	0
B	1097.9	-5.0	0.0	0.0	0.0	0.0	0.0	0.0	1	
C	1098.6	54.2	5.0	0.0	0.0	0.0	0.0	0.0	0	
D	1103.6	118.4	0.0	0.0	0.0	0.0	0.0	0.0	2	
E	1105.6	185.4	0.0	0.0	0.0	0.0	0.0	0.0	0	

Arrival Times + Fudge T and Layers represented

Geo	Elev	X-Loc	Y-Loc	SP A	SP B	SP C	SP D	SP E
				—T—L	—T—L	—T—L	—T—L	—T—L
1	1097.9	0.0	0.0	45.8 3	13.3 1	36.5 2	69.5 0	92.8 0
2	1097.1	4.3	0.0	48.4 3	23.8 1	33.5 2	65.1 0	88.9 0
3	1097.1	9.4	0.0	48.0 3	33.5 2	29.5 2	63.0 3	86.3 3
4	1097.1	14.7	0.0	48.4 3	38.8 2	24.5 2	58.5 3	85.4 3
5	1097.2	19.6	0.0	51.5 3	43.6 2	20.3 2	55.4 3	82.8 3

6	1097.6	24.6	0.0	53.3 3	45.4 2	14.1 2	50.1 3	78.4 3
7	1097.8	29.5	0.0	54.1 3	46.6 2	12.1 2	48.1 3	76.0 3
8	1098.0	34.5	0.0	55.4 3	48.9 2	9.4 2	46.8 3	73.1 3
9	1098.7	40.1	0.0	55.0 3	50.1 2	6.6 2	46.3 3	70.9 3
10	1098.6	44.6	0.0	54.1 3	51.0 2	4.0 2	47.1 3	70.0 3
11	1099.1	49.6	0.0	54.1 3	52.4 2	3.1 2	47.8 3	70.5 3
12	1099.6	54.2	0.0	53.6 3	56.8 3	4.9 1	48.9 3	71.3 3
13	1099.6	59.7	0.0	55.9 3	59.0 3	4.9 2	48.0 3	72.1 3
14	1100.4	64.3	0.0	57.6 3	59.9 3	9.3 2	48.0 2	71.6 3
15	1099.9	69.5	0.0	59.0 3	62.5 3	12.9 2	46.3 2	71.8 3
16	1100.3	74.5	0.0	61.1 3	64.3 3	15.5 2	42.8 2	70.4 3
17	1100.5	79.3	0.0	63.4 3	66.9 3	19.4 2	38.3 2	68.1 3
18	1100.8	84.2	0.0	65.5 3	67.3 3	23.8 2	35.6 2	66.0 3
19	1101.2	89.1	0.0	67.3 3	69.0 3	26.5 2	31.3 2	64.6 3
20	1101.7	94.0	0.0	68.6 3	68.1 3	28.1 2	21.6 2	63.4 3
21	1102.1	99.0	0.0	69.0 3	69.5 3	30.0 2	19.0 2	61.6 3
22	1102.5	104.1	0.0	70.9 3	70.0 3	35.3 2	20.8 2	59.9 3
23	1102.9	109.3	0.0	71.8 3	71.8 3	36.5 2	16.4 1	59.0 3
24	1103.6	113.4	0.0	72.6 3	70.9 3	37.0 2	11.0 1	58.0 3

### Layer 1 Velocity from direct arrivals

Spread A	SP	Geo	DD	V	Avg V
	B	1	5.0	376	
	B	2	9.3	392	
				384	
	C	12	5.1	1041	
				1041	
	D	23	9.1	557	
	D	24	5.0	455	
				506	

Wtd Avg Velocity computed for Layer 1 = 564

Layer 2 Velocity computed by regression of raw uncorrected arrivals

Spread A									
V	Ti	Geos	<-SP->	Geos	Ti	V	Avg V	Avg Ti	Pts
-----	-----	-----	-----	-----	-----	-----	-----	-----	-----
		B	3 11	30.8	2340		2340	30.8	9
1361	-4.6	1 11	C	13 24	2.7	1613	1482	-1.0	23
1239	6.1	14 22	D				1239	6.1	9
							Avg =	1539	for 41 Pts

### Layer 2 Velocity computed by Hobson-Overton method

Spread A		Avg	Std Err	4 Highest	Std Err	at geophones						
SPs	Geos	V	TdSP	Overall	Err	Geo	Err	Geo	Err	Geo	Err	Geo
B C	3 11	1799	26.7	3.185	-5.642	3	4.846	6	-3.964	11	2.643	7
C D	14 22	1376	-8.8	1.801	3.838	20	-2.847	22	-1.751	16	1.195	14

Wtd Avg Velocity computed for Layer 2 = 1562

Layer 3 Velocity computed by regression of raw uncorrected arrivals

Spread A									
V	Ti	Geos	<-SP->	Geos	Ti	V	Avg V	Avg Ti	Pts
		A	1 24	33.9	4376		4376	33.9	24
		B	12 24	44.1	4097		4097	44.1	13
3814	28.9	3 13	D			3814	28.9	11	
4289	41.7	3 24	E			4289	41.7	22	
Avg = 4199 for 70 Pts									

Layer 3 Velocity computed by Hobson-Overton method

Spread A										Avg	Std Err	4 Highest Std Err at geophones	
SPs	Geos	V	Td	SP Overall	Err	Geo	Err	Geo	Err	Geo	Err	Geo	Err
A D	3 13	5110	1.9	4.673	-7.274	3	6.512	8	5.868	7	-5.104	12	
A E	3 24	4279	-8.3	3.270	6.060	8	-5.405	15	5.240	9	-4.245	16	
B D	12 13	3544	9.3	0.000	-0.000	13	-0.000	12					
B E	12 24	3919	2.9	1.209	2.039	19	-1.899	24	-1.641	15	1.450	17	
Avg = 4341 for 48 Pts													

Wtd Avg Velocity computed for Layer 3 = 4281

Arrival times Td corrected to datum. (Datum Elev = 1096.490 + 0.055x) for SPREAD3.SIP

Spread A		SP A	SP B	SP C	SP D	SP E		
Datum Elev . . . . .		1093.7	1096.2	1099.5	1103.0	1106.7		
Geo .	X-Loc	Cor T	0.0	-3.0	1.6	-1.0	0.0	
			-Td-	-Td-	-Td-	-Td-	-Td-	
1	1096.5	0.0	-2.5	43.3	7.8	35.6	66.0	90.3
2	1096.7	4.3	-0.7	47.7	20.2	34.4	63.4	88.2
3	1097.0	9.4	-0.2	47.8	30.4	30.9	61.8	86.1
4	1097.3	14.7	0.4	48.8	36.2	26.4	57.9	85.8
5	1097.6	19.6	0.7	52.2	41.3	22.5	55.1	83.5
6	1097.9	24.6	0.4	53.7	42.9	16.1	49.6	78.8
7	1098.1	29.5	0.6	54.7	44.2	14.2	47.7	76.6
8	1098.4	34.5	0.7	56.1	46.6	11.7	46.5	73.8
9	1098.7	40.1	0.0	55.0	47.1	8.2	45.3	70.9
10	1099.0	44.6	0.6	54.7	48.6	6.2	46.7	70.6
11	1099.2	49.6	0.2	54.3	49.6	4.9	47.0	70.7
12	1099.5	54.2	-0.2	53.4	53.6	6.3	47.7	71.1
13	1099.8	59.7	0.3	56.2	56.4	6.8	47.3	72.4
14	1100.0	64.3	-0.6	57.0	56.3	10.2	46.4	71.0
15	1100.3	69.5	0.8	59.8	60.3	15.2	46.1	72.6
16	1100.6	74.5	0.6	61.7	61.9	17.6	42.4	71.0
17	1100.9	79.3	0.7	64.1	64.6	21.6	38.0	68.8
18	1101.1	84.2	0.6	66.1	64.9	26.0	35.2	66.6
19	1101.4	89.1	0.4	67.7	66.4	28.5	30.7	65.0
20	1101.7	94.0	-0.0	68.6	65.1	29.7	20.6	63.4
21	1102.0	99.0	-0.2	68.8	66.3	31.3	17.8	61.4
22	1102.2	104.1	-0.4	70.5	66.6	36.4	19.4	59.5
23	1102.5	109.3	-0.6	71.2	68.2	37.4	14.8	58.4
24	1102.8	113.4	-1.5	71.1	66.4	37.1	8.5	56.5

Arrival times Tc corrected to top of Layer 2 and Elev of top of Layer 2 for SPREAD3.SIP

Spread A		SP A	SP B	SP C	SP D	SP E
Elev . . . . .		0.0	1093.1	1098.4	1103.3	0.0
Geo .	X-Loc	Cor T	8.6	8.6	0.4	0.5
—	—	—	-Tc-	-Tc-	-Tc-	-Tc-
1	1093.6	0.0	7.7	31.1	0.0	28.4
2	1094.4	4.3	4.7	36.6	0.0	28.4
3	1094.4	9.4	4.7	36.2	20.2	24.4
4	1094.2	14.7	5.1	36.3	25.1	19.0
5	1094.4	19.6	5.0	39.4	30.0	14.9
6	1095.0	24.6	4.6	41.6	32.2	9.1
7	1095.7	29.5	3.8	43.3	34.3	7.9
8	1096.4	34.5	2.9	45.4	37.4	6.1
9	1097.6	40.1	2.0	45.9	39.5	4.2
10	1098.1	44.6	0.9	46.2	41.6	2.7
11	1098.9	49.6	0.3	46.7	43.5	2.4
12	1098.4	54.2	2.1	44.4	46.1	0.0
13	1098.0	59.7	2.8	46.0	47.6	1.7
14	1097.8	64.3	4.6	45.9	46.7	4.3
15	1097.8	69.5	3.7	48.2	50.2	8.8
16	1096.8	74.5	6.2	47.9	49.6	9.0
17	1096.5	79.3	7.1	49.3	51.3	12.0
18	1096.9	84.2	7.0	51.5	51.8	16.5
19	1097.8	89.1	6.1	54.2	54.4	20.0
20	1099.2	94.0	4.4	57.2	55.1	23.3
21	1100.8	99.0	2.4	59.6	58.5	27.2
22	1100.6	104.1	3.4	60.5	58.1	31.5
23	1102.5	109.3	0.7	64.1	62.6	35.5
24	1102.8	113.4	1.4	64.1	60.9	35.2

## Faro - SRK - Rock dump - Spread 3 - East to West

Spread A Points of emergence of refracted rays below target geophones for SPREAD3.SIP

Geo	SP A	SP B	SP C	SP D	SP E
	L	L	L	L	L
1	X-Loc -3.6 3	— 1	3.0 2	— 0	— 0
	Elev 1068.4	—	1094.2	—	—
2	X-Loc -0.5 3	— 1	5.1 2	— 0	— 0
	Elev 1065.9	—	1094.6	—	—
3	X-Loc 1.7 3	8.3 2	10.3 2	34.9 3	33.8 3
	Elev 1066.6	1094.5	1094.4	1071.1	1072.1
4	X-Loc 4.5 3	13.4 2	15.9 2	36.6 3	38.3 3
	Elev 1067.4	1094.2	1094.2	1074.4	1072.8
5	X-Loc 4.5 3	18.5 2	21.1 2	36.4 3	38.2 3
	Elev 1066.0	1094.2	1094.5	1075.3	1073.2
6	X-Loc 22.9 3	24.0 2	26.0 2	37.3 3	39.4 3
	Elev 1067.4	1094.9	1095.2	1079.1	1076.2
7	X-Loc 32.1 3	29.0 2	30.6 2	40.7 3	42.5 3
	Elev 1069.8	1095.6	1095.8	1079.4	1076.8
8	X-Loc 36.3 3	34.1 2	35.5 2	42.3 3	42.9 3
	Elev 1070.3	1096.3	1096.5	1079.0	1077.7
9	X-Loc 38.7 3	39.9 2	40.6 2	47.1 3	47.1 3
	Elev 1071.8	1097.6	1097.6	1078.1	1078.2
10	X-Loc 41.4 3	44.4 2	44.8 2	50.1 3	49.8 3
	Elev 1072.8	1098.1	1098.1	1075.9	1077.4
11	X-Loc 42.9 3	49.6 2	49.7 2	54.1 3	53.8 3
	Elev 1073.5	1098.9	1098.9	1074.1	1075.7
12	X-Loc 45.6 3	44.9 3	— 1	61.1 3	60.6 3
	Elev 1075.9	1073.9	—	1072.8	1074.7

13	X-Loc	48.0	3	47.1	3	59.0	2	66.8	3	66.7	3
	Elev	1075.3		1073.4		1098.1		1072.5		1073.0	
14	X-Loc	50.6	3	49.9	3	63.1	2	65.4	2	71.4	3
	Elev	1076.2		1075.0		1097.8		1097.8		1073.6	
15	X-Loc	55.9	3	54.6	3	68.8	2	69.7	2	80.2	3
	Elev	1074.7		1072.5		1097.9		1097.8		1071.4	
16	X-Loc	61.8	3	60.8	3	72.2	2	75.8	2	87.3	3
	Elev	1074.8		1072.8		1097.2		1096.5		1073.5	
17	X-Loc	66.9	3	65.7	3	77.6	2	81.1	2	91.9	3
	Elev	1074.2		1072.0		1096.5		1096.6		1075.3	
18	X-Loc	71.7	3	71.3	3	82.9	2	86.4	2	97.2	3
	Elev	1073.2		1072.5		1096.7		1097.1		1076.5	
19	X-Loc	77.9	3	77.6	3	88.3	2	91.4	2	105.2	3
	Elev	1072.1		1071.4		1097.5		1098.4		1077.3	
20	X-Loc	86.8	3	87.1	3	93.9	2	95.6	2	112.7	3
	Elev	1071.5		1072.7		1099.2		1099.7		1078.0	
21	X-Loc	91.7	3	91.8	3	98.9	2	99.3	2	113.7	3
	Elev	1071.7		1072.0		1100.8		1100.8		1077.9	
22	X-Loc	97.3	3	97.6	3	102.9	2	105.8	2	116.0	3
	Elev	1072.2		1073.6		1100.3		1100.9		1077.6	
23	X-Loc	105.3	3	105.4	3	109.3	2	—	1	121.4	3
	Elev	1072.2		1072.9		1102.5		—		1077.6	
24	X-Loc	112.3	3	112.4	3	113.1	2	—	1	125.3	3
	Elev	1075.2		1077.3		1102.7		—		1078.4	

#### Spread A Points of entry of refracted rays below source shotpoints:

L=2	Right	X-Loc	---	-2.5	54.3	--	--
		Elev	--	1093.0	1098.4	--	--
L=2	Left	X-Loc	--	--	54.1	118.3	--
		Elev	--	--	1098.4	1103.2	--
L=3	Right	X-Loc	5.9	5.9	--	--	--
		Elev	1064.4*	1064.4	--	--	--
L=3	Left	X-Loc	--	--	--	112.8	112.8
		Elev	--	--	--	1079.9	1079.9*

Faro - SRK - Rock dump - Spread 3 - East to West

### Spread A Depth and Elev of layers directly beneath SPs and Geos for SPREAD3.SIP

SP	Surface		Layer 2		Layer 3	
	X-Loc	Elev	Depth	Elev	Depth	Elev
B	-5.0	1097.9	4.8	1093.1	30.2	1067.7
C	54.2	1098.6	0.2	1098.4	23.8	1074.8
D	118.4	1103.6	0.3	1103.3	25.6	1078.0
			Geo			
1	0.0	1097.9	4.3	1093.6	31.1	1066.8
2	4.3	1097.1	2.7	1094.4	31.0	1066.1
3	9.4	1097.1	2.7	1094.4	30.8	1066.3
4	14.7	1097.1	2.9	1094.2	30.4	1066.7
5	19.6	1097.2	2.8	1094.4	30.1	1067.1
6	24.6	1097.6	2.6	1095.0	29.6	1068.0
7	29.5	1097.8	2.1	1095.7	28.1	1069.7
8	34.5	1098.0	1.6	1096.4	25.8	1072.2
9	40.1	1098.7	1.1	1097.6	23.9	1074.8
10	44.6	1098.6	0.5	1098.1	22.9	1075.7
11	49.6	1099.1	0.2	1098.9	23.6	1075.5
12	54.2	1099.6	1.2	1098.4	24.8	1074.8
13	59.7	1099.6	1.6	1098.0	25.8	1073.8

14	64.3	1100.4	2.6	1097.8	27.1	1073.3
15	69.5	1099.9	2.1	1097.8	27.0	1072.9
16	74.5	1100.3	3.5	1096.8	27.9	1072.4
17	79.3	1100.5	4.0	1096.5	28.3	1072.2
18	84.2	1100.8	3.9	1096.9	28.6	1072.2
19	89.1	1101.2	3.4	1097.8	28.5	1072.7
20	94.0	1101.7	2.5	1099.2	28.2	1073.5
21	99.0	1102.1	1.3	1100.8	28.2	1073.9
22	104.1	1102.5	1.9	1100.6	27.7	1074.8
23	109.3	1102.9	0.4	1102.5	26.8	1076.1
24	113.4	1103.6	0.8	1102.8	26.7	1076.9

SPREAD3.SIP

Velocities used, Spread A

	Layer 1	Layer 2	Layer 3
Vertical	564	1562	4281
Horizontal			

